ANALYSIS OF EXCAVATION SUPPORT SYSTEM WITH SOIL NAIL OF DIFFERENT PROFILES

Submitted to

DELHI TECHNOLOGICAL UNIVERSITY

in partial fulfilment of the requirements for the award of the degree of

DOCTOR OF PHILOSOPHY

In

CIVIL ENGINEERING

By

ARCHITA GOYAL
(Reg. No. 2K16/PhD/CE/08)

Under the supervision of

Prof. (Dr.) Amit Kumar Shrivastava

DEPARTMENT OF CIVIL ENGINEERING

DELHI TECHNOLOGICAL UNIVERSITY

SHAHBAD, DAULATPUR, BAWANA ROAD, DELHI - 110042 (INDIA)

November, 2023

Dedicated to my family

DELHI TECHNOLOGICAL UNIVERSITY

Shahabad Daulatpur, Main Bawana Road

Delhi-110042 (India)

DECLARATION

I hereby declare that the thesis entitled **"ANALYSIS OF EXCAVATION SUPPORT SYSTEM WITH SOIL NAILS OF DIFFERENT PROFILES"** submitted by me for the award of the degree of ***Doctor of Philosophy*** to **Delhi Technological University (Formerly Delhi College of Engineering)** is a record of bonafide work carried out by me under the guidance of Prof. (Dr.) Amit Kumar Shrivastava, Department of Civil Engineering, Delhi Technological University.

I further declare that the work reported in this thesis has not been submitted and will not be submitted, either in part or in full, for the award of any other degree or diploma in this Institute or any other Institute or University.

Archita Goyal

Reg No: 2K16/PhD/CE/08

Department of Civil Engineering

Place: New Delhi

Date:

DELHI TECHNOLOGICAL UNIVERSITY

Shahabad Daulatpur, Main Bawana Road

Delhi-110042 (India)

CERTIFICATE

This is to certify that the thesis entitled **"Analysis of excavation support system with soil nails of different profiles"** submitted by **Ms. Archita Goyal** to **Delhi Technological University (Formerly Delhi College of Engineering)**, for the award of the degree of "*Doctor of Philosophy*" in Civil Engineering is a record of bonafide work carried out by her. Archita Goyal has worked under my guidance and supervision and has fulfilled the requirements for the submission of this thesis, which to our knowledge has reached the requisite standards.

The results contained in this thesis are original and have not been submitted to any other university or institute for an award of any degree or diploma.

Dr. Amit Kumar Shrivastava

Professor

Department of Civil Engineering

Delhi Technological University (DTU)

Bawana, Delhi-110042

ACKNOWLEDGEMENTS

First of all, I am thankful to the almighty god who made this work possible from beginning to end and gave me strength and patience during my PhD journey.

I would like to express my wholehearted gratitude and sincere appreciation and thanks to my Ph.D. supervisor, Dr. Amit Kumar Shrivastava, Professor, Department of Civil engineering, Delhi Technological University for his inspiring guidance and continuous support through my PhD journey. Without his active involvement and constant guidance, this research would not exist in its current form. The lines are dedicated to my guide:

"सब धरती कागज करूँ, लेखनी सब बनराय/

सात समुंदर की मसि करूँ, गुरु गुण लिखा न जाय//"

His exceptional guidance and advice helped me during every stage of this research work. He will always remain a source of inspiration for me throughout my life.

I am equally appreciative of the support I received from the department head, Professor V.K. Minocha, during my doctoral journey. I hold him in high regard and will always be respectful of his

contributions. I extend my sincere thanks to the heads and faculty members of the Department of Civil Engineering at Delhi Technological University, Delhi, for their cooperation and assistance. I am also very much thankful to Ajay Kumar Garg Engineering College for providing me lab facility and their kind support in completing my experimental work.

Special gratitude goes to external examiners and the members of the SRC, Professor S. K. Singh from the Department of Civil Engineering at PEC University of Technology, Chandigarh, and Ex. Professor Dr. Sarvesh Chandra from the Department of Civil Engineering, IIT Kanpur. I am also thankful to Professor K. C. Tiwari Delhi Technological University under whom I have successfully completed my course work and also Professor S. Anbu Kumar and Professor Vijay Gautam from Delhi Technological University for their insightful and constructive feedback.

There are no words sufficient to express my deepest thanks to my beloved husband Mr. Yatan Kumar Bansal and my parents Shri. Daulat Ram Goyal and Smt. Vanita Goyal for all of their sorrow and suffering in bringing me to this stage. Throughout this journey, they are a source

of motivation and encouragement for me. My special thanks to my lovely daughter Miss Inika Bansal and son Master Tanay Bansal for their love, patience, and support during the study. I extend my appreciation to my younger sister Mrs. Swati Goyal and younger brother Mr. Devansh Goyal for their moral and emotional support.

My sincere thanks to my fellow researcher and friends Dr. Parvesh Kumar, Dr. Sandeep Panchal, Mr. Abhishek Paswan, and Mr. Rajat Gautam, Mr. Prateek Roshan, Mr. Indrajeet Singh for their cooperation during my research work. The acknowledgement will be incomplete without thanking my dearest friend Dr. Pankaj Sharma for constantly helping and motivating me in this PhD Journey. Your unwavering support during my PhD journey, particularly on those days when I felt lost and lacked motivation, will forever remain etched in my memory.

I would like to appreciate the efforts of the anonymous reviewers for reviewing our research papers and giving constructive feedback which ultimately improved the quality of our research publications over time. And at last, I would like to express my gratitude to everyone who has helped me achieve this goal, whether directly or indirectly.

Archita Goyal

ABSTRACT

Stabilizing excavations in various soil types involved the implementation of soil nailing, which entailed inserting reinforcement elements, such as nails, into the soil. Conventional soil nailing systems used straight nails, but newer systems utilized helical nails, featuring a twisted shape that offered enhanced stability and load-bearing capacity. Understanding the effectiveness of soil nailing systems required a thorough analysis of their behavior under different conditions.

This study's primary aim was to compare and analyze conventional soil nail (CN) and helical soil nailing (HN) systems. Both finite element analysis (FEA) and limit equilibrium methods (LEM) were employed to study the behavior of these systems. The goal was to optimize the performance of helical soil nailing using Response Surface Methodology (RSM) and a Hybrid Deep Belief Network (DBN)-Coot optimization algorithm. The study included conducting pullout tests and analytical methods to compare the pullout behavior of CN and HN in cohesive soil. Initially, stability comparison was achieved by FEA with PLAXIS-2D and theoretical calculations. CN and HN were assessed for their factor of safety using both FEA and LEM methods. Under comparable soil and loading conditions, the findings demonstrated that HN exhibited reduced deformation and a higher safety factor compared to CN. The study was then extended to optimize soil nailing parameters like inclination angle, surcharge pressure, helical pitch, and shaft diameters for HN. The optimization study used an RSM-based box behnken design (BBD) with 40 experimental runs obtained from RSM-BBD. Additionally, a hybrid DBN-COOT machine learning model was developed and trained to predict the pullout characteristics of HN used in this study. The RSM-BBD was performed using Design Expert software, whereas DBN-CO was developed using MATLAB. While validating both RSM-BBD and DBN-CO models, 3% more optimization accuracy was achieved from DBN-CO than RSM-BBD due to the use of coot optimization in DBN's weight optimization process. Overall, the study offered significant insights into the behavior of soil nailing systems and underscored the potential of utilizing advanced modeling and optimization techniques to enhance their performance.

TABLE OF CONTENTS

LIST OF FIGURES

LIST OF TABLES

LIST OF ABBREVIATIONS AND ACRONYMS

c	Cohesion
Φ	Angle of internal friction
G_s	Specific Gravity of soil
D_{10}	10% of the particles are finer than this size.
D_{30}	30% of the particles are finer than this size
D_{60}	60% of the particles are finer than this size
D_{50}	Average grain size
C_c	Coefficient of curvature
C_u	Coefficient of uniformity
RD	Relative density
Y_d (max)	Maximum dry unit weight
Y_d (min)	Minimum dry unit weight
M_d	Diameter of shaft in model
P_d	Diameter of shaft prototype
K	Scale factor
ds	Minimum shaft diameter
Er	Effective radius of the helix
D_{sc}	Shaft diameter for conventional nail
D_{hh}	Helical diameter for helical nail
E	Modulus of elasticity
F_o	Null force
f	Residual factor
τ_s	Maximum value of shear stress
τ_p	Shear stress residual value
τ	Primary value of shear stress

q	Overburden pressure
EA	Axial stiffness
EI	Bending stiffness
E_{em}	Equivalent modulus of elasticity
E_n	Modulus of elasticity of nail material
E_g	Modulus of elasticity of grout
Ac	Cross-sectional area of helical soil nail
A	Gross area of soil nail
A_{cc}	Cross-section area of grouted soil nail
D_{on}	Overall nail diameter
S_u	Unit spacing
R_{ifs}	Strength reduction factor
$\sum Msf$	Mean of a total multiplier
CN	Conventional soil nail
HN	Helical soil nail
RSM	Response surface methodology
DBN	Deep belief network
ANN	Artificial neural network
COOT	Conformational optimization on target

CHAPTER 1

INTRODUCTION

1.1. General

In densely inhabited places, deep excavation is a typical development practice to make use of underground space (Liu et al. 2016). The construction of underground structures often requires the excavation of soil, which can create instability and potentially hazardous conditions if not properly supported. Excavation support is a term used to describe an engineered solution that aims to provide stability to an excavation (Han et al. 2020). Typically, an excavation support is necessary for excavations that lack a sloped configuration. Supporting deep excavations exceeding 4.5 meters involves additional reinforcement for retaining wall stability. Deep excavation support systems are essential for construction projects with significant depth (Issa et al. 2022). These systems are designed to keep the soil or rocks stable and safe while excavating so that the walls of the excavation don't collapse or fail.

Deep excavation is primarily concerned with securing neighbouring ground structures or properties. Various conventional methods, such as retaining walls and anchors, have been employed during the deep excavation process to preserve the excavation slope or prevent the slope from collapsing. Deep excavations have been extensively utilized for various purposes like tall building foundations, subway systems, shopping malls, and underground parking lots. In megacities, excavations often extend both deeper and wider. The process of excavation unavoidably changes the stress conditions in the soil, leading to potential deformations in walls and movements in the ground that can affect the nearby structures (Byrne et al. 1998).

Designers are primarily concerned with ensuring the stability of deep excavations. Excavation failures are commonly identified by the significant inward movement and support system collapse. As a result, if excavations fail, there would be both economic losses and casualties. Deep excavations can negatively impact nearby building’s structural integrity, especially when the surrounding soil is soft. When deep excavations occur in urban areas, they can lead to stability

issues caused by substantial ground settlement and significant movements along the excavation walls (Farrokhzad et al. 2021).

In urban regions, soil nailing proves to be a highly adaptable technique, offering great efficacy in stabilizing slopes, especially those that are vertical. Using this technique, a reinforced shotcrete wall is constructed on the excavation face, fortified by numerous nails. Over time, numerous individuals have employed this approach to stabilize both natural slopes and earth-retaining structures (Gareh et al. 2015). These nails remain inactive until the soil mass starts moving, providing a passive stabilizing mechanism. Additionally, it serves as a cost-effective and time-saving alternative to conventional retaining systems for slope stability. The incorporation of inclusions in the soil through soil nailing results in reduced deformation compared to slopes lacking such reinforcement, as it enhances shear strength and diminishes horizontal displacement.

The following are the traditional methods of supporting excavations including retaining walls, anchors, and tiebacks. These methods are commonly used in construction to stabilize soil during excavation activities. Retaining walls are vertical or sloping structures built along the edges of an excavation to hold back the surrounding soil. Diverse materials including concrete, steel, and timber, can be employed to construct retaining walls. The primary purpose of these walls is to resist the soil pressure and uphold the excavation's stability (Han et al. 2020). Anchors made mainly of steel, are tensioned structural components installed horizontally into the ground behind the excavation. Their role is to furnish supplementary support and stability to the soil. This is achieved by transferring the load from the soil to the anchor, effectively preventing inward soil movement and preserving the excavation's stability.

Tiebacks are similar to anchors but are installed at an angle (Seo et al. 2019). They consist of steel rods or cables that are inserted into the soil behind the excavation and are then tensioned to provide lateral support. The tiebacks help distribute the forces and prevent the soil from collapsing inward. Throughout various construction sites, traditional methods have gained widespread acceptance for supporting excavations, effectively ensuring stability and safety. In contrast, soil nailing presents an alternative approach to support excavations. While retaining walls, anchors, and tiebacks are

indeed traditional methods of supporting excavations, soil nailing is considered a modern and innovative technique that offers certain advantages over these traditional methods (Raju 1996).

Here's why soil nailing is often considered better:

i. Cost-effectiveness-When compared to traditional methods, soil nailing typically offers greater cost-effectiveness. It requires less material and construction time compared to retaining walls, anchors, or tiebacks.
ii. Versatility- The technique of soil nailing showcases its versatility in addressing various soil types and excavation conditions. Cohesive soils, including clay, and granular soils, like sand or gravel, both find practical applications for this method.
iii. Minimal disruption- Soil nailing causes minimal disruption to the surrounding environment and nearby structures. The installation process is relatively quiet and vibration-free, making it suitable for urban areas.
iv. Enhances stability- Soil nailing provides additional tensile strength to the soil, improving its stability and preventing excavation failure.
v. Increased constructability-Soil nailing is a relatively simple and efficient construction technique.

Here are further details on soil nailing and its history, the components of soil nailing, factors related to soil nailing, the process involved, details of conventional soil nails, their advantages and disadvantages, and the development of helical soil nails.

1.2. Soil Nailing

The application of soil nailing involves stabilizing unstable slopes to prevent collapse or sliding, making it a valuable technique for slope stabilization (Goyal and Shrivastava 2021). The method involves the installation of steel or fiberglass nails (or rods) into the slope, which are then grouted with a cementitious material to provide additional support. Employing soil nailing prevents the collapse or sliding of unstable slopes, serving as a technique to stabilize them (Figure 1.1).

Figure 1.1. Soil nailing (Raju 1996)

The procedure entails making holes in the slope at designated angles and intervals, then inserting steel or fiberglass nails that are grouted with a cementitious material. This creates a reinforced zone that increases the slope's strength, with the nails installed in a pattern that maximizes their effectiveness. Finally, a facing material like shotcrete or concrete is applied to the slope to protect it from erosion and weathering. In diverse slope stabilization applications, such as retaining walls, embankments, and cut slopes, soil nailing emerges as a flexible and adaptable technique (Dhakal and Acharya 2019). It is particularly useful in situations where traditional retaining walls or other slope stabilization techniques are impractical or costly. Soil nailing is an effective and reliable method that is often used in combination with other techniques to provide a comprehensive and long-lasting solution for slope stabilization.

The positioning procedure of the soil nail on the ground surface is done through drilling and its strengthening is done through grouting together which increases the soil’s shear strength or cuts. To ensure both external and internal wall stability soil nails are installed in a pattern design. Generally, steel bars are used as a nail in construction, which resists shear and tensile stresses and bending moment. The soil nails are constructed with consistent cross-sectional dimensions and length. The soil nail length typically ranges from 60% to 80% of the wall height, adjusted

according to the specific soil conditions (Byrne et al. 1998). Soil nails are tested to find out the soil nail adhesion and its resistance to pullout failure.

The soil nail wall design considers various parameters, including soil properties, wall geometry, external loads, and groundwater conditions. The specific characteristics of the soil play a crucial role in determining the design of a soil nail wall. Various aspects, including cohesion, shear strength, and internal friction angle, all contribute to determining the ideal length, diameter, and spacing of the soil nails. Moreover, the geometric characteristics of the wall, such as its height, slope inclination, and overall configuration, also play a significant role in the selection of appropriate design elements for the project. A thorough understanding of these factors is crucial for a successful and reliable soil nail wall design. External loads that the soil nail wall is expected to bear are another important consideration. Surcharge loads or seismic forces that will act on the wall are taken into account during the design process (Chavan et al. 2017). Groundwater conditions are also a significant factor. The presence of groundwater can impact the stability of the wall, and therefore, drainage measures and grouting techniques are considered in the design to ensure appropriate performance and durability.

1.2.1 History of soil nail development

Soil nailing was initially created by Henri Vidal, a French engineer, in the 1970s, marking its origin in history (Alhabshi 2006). During its initial stages of development in the 1970s, soil nailing primarily targeted slope stabilization. The process involved drilling holes into the soil and inserting U-shaped steel bars, which were then secured with grout to reinforce the tension. Advancements in the late 1970s enabled the technique to be applied to the construction of retaining walls, demonstrating its efficacy in minimizing lateral loads on the walls. During the 1980s, soil nailing gained extensive popularity in the United States, and it became a popular method for slope stabilization and retaining wall construction (Jewell 1980). The technique was extensively utilized during this time. In 1985, the Federal Highway Administration released the first-ever comprehensive design manual for soil nailing, which played a vital role in standardizing the technique and promoting its increased usage (Elias and Juran 1991).

In the subsequent years, soil nailing techniques underwent continuous improvement due to the progress in drilling technology and construction materials. Advanced grouting materials and high-strength steel bars were introduced, increasing the durability and strength of soil nails (Bhuiyan et al. 2022). Additionally, the development of self-drilling soil nails streamlined the installation process. Currently, soil nailing has become a prevalent and extensively used technique in geotechnical engineering, and it has proven its efficacy in various projects such as highway and railway construction, building foundations, and slope stabilization. Continuous research and development in this field aim to refine the technique and enhance its effectiveness, particularly in challenging soil conditions.

1.2.2 Components of soil nailing

The components of a soil nailing system work together to provide a stable and durable reinforcement solution for excavations, soil slopes, as well as retaining walls. The following components of a typical soil nail wall shown in Figure 1.2 are a head stud, nail head, bearing plate, reinforcement, facing, grout, centralizer, end cap, welded wire mesh, drainage, coupler, tendon, corrugated plastic sheathing, and waler bars. The details of the above-mentioned components are as follows.

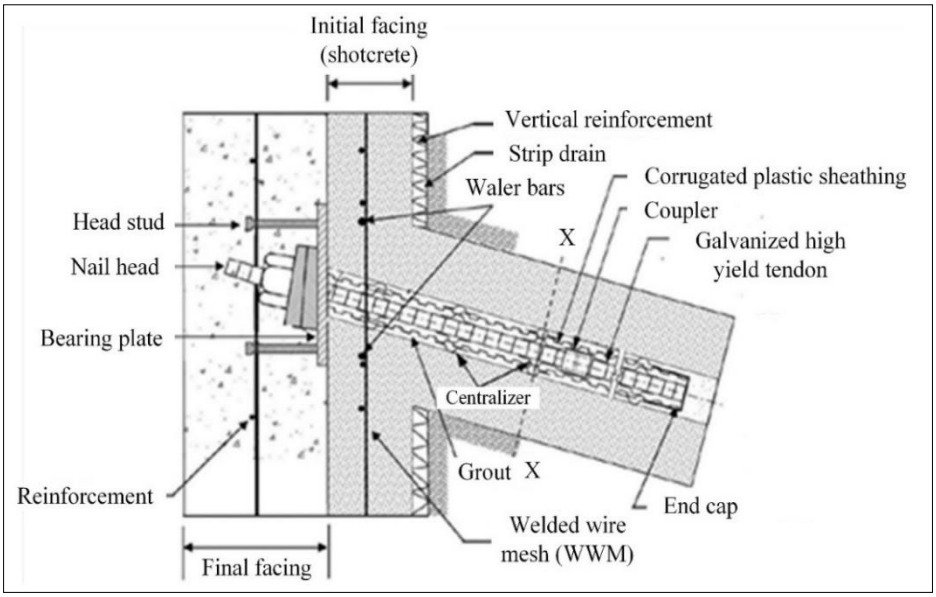

a

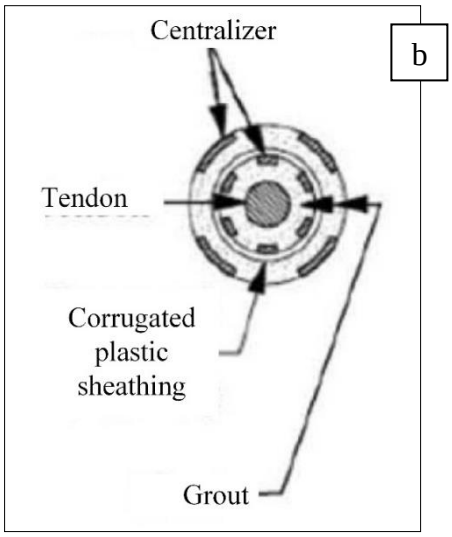

Figure 1.2. (a) Soil nail wall cross-section (b) Soil nail Cross Section at X-X (Goyal and Shrivastava 2020)

1.2.2.1. Head stud

Head studs are normally steel bars that are fixed into the soil and sprout out of the soil face and are used in soil nail walls (Gassler and Gudehus 1981). The head studs act as points of attachment for the face system, which might be either a shotcrete layer or a concrete panel. To install the head studs, a hole must first be drilled into the ground, then the steel bar must be inserted into the hole. Geotechnical or structural engineers typically design the spacing and orientation of the head studs based on their expertise in soil nail walls, as these factors affect the wall's stability and performance (Gareh 2015).

1.2.2.2. Nail head

The top of the soil nail, usually a flat or slightly curved plate, is essential for transferring the force from the soil nail to the surface structure like an excavation support system or retaining wall (Kotake and Sato 2021). It remains exposed and visible above the ground in the soil nail system. To prevent deformation or failure under applied loads and ensure a long service life, the nail head in a soil nail system is usually made of steel with sufficient strength and stiffness and is coated with a protective layer against corrosion. Within a soil nail system, the head of the nail acts as a point of anchorage for the installation equipment and facilitates load transfer (Dey 2015). Allowing

the contractor to apply the necessary tension and torque during installation, ensures that the soil nail achieves the desired bond strength with the surrounding soil.

1.2.2.3. Bearing plate

In the soil nail system, a bearing plate serves as a vital component responsible for effectively transmitting the tensile and shear forces, which is achieved by applying a steel plate against the excavated soil face (Joshi 2003). The bearing plate is engineered with ample thickness and strength to safeguard against any deformations or failures that may occur due to external forces. The bearing plate in the soil nail system plays a vital role in ensuring a strong bond with the surrounding soil and effectively distributing the load.

1.2.2.4. Reinforcement

Reinforcement in a soil nail system refers to steel bars or rods that are inserted into the soil to offer extra support and strength to the soil mass (Patra and Basudhar 2005). By enhancing the stability and load-bearing capacity of the soil mass, reinforcement is particularly beneficial in soils susceptible to instability, erosion, or low shear strength in a soil nail system. By combining grout and mechanical anchors like soil nails or rock bolts, the reinforcement becomes anchored in the soil. This creates a composite structure that merges the strength and stiffness of the steel reinforcement with the resistance and resilience of the soil mass (Juran and Elias 1991).

1.2.2.5. Facing

The integrity of the soil-nail system relies on achieving local stability between the soil and the soil nail through a facing process (Babu and Singh 2009). This process not only offers resistance against outward deformation but also protects the soil-nailing system from surface erosion, weathering effects, and moisture loss. Additionally, the facing contributes to improving the overall aesthetic appearance of the nailed structure (Azzam and Sobhey 2019). Depending on the slope's inclination, facings of varying thicknesses (ranging from 150 mm to 200 mm) are used, with thinner facings for inclined formations and thicker facings for vertical permanent cuts (Ayazi and Tangri 2022). The soil-nail facing comprises two main components. The initial part involves meshed wires that are welded together and fixed along the entire excavation face using appropriate

lap splices. Waler bars and vertical bars are placed around the nail head to ensure horizontal and vertical bending stresses. The initial facing is completed by shotcreting the reinforcements positioned around the nail heads. There are two types of shotcreting methods used: the wet mix method, where aggregate, cement, and water are mixed in a batch plant and conveyed to the nozzle, and the dry mix method, where water is added at the nozzle end of the shotcrete gun, fed with a blend of dry aggregates and cement (Dey 2015).

To achieve low permeability, significant durability, and high strength, it is recommended to maintain a water-cement ratio of less than 0.45. Among the shotcrete methods, the wet type is preferred due to its higher production rate (ranging from 1.68 m^3/hour to 3 m^3/hour) and better bonding properties, resulting in less loss due to rebound. The final facing components are comprised of cast-in-place (CIP) reinforced concrete panels. A recent advancement in facing involves the use of steel fiber reinforced shotcrete (SFRS) instead of mesh reinforcement. The SFRS utilizes steel elements with hooked ends, which are mixed as aggregates in the concrete mix and employed during the facing process (Ortigao et al., 1995). The completed final facing typically has a thickness ranging from 150 to 300 mm, excluding the initial facing thickness. This thickness is achieved by applying successive layers of shotcrete in a bottom-up manner. During the final facing with reinforced shotcrete, the use of waler bars is eliminated.

1.2.2.6. Grout

The grouting is done to install and reinforce the tendons inside the drilled hole. After placing the tendons through the centralizers which ensure the center alignment of the bar (Tan and Chow 2004), the process of grouting is carried out under gravity using the tremie method. The effective gap between the tendon and the soil is provided by the centralizers so that the grout is penetrated effectively around the tendon. The typical grout mixture contains a combination of Portland cement and water. Grouting is a commonly employed procedure to strengthen the bond between the soil and tendon (nail), while also providing increased corrosion protection. This process fosters a robust interaction between the soil and the nail, ensuring the effective transfer of shear stress between the tendons and the deforming ground. Furthermore, tensile stresses from the tendons can also be transferred from tendons to surrounding stable soil through the grout. The recent

advancements in the tendons led to the eliminate the usage of grouting and drilling (Bhuiyan et al. 2022). The latest tendons used contain equal-spaced helical plates which are attached around the tendons in the form of screws that can be applied through torque.

1.2.2.7. Centralizer

In the context of reinforcing and stabilizing soil or rock slopes, the centralizer plays a critical role in the soil nail system. This vital component ensures that the soil nails are installed in a closely spaced pattern, preventing any deviations from the intended alignment or improper installation angles. Without centralizers, the performance and effectiveness of the entire system may be compromised. Centralizers come in different forms, but they typically consist of a sleeve or collar that is attached to the soil nail to prevent it from rotating or shifting during installation. This ensures that the nail is installed vertically or at the desired angle, which is crucial for achieving the required soil reinforcement and stability. Centralizers used in soil nailing systems can be designed and constructed with different materials to suit the particular application and soil conditions. Furthermore, the spacing of these centralizers can be customized according to factors such as the soil nail's size and length, and the soil's properties that require reinforcement (Goyal and Shrivastava 2022).

1.2.2.8. End cap

In soil nail systems, an end cap is a crucial element responsible for anchoring the soil nail securely into the ground (Benmebarek et al. 2022). Constructed from steel, its primary purpose is to prevent the soil nail from being extracted by external forces. During installation, a hole is drilled into the ground, and the soil nail is inserted before the end cap is positioned at its termination point. Grouting further enhances reinforcement and stability by firmly securing the end cap in place (Kim et al. 2013). Depending on various factors like soil characteristics applied loads, and project specifications, different types of end caps, such as flat plates, mushroom caps, and bulb caps, can be employed.

1.2.2.9. Welded wire mesh

In slope and retaining wall applications, the use of welded wire mesh is prevalent to reinforce the soil (Kotake and Sato 2021). This specific mesh type is constructed by welding wires together at their intersections, forming a grid pattern. Soil nails, which are lengthy steel bars, are drilled and grouted into the soil to offer support and stability to the slopes and retaining walls. Positioned between the soil nail heads and the shotcrete or concrete facing, the welded wire mesh serves multiple purposes. It evenly distributes the load from the soil nails across the facing, provides additional support to the facing, and prevents cracking and spalling of the facing material. Thus, the integration of welded wire mesh plays an essential role in ensuring the stability and long-lasting performance of soil nail systems used in these applications (Lazarte et al. 2015).

1.2.2.10. Drainage

The drainage system is necessary to provide satisfying serviceability to the soil-nailing system. The implementation of a drainage system can be done either behind the primary face or in proximity to the excavation face. When considering the soil nailing system, the presence of underwater pressure can lead to the generation of pore water pressure. This can be regulated by providing proper drainage in the soil nailing system. Furthermore, the excessive hydrostatic pressure generated is minimized which in turn protects the deterioration of facing and increases the sustainability of the soil nail bonding. The presence of a drainage system demonstrates its effectiveness in preserving the structural performance and stability of the soil-nail system both during and after the excavation process. The wall saturation can be eliminated with less water accumulation by using a deep shallow drainage structure (Bruce and Jewell 1986). In some cases, the drainage for the soil nailing system is provided above and below of soil-nail (Raju 1996). The advanced drainage system mostly consists of strip drains in vertical positions. The strip drains are made up of synthetic polymer in the form of drain cores. These cores are wrapped around using a geotextile to accompany filtration. If groundwater behind the soil nail structure is abundant, pipe drains in a horizontal position are utilized.

1.2.2.11. Coupler

Within the soil nail system, a coupler plays a crucial role in linking two or more soil nails together, effectively increasing their length and enhancing soil reinforcement (Liu et al. 2016). The process

involves drilling holes in the ground and inserting threaded steel bars or rods, which are subsequently grouted into the soil to form a secure bond with the surrounding earth. Couplers are utilized to increase the length of soil nails by connecting them end-to-end. Typically, couplers are cylindrical sleeves composed of high-strength materials such as steel, with internal threads that match those on the soil nails. To join two soil nails together, a coupler is screwed onto the end of one nail, followed by the other nail at the other end of the coupler. This process can be repeated as necessary to create longer soil nails. Employing couplers grants enhanced adaptability in the design and construction of soil nail systems, enabling them to adjust to varying ground conditions with greater flexibility (Mickovski et al. 2016).

1.2.2.12. Tendon

Generally, steel bars are used as tendons but other elements with better resistance towards tensile stress can also be utilized. An ideal tendon should have higher resistance towards shear, bending, and tensile stresses respectively. As per the conditions of the soil in the particular area, hollow or solid steel bars can be used. When the working area allows for drilling and grouting, solid bars are utilized. However, in less stable conditions where the drilling capacity is limited, hollow bars are employed. In both cases, the drilling and grouting process is conducted simultaneously. The latest advancement in the soil nailing field gives rise to the utilization of innovative fiber-reinforced plastics (FRP) as tendons. These FRP materials are produced by mixing different types of resins with glass fibers (Ortigao et al. 1997). Tendons have also been made up of renewable resources like Moso bamboo, which has high tensile strength for short periods but is cost-effective (Dai et al. 2016).

1.2.2.13. Corrosion protection

According to the corroding ability of the surrounding soil, the tendons are exposed to corrosion. So, protection against corrosion should be provided to the tendons as per the requirements, which increases their working life. Even though a certain level of protection is provided by the grouting, it is not enough for higher concentrated soils. So, for permanent applications corrosion resistance is significant. Encapsulating the tendon in a corrugated outer sheath of PVC with an inner cement annulus provides long-term protection against corrosion (Gassler 1995; Warner and Barley 1997).

More methods like the epoxy coating, cathodic protection method, sacrificial steel method, and galvanization, are also available for protecting the tendons against corrosion.

1.2.2.14. Waler bars

Waler bars play a vital role in strengthening soil nail systems and providing stability to excavation faces and retaining walls. These bars, typically made of steel, are positioned horizontally and perpendicular to the vertical soil nails, which are inserted into the soil through drilling or grouting. Placed at regular intervals along the length of the soil nail wall, the waler bars are connected to the heads of the soil nails. Their primary function is to evenly distribute the load from the soil and any retained material across the wall, preventing localized failure or deformation (Milligan and Tei 1998). Integrating waler bars into the soil nail system enhances its overall performance by increasing resistance to lateral forces and imparting greater stiffness and rigidity to the wall. They are commonly used in combination with other geotechnical techniques, such as reinforced concrete facing or shotcrete, to create a durable and reliable retaining structure.

1.2.3. Soil nail installation process

The soil nail installation should be done by following some important procedures as discussed in Figure 1.3. The installation steps for the soil nailing process are explained below:

- Step 1- Excavation of an un-stabilized slope to produce a self-standing platform for the drilling equipment.
- Step 2- The drilling process is done by inserting the nail in the slope at a particular angle of inclination.
- Step 3- The first nail is inserted with the help of a centralizer and filled with grout in between the gap of soil and nail.
- Step 4- Initial facing is also done with the installation of a head plate and drainage setup. Optional meshing can also be provided before the initial facing to obtain more stability. Most of the facing is done through shotcrete construction.

- Step 5- Excavation is conducted again to install the next soil nail below the current soil nail level. The drainage system should be extended to the toe of the slope during each nail installation.
- Step 6- Repeat the above steps until you reach the required stability, by placing the soil nails in an equally distributed manner of spacing and the final facing is done by a repeated layer of shotcrete construction.

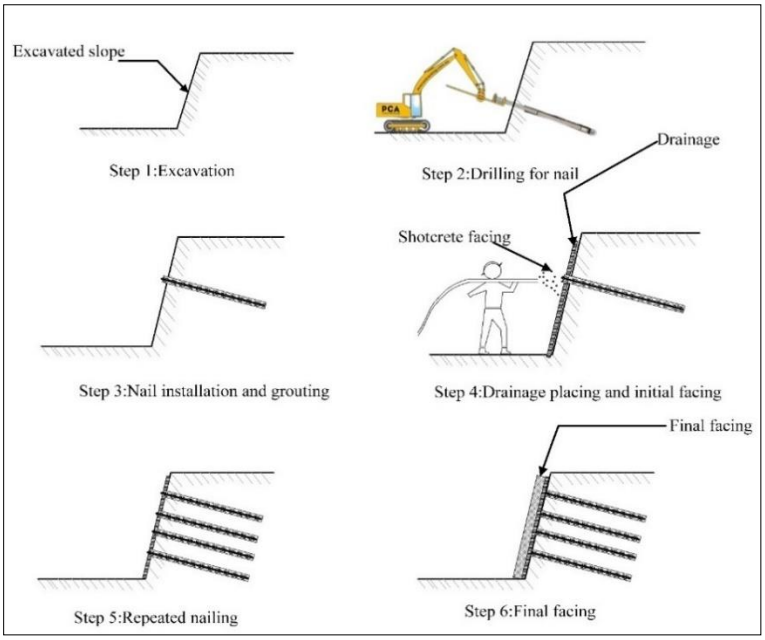

Figure 1.3. Soil nailing installation process (Byrne et al. 1998)

1.2.4. Factors affecting the performance of soil nails

The performance of soil nails can be affected by various factors (Dey 2015), including:

- Soil type
- Nail length and diameter
- Installation method
- Corrosion resistance
- Slope angle
- Soil nail spacing

- Groundwater conditions

1.2.4.1. Soil type

The performance of soil nails is significantly impacted by the type of soil in which they are installed. Soil with high plasticity or moisture content can result in lower nail performance due to lower soil nail bond strength.

1.2.4.2. Nail length and diameter

The soil nail's diameter and length used in a project are also significant factors that can affect their performance. Longer and thicker nails can provide higher resistance against pullout and bending.

1.2.4.3. Installation method

The method used to install soil nails can also affect their performance. If soil nails are not installed at the correct angle or depth, it can result in lower bond strength between the soil and the nail.

1.2.4.4. Corrosion resistance

Corrosion resistance is also a significant factor in the performance of soil nails since they are usually made of steel, which can corrode over time.

1.2.4.5. Slope angle

The angle of the slope where the soil nails are installed can also affect their performance. Soil nails installed on steep slopes may require thicker and longer nails to provide adequate reinforcement.

1.2.4.6. Soil nail spacing

Additionally, the spacing between soil nails can affect their performance. Too much spacing may not provide enough reinforcement, while too little spacing may result in nail interference, which can affect their performance.

1.2.4.7. Groundwater conditions

Finally, groundwater conditions can also affect the performance of soil nails. High groundwater levels can weaken the soil nail bond strength and cause corrosion. It's crucial to consider all of

these factors during the design and installation of soil nail systems to ensure their optimal performance.

1.3. Conventional Soil Nail

Traditional soil nailing encompasses the utilization of reinforcing components called soil nails, which are inserted into the soil to improve its stability and load-bearing capabilities (Goyal and Shrivastava 2020). These soil nails are commonly crafted from steel bars or tubes, having diameters spanning from 20 to 50mm. Their installation angle usually ranges from 10 to 20 degrees relative to the horizontal plane, and their lengths can vary from a few meters to several tens of meters. The subsequent section outlines the different types of conventional soil nailing methods.

- Grouted soil nailing
- Self–drilling soil nailing
- Jet-grouted soil nailing
- Driven nailing
- Launched nailing
- Corrosion-protected nailing

1.3.1. Grouted soil nailing

This nailing system uses smooth threaded surface solid bars which are inserted into the 100 mm to 150 mm diameter range of pre-drilled holes where low-pressure grouting or grouting under gravity is carried out previously (Kim et al. 2013). The drilling methods are varied as per the ground conditions available which are named down-the-hole hammer, rotary drilling, and rotary percussive drilling techniques. The tendon diameter typically ranges between 15 mm to 46 mm. The space between the drill hole and the placed tendon is selected according to the grout coverage needed for the system, which will be in the range of 30 to 80 mm, surrounding the soil nail. To ensure uniform grout coverage, centralizers are placed at intervals of 1.5 to 2.0 m along the nail. Since, the surface area of the soil nail increases due to the grouting process, which also provides improved roughness. Thus, soil-nail interaction is consequently increased, and the grouted soil nail archives better bonding strength which simultaneously improves the pullout resistance (Palmeria

and Milligan 2015). The grouting layer also provides better protection to the soil nail against corrosion. The soil nails are equally placed at a 1 m to 3 m spacing range in both vertical and horizontal directions. This range is selected according to the soil type in the slope area.

1.3.2. Self-drilling soil nailing

In this process, the drilling and grouting techniques take place simultaneously to install the hollow bars. The bar acts as both a drill tool and a grouting pipe as shown in Figure 1.4. The drill bit is sacrificed for each nailing process because all the process takes place simultaneously and the drill bit is under the hole. The whole process is completed faster than the other nailing process. Other process uses air and water as a flushing medium but here cement grout flushes the impurities. The drill hole stability is assured due to the simultaneous drilling and grouting process (Mickovski et al. 2016). The bond strength between soil and tendon is increased with the permeation of grout into the surrounding soil, which in turn increases the pullout capacity of the soil nail. The annular space between the tendon and the drilled hole is also grouted because the grout comes out of the drill bit. The usage of centralizers and casing is eliminated in the self-drilling soil nails. The time and cost of this soil nail installation are less when compared to other soil nail systems.

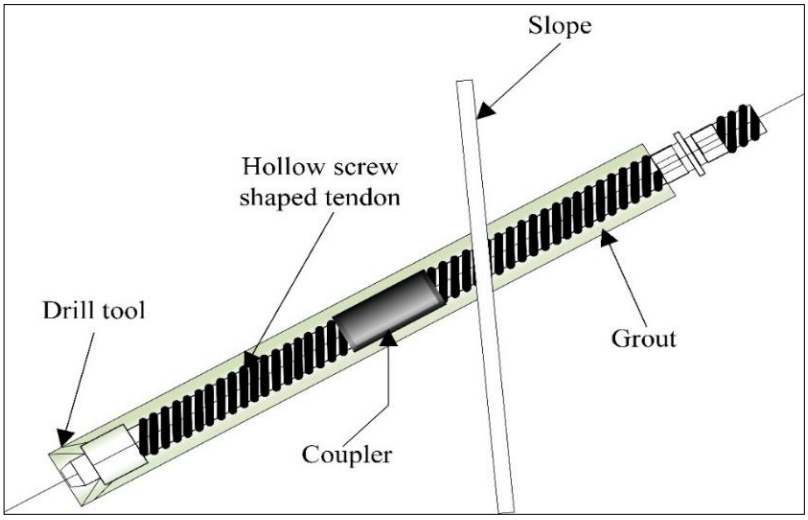

Figure 1.4. Self-drilling soil nail (Mickovski et al. 2016)

1.3.3. Jet-grouted soil nailing

Based on the technique of installation and pressure applied for grouting, Jet-grouted soil nailing differ from other nailing technique. By using high frequency hammer the nails are installed and cement grouting is performed. Steel tube in jet grouted nails used to protect against corrosion. A percussion driving grouting jet with 20MPa high pressure is employed in the grouting and drilling process. Re-compaction and hydraulic fracturing of the surrounding soil are caused by the high grouting pressure. Also, the pullout resistance of soil nails is increased consequently due to the enhanced soil nail interaction. The central steel rod included inside the soil grout composite should have an overall thickness range of 30 to 40 cm. In this nailing system, pre-drilling and high-pressure grouting are simultaneously carried out, which is similar to self-drilling nails.

1.3.4. Driven nailing

The driven nailing system consists of 20 mm to 50 mm range of nominal diameter steel rods or angle rods with a yield strength of 350MPa. While used as driven nails, the tendon's maximum driven length is limited to 20 m with a contact area pressure range of 2 to 4 bars per m^2. The rod used for driven nailing should have a higher ductility rather than brittle property so that the brittle failure of the soil nail is avoided. The percussion method using a hammering device is used in driving the soil nail. In some cases, the vibratory method using a vibrator mechanism is used to drive the nail. Since this method uses force to drive the nail into the soil, a pre-drilling process is not required for this system. This reduces the installation time drastically and this is viable in retaining collapsible soils.

1.3.5. Launched nailing

In launched soil nailing, the tendons of soil nails are forced into the soil by a ballistic method of utilizing a compressed air launcher. Speed and energy transfer at nail installation are 200 mph and 100 KJ respectively. The ground around the nail is displaced and compressed during penetration. The major advantage of using launched nails is rapid installation, as 4 to 6 nails can be installed per hour. Since these nails are launched rapidly, the surrounding soil has fewer disturbances. But, these types of soil nails are difficult to install in boulders. Also, soil nail interaction is less due to the driving action. Figure 1.5 shows the equipment used in the launched nailing process.

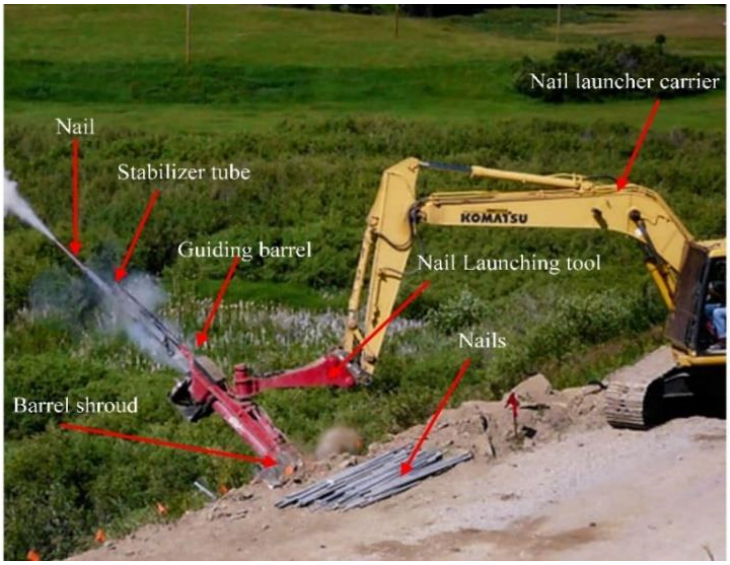

Figure 1.5. Launched nailing system (Goyal and Shrivastava 2021)

1.3.6. Corrosion-protected nailing

The grout cover around the tendons achieved partial corrosion resistance along the soil nail's total length. So, a protective layer of corrosion-resistance material is used to cover the nails, which are said to be corrosion-protected soil nails. These soil nails are suitable for the permanent application of soil nailing. For aggressive environments, where the soil corrosion concentration is high, full encapsulation of the nail is recommended.

1.4. Advantages and Limitations of Conventional Soil Nail

Soil nailing offers several advantages compared to other stabilization methods, which are listed below:

- Faster Installation: Soil nails can be installed quickly using smaller equipment, even in remote areas. Their simple installation procedure and minimal construction materials result in less environmental impact.
- Cost Efficiency: Since soil nails are shorter than anchors, soldier beams are not needed, reducing costs by up to 10 to 20% compared to anchors (Burns 2006).
- Fewer Field Adjustments: Soil nails require only a few adjustments when encountering obstacles like cobbles, boulders, piles, or underground utilities during construction.

- Unobstructed Working Environment: Unlike braced excavations, soil nails do not create congested bottoms, providing an obstruction-free working environment.
- Flexibility and Settlement Accommodation: Soil nail walls are flexible and can handle significant total and differential settlements. The maximum horizontal displacement at the end of construction is limited to 0.3% of the excavation depth (Han et al. 2020). In seismic regions, their low stiffness improves wall performance (Gassler and Gudehus 1981).

Soil nailing has some limitations that need consideration:

- It cannot be used on slopes with certain soil types that cannot handle a 1.2 to 1.8-meter excavation without support for 2 to 3 days. The soil should have specific cohesion properties for successful soil nailing.
- Soil nailing requires a certain amount of soil deformation to work effectively, which makes it unsuitable for structures sensitive to deformation control. Post-tensioning can help but at a higher cost.
- Higher water tables are not ideal for soil nailing due to difficulties in excavation and drilling, increased corrosion risks, and potential seepage issues affecting grout quality.
- Dry and less cohesive soil can lead to drill hole collapses. While simultaneous drilling and grouting can address this, corrosive dry soil may reduce the system's durability and pullout capacity (Juran and Elias1991).

1.5. Development of Helical Soil Nail

In congested areas, soil nailing has become important due to its efficient placement and fast execution. Recent developments in soil nailing aim to simplify the installation process by reducing soil damage and minimizing disturbances to the surroundings. One such advancement is the helical soil nailing (HN) technique, which involves attaching helices to the nail shaft. This approach allows for easier installation with minimal soil disruption and provides greater tensile strength and efficiency compared to traditional soil nails.

Researchers have studied conventional soil nails through experiments and theories, but to overcome their limitations, helical soil nails are now used in soil nailing applications (Rawat and

Gupta 2016, Seo et al. 2019). Design parameters for helical soil nails differ from conventional ones, and there is still a limited understanding of these parameters. Recent research on helical soil nailing includes exploring the effects of helix size, number of helices, and spacing between them on pullout capacity under varying surcharge pressure. Additionally, a numerical model has been developed to optimize the nail's inclination angle, and the shaft diameter is also an important factor for installation and pullout. The performance of helical soil nails can be further enhanced by adjusting the number of helices and their pitch.

The following are types of helical soil nails; solid shaft helical soil nails and hollow bar helical soil nails. Solid shaft helical soil nails are helical soil nails that consist of a solid steel shaft with a helix at the end. The helix is usually made of one or more plates that are welded to the shaft. These nails are typically used in cohesive soils, where the helix can create a bond with the soil. Hollow bar helical soil nails are helical soil nails that consist of a hollow steel bar with one or more helices. The bar is drilled into the soil, and grout is injected through the center of the bar to fill the annular space between the bar and the soil. These nails are typically used in non-cohesive soils, where the grout can provide additional support to the soil (Rawat 2017).

1.5.1. Advantages of helical soil nails

- Special equipments are not required- Installation of helical soil nails done by simple drill motor.
- Instant reinforcement and quick installation- Within a short time helical soil nails can be drilled into the ground. After installation, the soil reinforcement is available immediately.
- Compared to conventional soil nails, soil nailing using helical nails is more economical. Since it does not require a stable soil condition that can withstand unsupported cutting for 1 to 2 days as the helical nails can penetrate the soil at a rate compatible with the helices' pitch.
- Building-pore water pressures are eliminated by helical soil nails, therefore useful for construction in soil conditions below the groundwater table.
- Helical soil nails are applicable for rehabilitating damaged retaining structures.

- Since helical soil nailing does not need drilling, better soil-nail interaction is achieved. Thus, improving the pullout capability.
- It is applicable for various conditions of soils like sand and gravel.
- The requirement of grouting during the installation of soil nails is eliminated.
- The pore water pressure buildup in slopes and earth-retaining structures are effectively reduced while using helical soil nail.
- The failure behavior of helical soil nails is better than that of conventional soil nails.
- For the rehabilitation of distressed retaining structures, helical soil nails are highly suitable.
- The versatility of helical soil nails allows for their application in a wide range of soil slope conditions. These conditions encompass various soil types, including naturally cemented or dense sand, gravel, weathered rock lacking unfavorable oriented joints or low shear strength, sand with apparent cohesion due to capillary effects, and stiff cohesive soils like clayey or sandy silts. Additionally, helical soil nails can be effectively used in low-plasticity clays that do not exhibit susceptibility to creep.

1.5.2. Application of helical soil nail

The following are some of the applications of helical soil nails:

- Excavation support- Excavation work can also be supported by helical soil nails, which are installed at an angle into the soil to provide temporary stability and prevent soil collapse.
- Retaining walls- Retaining walls can also benefit from the support and stability provided by helical soil nails, which are inserted into the soil behind the wall and anchored to prevent collapse.
- Foundation repair- Helical soil nails can also repair and strengthen existing foundations by being inserted into the ground around the foundation and securely anchored for support.
- Slope stabilization- Helical soil nails are a useful technique for slope stabilization, preventing collapse by being installed at an angle and anchored firmly into the soil.

1.5.3. Behaviors of helical soil nail in various soil types and conditions

The behavior of helical soil nails depends on several factors such as soil strength, stiffness, soil type, loading conditions, and slope geometry. Helical soil nails are capable of creating a bond with cohesive soils which results in a pullout resistance proportional to the helix's surface area. This bond reduces the slope instability and provides additional lateral support to the soil. In non-cohesive soils, helical soil nails mainly rely on grout and lateral earth pressure to provide support. The lateral earth pressure on the helix plays a critical role in the behavior of soil nails in non-cohesive soils. It induces bending moments on the soil, reducing its pullout resistance and increasing the risk of nail failure.

The slope geometry including slope height, slope angle, and slope curvature can affect the behavior of helical soil nails by influencing soil stresses and nail forces. Slope curvature also affects the behavior of helical soil nails by inducing bending moments and shear forces on the nails, making curved slopes require special attention during the nail design process to ensure adequate resistance to soil movement. The behavior of helical soil nails is affected by loading conditions on a slope or wall. Lateral loads like wind or seismic loads can cause significant bending moments and shear forces on the nails, affecting their pullout and bending resistances. Vertical loads such as the weight of the structure or soil above the nail can impact nail capacity and soil stress distribution, as well as cause soil settlement or heave that affects the nail bond and grout properties.

1.6. Parameters to be Considered in the Helical Soil Nailing Process

The following parameters are considered in the soil nailing process;

- Surcharge pressure
- Shaft diameter
- Helix pitches
- Inclination angle
- Pullout capacity
- Deformation behavior
- Installation torque
- Factor of safety

1.6.1. Shaft diameter

The shaft used in the soil nails is meant by tendons. These tendons are installed in holes drilled into the soil or weak rock materials and then grouted in place. They can be hollow or solid steel rods with mostly threaded outer surfaces. The diameter of the shaft mostly ranges between 25 to 35 mm.

1.6.2. Helix pitches

A helical plate in soil nails refers to a circular steel plate that is shaped into a spiral and joined to a central steel shaft. Its purpose is to assist in the installation of soil nails by generating thrust along the longitudinal axis of the nail as it is rotated into the ground. The plate's role is to transfer the axial load to the soil through bearing. The helix pitch is the distance measured along the shaft's axis between the leading and trailing edges of the helical plate. Figure 1.6 illustrates the dimensional parameters of the helical soil nail.

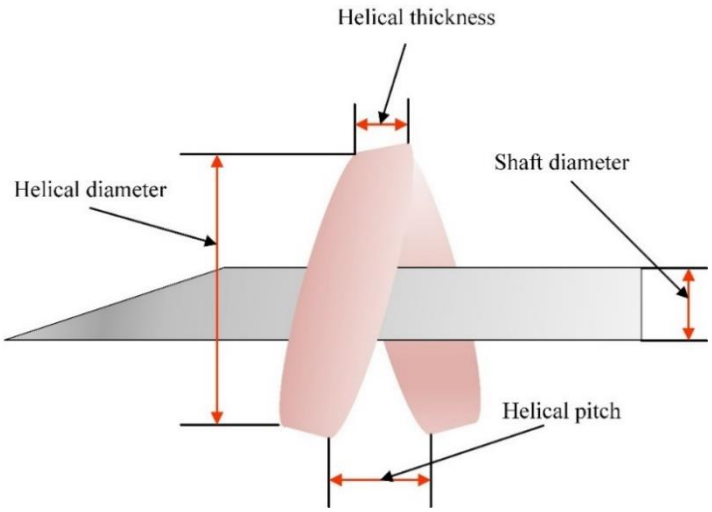

Figure 1.6. Parameters in helical soil nail (Sharma 2021)

1.6.3. Surcharge pressure

The excess load applied on the slope surface which develops a long-term accelerated consolidation is known as surcharge pressure. It is the result of objects on the surface that add loading to the protective system, which means the loads of spoil embankments, streets or highways, and

construction machinery act on the surface of soil near the excavation area. The main reason to use surcharge pressure is to relieve protective systems and support systems.

1.6.4. Pull-out resistance

The resistance exerted by the soil nails which are nailed into the ground towards the force applied to pull out the nail is known as pull-out resistance. It represents the amount of stress mobilized per unit area at the interface between the nail and soil. When designing the soil nails, pullout resistance is a key parameter to be considered to obtain efficient performance from the soil nail.

1.6.5. Inclination angle

The inclination angle is one of the significant parameters in the soil nailing system. It is the angle at which the tendon of the nail is concerning the horizontal plane. It affects the stabilization reinforcement efficiency and the pullout behavior of the soil nail. As the steep angle of the slope increases the inclination angle concerning the horizontal plane is decreased to obtain a better factor of safety (Alsubal et al. 2017).

1.6.6. Deformation behavior

The change in size or shape of the material, when external force is applied is known as the deformation behavior of the material. The deformation of the soil nail depends on the stress and strain acting on it, due to the movement in the slopes. Generally, the soil nail walls may deform during and after construction in both horizontal and vertical directions. The magnitude of both displacements is the same at the top of the slope and the displacement is high at the top of the slope.

1.6.7. Factor of safety

The ratio between ultimate soil nail strength or nominal resistance and the nominal or service load used while designing the soil nail component is known as the factor of safety in soil nails. It can also be termed as the maximum allowable stress in the design. In the pullout analysis of the soil nail, the ratio of the pullout capacity of the nail to the maximum axial force developed in the nail provides its safety factor.

1.7. Methods used in Soil Nail Analysis

There are several methods used in soil nail analysis, including;

- Analytical methods
- Empirical methods
- Field testing
- Limit equilibrium method (LEM)
- Finite element method (FEM)

1.7.1. Analytical methods

The use of analytical methods is a common practice in assessing the stability of soil slopes and retaining walls supported by soil nails. These methods involve applying mathematical equations and formulas, which are particularly useful for analyzing simple structures that satisfy the assumptions made during the analysis (Yin et al. 2021).

1.7.2. Empirical methods

Empirical methods are utilized to predict the behavior of soil slopes and retaining walls reinforced with soil nails by utilizing data from prior projects or experiments, particularly when there is limited data accessible or when the structure being studied is comparable to those previously analyzed.

1.7.3. Field testing

By conducting field tests to assess the performance of soil nails in specific soil types and conditions, valuable data can be gathered to improve the accuracy of soil nail analysis and refine assumptions made in other analysis methods (Park et al. 2021) and (Kwong and Lee 2008).

1.7.4. Limit equilibrium method

The limit equilibrium method (LEM) is a widely used approach in soil nail stability analysis which utilizes the principle of equilibrium to assess the stability of a soil mass. Due to its simplicity and ability limit, LEM provides a reasonable factor of safety for retaining walls or slopes. LEM involves dividing the soil mass and computing the forces acting on soil mass. The method also

takes into account the resisting forces, such as the shear strength of the soil, the bond strength between soil and soil nails, and the frictional resistance between the soil and retaining wall. The factor of safety of the soil mass can be determined by balancing the forces and comparing them to the resisting forces (Arvin et al. 2021), (Rabie 2016) and (Shiu et al. 2007).

1.7.5. Finite element method

In finite element analysis (FEA), calculations, models, and simulations are used to predict the behavior of a material or component when subjected to different physical conditions like pressure temperature, and types of materials. This analysis is mostly used by engineers and researchers in finding the errors and vulnerabilities in their prototype designs and products. Finite element analysis provides a safe simulation against potentially dangerous and destructive load conditions of load and failure modes, allowing researchers to discover physical responses at any location in the system. Since the physical stress that may affect the model is analyzed beforehand, the accuracy of the model is enhanced as an additional benefit. The finite element analysis works based on three major phases which include problem classification, discretization, and modelling. Even though this analysis method has many advantages it also has certain limitations which are errors occurred while modelling, incorrect boundary conditions, automatic and non-uniform meshing errors, and cost of the analysis tools. Some commonly utilized FEA software tools are PLAXIS 2D and ANSYS. These tools contain various pre-determined materials which can be used while modelling any components. Some of the finite element analysis tools used in different sectors are shown in Figure 1.7.

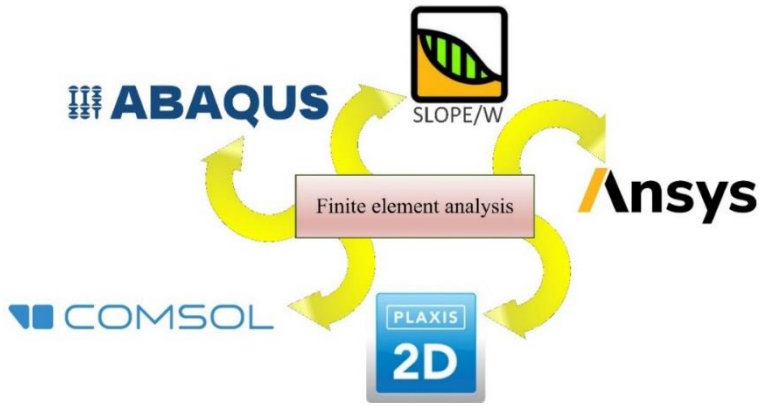

Figure 1.7. Software tools used in FEA analysis

1.7.5.1. SLOPE/W

The SLOPE/W is one of the leading rock and soil stabilization analysis software which is developed by a sequent software company. Both simple and complex problems in slip surface shapes, pore-water pressure conditions, soil properties, and loading conditions can be analyzed effectively using SLOPE/W software. To assess the geometrical stability of the given slope, limit equilibrium approach is used in this software. The limit equilibrium method identifies force-displacement relationships, simply by using the given material and geometric properties of the different members. The advantages of using limit equilibrium approaches are, that slope bending moments are unconservative when more than one support level is used and well-understood limit conditions are assumed.

Even though this analysis tool uses a limit equilibrium approach, some finite element approaches such as stability and dynamic stability analyses are also used in this tool. It uses finite element computed stresses from other tools to calculate a stability factor by computing both total shear resistance and mobilized shear stress along the entire slip surface. GeoStudio is a platform developed by the same sequent software company to combine the analyzed results from different products into a single modeling project, by using the results from one as the starting point for another. Using this tool, the application of SLOPE/W widened to many sectors in construction and stabilization.

1.7.5.2. ABAQUS

The ABAQUS is a tool used for both design and analysis of the mechanical components, as well as visualizing their assembling by visualizing or simulation using finite element analysis. It was developed by Dassault Systems and the first version was released in 1978. When compared to other finite element analysis platforms, ABAQUS may have the simplest coding, which is a major advantage. A powerful, object-oriented scripting language, python is widely used in ABAQUS. Python has been embedded within the ABAQUS software products. For faster simulation, the Computing Power of GPU is used by the ABAQUS. The minimum system requirement needed to run the ABAQUS software is 8 GB of RAM with a 32-bit operating system. This software takes up to 4 GB ram to its working. ABAQUS is mostly suited for static, low-speed dynamic, and

steady-state transport applications. In one single simulation, analyses of both the time and frequency domain of a model are possible in this software tool also it delivers highly accurate stress analysis results.

1.7.5.3. ANSYS

ANSYS is a multi-purpose modeling and finite element analysis package developed to numerically solve a wide variety of mechanical problems in different analysis stages as well as types. Initially, the ANSYS software was developed by Swanson Analysis Systems Inc. (SASI) and later the name of the developer company was changed to the software name itself. The first commercial version of Ansys software was labeled as version 2.0 and released in 1971. At the time, the software was made up of boxes of punch cards, and the program was typically run overnight to get results the following morning. Now due to the technology developments, the result processing time is reduced. The difficulties in the modelling include static/dynamic, structural analysis, heat transfer, and fluid problems, as well as acoustic and electromagnetic.

This software provides a platform that spans the entire range of physics as well as access to virtually any field of engineering simulation that a design process requires. ANSYS is a trustable software around the industrial sectors in providing better simulation results. A powerful structured scripting language known as Ansys Parametric Design Language (APDL) is used to interact with the Ansys Mechanical solver. The meshing process in the ANSYS simulation workbench takes place in two forms namely, fully automatic and manually directed automatic meshing. The minimum system requirements needed for the installation of this software are 8 GB RAM, Graphics Card with 2 GB memory, and an i3 or above processor with 2.5 GHz.

1.7.5.4. COMSOL

COMSOL Multiphysics which was formerly named FEMLAB is developed by COMSOL Multiphysics Pvt. Ltd., as a simulation software, which is based on advanced numerical methods. Fully coupled multiphysics and single-physics modeling capabilities allow to simulate electromagnetics, structural mechanics, acoustics, fluid flow, heat transfer, and chemical phenomena in an environment. Most engineers use COMSOL Multiphysics software to simulate

designs, device modeling, and processes in all fields of engineering, manufacturing, and scientific research sectors. This software is coupled with multiphysics and single-physics modeling capabilities. The modeling section of this software contains almost all the processes of modeling workflow such as geometric definition, properties of material, and the physics that determines the specific phenomena for performing computations and evaluating the results. Some of the advantages of COMSOL software include complete modeling workflow, geometry to results evaluation, streamlining the modeling workflow, understanding product behavior, facilitating collaboration, providing results quickly, and user-friendly tools for building as well as deploying simulation apps. The system requirements of COMSOL are 4GB of RAM, 13GB of ROM, windows 64-bit Intel, and AMD processor. COMSOL takes more time in the design process. Combining the physical equation gives better results for real phenomena in the design model

1.7.5.5. PLAXIS 2D

For 2D analysis of deformation and stability in geotechnical engineering and rock mechanics, a powerful and user-friendly finite element analysis software known as PLAXIS 2D is utilized by worldwide top engineering companies and institutions in the civil and geotechnical engineering industry. This analysis software is developed by Bentley Systems. For simulating both non-linear, anisotropic soil behavior and interaction with structures accurately PLAXIS 2D offers a complete 2D solution for geometric design and analysis. Optional dynamic, transient groundwater flow and thermal capabilities are also available for improved performance. To create efficient models with a logical geotechnical workflow PLAXIS guides users across several modes. For modeling different geometrical components like modeling capabilities of CAD through PLAXIS 2D, various predefined shapes and structural elements with different loading conditions are available which leads to the fast and efficient finite element model development.

The major intention of developing PLAXIS 2D software is to provide a practical analysis tool that can be useful for geotechnical engineers, even though they have low knowledge of numerical analysis. Using an open modeling environment developed by the same Bentley Systems, geotechnical data such as topology, boreholes, piezometers, other field instruments, and measurement devices can be visualized and manipulated. The design and construction of the

finished model can also be staged using this modeling software. The applications of PLAXIS 2D are extended to excavations, embankments, foundations for tunneling, mining of oil and gas, as well as reservoir geomechanics. Geometrical aspects indications such as axial, strain, and plane symmetry are handled by PLAXIS 2D original codes. The minimum system requirement for the installation and working of PLAXIS 2D is a 64-bit latest operating system operating on a dual-core processor with GPU with 256 MB OpenGL 3.3 and 4 GB RAM. For storage purposes, at least 2 GB of free space on the partition where the windows temporary directory resides, and 2 GB of free space on the partition where projects are saved, should be available on the system.

1.8. Optimization Models

1.8.1. Response Surface Methodology

The design of experiments based on response surface methodology contains some sets of statistical and mathematical tools to design and optimize the process and effect variables. The influence of various parameters in the process is recognized through RSM and helps in reducing the trial numbers. An adequate functional relationship between a response and controlling input variables is developed using mathematical and statistical techniques, which provide an approximate relationship by a low-degree polynomial model. The polynomial models are mostly first and second-degree polynomial models as shown in equations 1.1 and 1.2 respectively.

$$y = \gamma_0 + \sum_{i=1}^{k} \gamma_i x_i + \varepsilon \tag{1.1}$$

$$y = \gamma_0 + \sum_{i=1}^{k} \gamma_i x_i + \sum\sum_{i<j} \gamma_{ij} x_i x_j + \sum_{i=1}^{k} \gamma_{ii} x_i^2 + \varepsilon \tag{1.2}$$

Where x is the number of control variables

y is the response

γ is the vector of unknown constant coefficients referred to as parameters

ε is the random experimental error assumed to have a zero mean

The later research conducted on the response surface methodology led to the introducing many designing models which include central composite design, factorial design, and box behnken design (BBD). Among them, box behnken design estimates the parameters using a quadratic model with sequential building designs to determine the lack of fit in the model using blocks. These design models are explained in detail in the upcoming chapters.

1.8.2. Deep Belief Network

Due to the powerful self-learning and adaption of neural networks, it played an important role in many fields such as object classification and data fitting. After the creation of neural networks, the development in machine learning was drastic and gave rise to various kinds of neural networks such as BP-networks, SOMF-networks, and RBM-networks. The networks can be used for different problem-solving situations. Among deep learning, an algorithm of Deep Belief Network (DBN) is an effective method for problem-solving from neural network with deep layers, such as low velocity and the phenomenon of over fitting in learning process. The layers of machine learning in the deep belief network are shown in figure 1.8 and further deeply discussed in the later chapters.

Deep belief networks possess distinctive characteristics that set them apart. One such feature is their layer-by-layer learning approach, where the top-down, generative weights govern the interdependence between variables in different layers. As the learning process concludes, a singular, bottom-up pass becomes sufficient to deduce the values of latent variables in each layer. This pass begins with an observed data vector in the bottom layer and utilizes the reverse direction of the generative weights.

In essence, a deep belief net can be perceived as a conglomerate of elementary learning modules, each constituting a particular type of Boltzmann machine learning technique. It comprises a layer of visible units, which serve as representations of the data, and a layer of hidden units that acquire the ability to capture complex features and higher-order correlations present within the data. These components work in synergy, allowing the deep belief net to learn and comprehend intricate patterns and structures in the input data. In machine learning the visible vector generation probability is shown in equation 1.3.

$$p(v) = \sum p(h|v, W)p(v|h, W) \tag{1.3}$$

Where,

$p(v)$ is the probability of visibility vector generation

W is the matrix of symmetrically weighed connections

$p(h|v, W)$ is the Posterior distribution over hidden vectors

$p(v|h, W)$ is the Posterior distribution over visible vectors

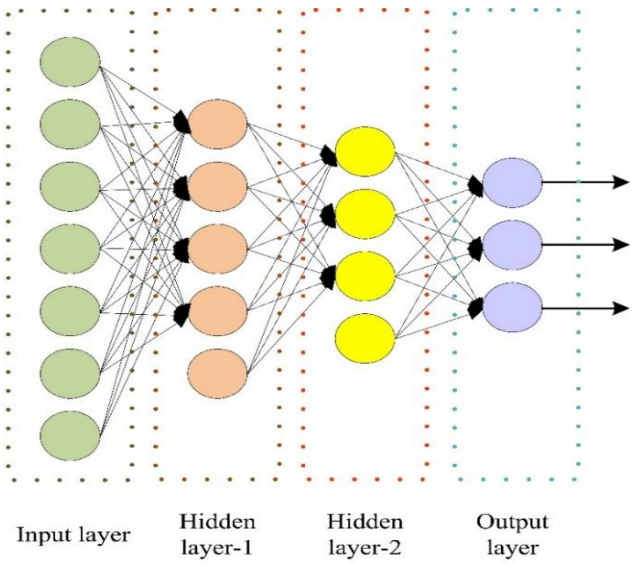

Figure 1.8. General structure of DBN (Liu et al. 2020)

1.8.3. COOT optimization algorithm

The coot is an aquatic habituated bird that is from the family rail of Rallidae. They constitute the genus Fulica, the name being the Latin for “coot”. frontal shields of the coot are considered as prominent decoration on the fore head, which has eyes of dark red color and bills of beautiful colors. Except for some coots, all of them have white colored under their tail. The literature on American coot behavior includes extensive work on breeding, habitat, and migratory behavior. The coots exhibit various movement patterns and behavior on the water's surface. These patterns

are used to develop a new optimization method. The behavior characteristics of coots that are considered for this optimization are given below

1. Side by side random movements
2. Chain formation movement
3. Adjustment of position based on group leaders
4. Movement towards optimal area, following the leader

1.8.3.1. Random movements

In the side-by-side movement, the coots just randomly wander around the water's surface as shown in figure 1.9 (a). In the searching phase, each coot moves toward the random position which allows it to explore each part of the search space. The random movements of the coots are considered as per equation 1.4. (Mirjalili et al. 2017).

$$Q = rand(1, d) \times (ub - lb) + lb \tag{1.4}$$

Where, Lower bound of the search space is lb

Upper bound of the search space is ub

In case of any huddles in the algorithm, the escape movement position update can be updated using equation 1.5

$$cootpos(i) = cootpos(i) + A * R2 * (Q - cootpos(i)) \tag{1.5}$$

Where, A is the random movement of coot that is calculated using equation 1.6

$$A = 1 - L * \left(\frac{1}{iter} \right) \tag{1.6}$$

Where, L is current iteration,

$iter$ is maximum iteration.

1.8.3.2. Chain formation movement

During the chain movement, the behavior of coots changes to regular chain formation and moves around the water surface as shown in figure 1.9 (b). The implementation of chain movement can be determined using the average position of two coots (Mirjalili et al. 2017). Another, method for the chain movement implementation is to calculate the distance between the two coots and then move the coot toward the other coot about half the distance. As per the first method, the new position of the coot is updated as equation 1.7

$$cootpos(i) = 0.5 * (cootpos(i+1) + cootpos(i)) \tag{1.7}$$

Where, $cootpos(i)$ is the current position of coot

$cootpos(i+1)$ is second coot position

1.8.3.3. Adjustment of position based on group leaders

A few coots in front of the group usually lead the whole group, and other coots adjust their position according to the leader's position by moving towards them. As more than one leader is present in the group, confusion arises in the leader selection and to solve this, the average position of the leaders is considered. Furthermore, the selected average leader position causes a premature convergence among the coot group as shown in figure 1.9 (c). To move towards the optimal area, leaders need to update their position. They always search for better positions around the present optimal position. The updated position based on the leader is shown in equation 1.8

$$cootpos(i) = leaderpos(K) + 2 * R1 * \cos(2R\pi) * (leaderpos(K) - cootpos(i)) \tag{1.8}$$

Where, $leaderpos(K)$ is the position of the leader

$R1$ is a random number between intervals [0, 1],

R is a random number between intervals [− 1, 1].

1.8.3.4. Movement towards optimal area

Sometimes leaders have to move away from the current optimal position to find better positions as shown in figure 1.9 (d). A good way of getting closer to the optimal location and getting away from the previous position is updated as per equation 1.9

$$leaderpos(i) = \begin{cases} B * R3 * \cos(2R\pi) * (gBest - leaderpos(i)) + gBest & R4 < 0.5 \\ B * R3 * \cos(2R\pi) * (gBest - leaderpos(i)) - gBest & R4 \geq 0.5 \end{cases} \quad (1.9)$$

Where $gBest$ is the best optimal position

$R3$ and $R4$ are random numbers between intervals [0, 1],

Also B is calculated using equation 1.10

$$B = 2 - L * \left(\frac{1}{iter} \right) \quad (1.10)$$

Where, L is current iteration,

$iter$ is maximum iteration.

Figure 1.9. Behavior of coots (Mirjalili et al. 2017)

(a) Random movements (b) Chain formation movement (c) Adjustment of position based on group leaders (d) Movement towards optimal area

1.9. Motivations

The motivation behind the analysis of conventional and helical soil nails using the finite element method and limit equilibrium method in cohesive soil is to evaluate the performance of these soil reinforcement techniques in cohesive soil conditions. To reinforce cohesive soils like clay and silt, which are difficult to work with due to their low permeability and high compressibility. Soil nailing is a popular technique used in construction projects for stabilizing slopes, retaining walls, and excavations. The use of finite element and limit equilibrium methods in the analysis allows for a detailed understanding of the behavior of soil nails under different loading conditions. The finite element method is a numerical analysis technique that allows for the modeling of complex soil geometries and non-linear soil behavior. The limit equilibrium method, on the other hand, is a simpler analytical method that provides a quick estimate of the stability of soil slopes and retaining walls. By comparing the results obtained from these two methods, the research aims to provide a better understanding of the behavior of conventional and helical soil nails in cohesive soil. This information can be used to optimize the design of soil nail walls, improve construction techniques, and provide more cost-effective solutions for construction projects in cohesive soils.

The motivation behind the optimization of helical soil nailing behaviors by RSM and hybrid DBN-COOT is to enhance the effectiveness and efficiency of soil nailing design. helical soil nails enhance their load-carrying capacity and overall performance. By utilizing RSM and DBN-COOT optimization methods, it is possible to determine the optimal values of parameters for helical soil nails to achieve optimal performance. RSM, a statistical modeling method, allows for the creation of mathematical models that illustrate the correlation between input parameters and output responses. DBN-COOT is an optimization technique that employs machine learning and combines DBN with COOT optimization methods. DBN is an artificial neural network that can recognize intricate connections between inputs and outputs, whereas COOT optimization is a metaheuristic optimization approach that can identify the optimal values for input parameters. Applying RSM and DBN-COOT to optimize the behavior of helical soil nailing can result in more precise and efficient design processes, lowered construction costs, and increased stability and performance of the soil nail structures. Furthermore, this research can offer valuable insights into the behavior of helical soil nails and the relationship between input parameters and output responses.

1.10. Objectives

Soil nailing is an efficient and commonly used technique in geotechnical engineering. The effectiveness of this method relies on understanding the pullout behavior and deformation characteristics of soil nails in the given soil conditions. Conventional soil nails have been extensively studied in the past, but recent advancements have introduced helical soil nails, which offer potential advantages over their conventional counterparts. The study aims to achieve the following objectives:

- To investigate the pullout behavior and deformation by experimental, mathematical, and numerical modelling for conventional soil nails in cohesive soils.
- To investigate the pullout behavior and deformation by experimental, mathematical, and numerical modelling of helical soil nails in cohesive soils.
- To compare the results obtained from the finite element and limit equilibrium methods to provide a better understanding of the behavior of conventional and helical soil nails in cohesive soil.
- To use RSM to determine the optimal values that maximize the performance of helical soil nails.
- To apply DBN-COOT optimization to further refine the design parameters and identify the optimal values of input parameters that provide the best performance of the helical soil nails.
- To optimize and validate the helical soil nailing outcomes using RSM and hybrid DBN-COOT optimization with different shaft diameters, helix pitches surcharge pressure, and inclination angle.

1.11. Scope

The scope of this research is to improve the soil nailing process by utilizing a helical soil nail. Also, evaluate the performance of these soil reinforcement techniques in cohesive soil conditions. By conducting the numerical analysis and finite element analysis, it is expected to improve the pullout and deformation behavior while using the helical soil nails. The analysis will focus on comparing the results obtained from the finite element and limit equilibrium methods to provide a

better understanding of the behaviour of conventional and helical soil nails in cohesive soil. The scope of optimization of helical soil nailing behaviors by RSM and hybrid DBN-COOT is to improve the efficiency and effectiveness of soil nailing design in geotechnical engineering. The optimization will focus on identifying the optimal values to achieve the best performance of the helical soil nails.

1.12. Thesis Organization

Chapter 1: This chapter provides a brief introduction to the types of slope stability reinforcement systems. Among them, the slope stabilization through soil nailing is discussed deeply and their parameters are also analyzed. The analysis and optimization used in enhancing the helical soil nailing process are also summarized.

Chapter 2: This chapter contains the literature survey conducted before starting the experiment. The literature on slope stabilization and its types are discussed. The evolution of the soil nailing process with their types is analyzed using the literature of different authors. Literature regarding numerical modelling and optimization using machine learning is analyzed in this chapter.

Chapter 3: This chapter covers the apparatus and equipment used in the current investigation. The properties of the materials and the measurement process of the material properties are also discussed.

Chapter 4: Analysis of soil and nail behavior using mathematical and numerical modelling is conducted in this chapter. Deformation, stress distribution, and load-carrying capacity are determined using these modelling techniques in this chapter.

Chapter 5: The prediction and optimization process of the soil nailing performance using RSM and Hybrid Deep Belief Network-COOT Optimization is conducted in this chapter.

Chapter 6: The results obtained from various analyses are collected and comparatively analyzed in this chapter.

Chapter 7: The concluding remarks obtained through the analysis from the previous sections are discussed in this chapter.

CHAPTER 2

LITERATURE REVIEW

2.1. General

Slope, rock falls, rock slips, road cut excavation, and embankment collapse are the most common manifestations of slope stability issues. The development of a region is often hindered by the presence of an unbalanced slope, which not only poses risks to human life but also raises numerous challenges. Ensuring slope stability is crucial for both global development and human safety. In response to these issues, various stabilization techniques have emerged over the years. This section will delve into a diverse array of topics, encompassing slope stabilization methods, the evolutionary history of soil nails, conventional soil nail behaviors, helical soil nails, and their availability, as well as performance analysis and optimization techniques for enhancing soil nail efficiency and performance measures.

2.2. Studies on Slope Stabilization

Löbmann et al. (2020) reviewed the influence of vegetation on the stability of shallow slopes. The soil stability was investigated at different depths, and the depths were classified as follows: soil with high root density, soil with low root density, unrooted soil, and bedrock. Evaluation of slope stability takes into account the root characteristics (root concentration, density, diameter, and tensile strength) as well as ecological factors. Both woody and herbaceous vegetation exhibits a great deal of variation in performance, which is influenced by the local environment, site-specific needs, species mix, and plant health.

Capilleri et al. (2016) investigated plant soil stabilization with the help of experimental and theoretical methods. Plant root properties such as diameter and tensile strength must be considered. The test outcomes reveal that the plants enhance the soil's shear resistance and stiffness. Moreover, the soil stabilization effectiveness differs based on the soil type. The experimental findings indicate that the root's tensile strength ranges from 2.5 to 8 MPa, suggesting its potential utilization in shallower slide stabilization and erosion prevention.

Benmebarek et al. (2022) evaluated the performance of pile slope stabilization and optimized it using the computation method. The pile location, pile spacing, and length of the piles are important criteria for pile slope stabilization. Positioning the fixed pile head at the slope's center improves stability and reduces the required length of the piles. Piles with a free head offer only a slight increase in the factor of safety for cohesive-frictional slopes. A comparative analysis was conducted to assess the performance of free head, fixed head, and hinged head piles. The findings demonstrate that as the pile length increased, both the bending moment and shear force experienced variations.

Lu et al. (2018) evaluated the stability of clay-rock composites used in the discrete element method. Employing a methodical approach, the numerical model closely approximated the rock's shape, considering its influence on the mechanical characteristics of mixed soils. For clay-rock slopes, the factor of safety is lower than that of clay slopes when the rock percentage falls below 60%. Test data indicated that a 60% or higher rock concentration led to increased soil stability. Notably, the form of the rock played a vital role in slope stability, with slopes containing smaller rocks demonstrating greater stability than those with larger rocks.

Kulczykowski et al. (2017) decided to investigate the effectiveness of soil nails in the preservation of historic buildings. Reinforced soil reduces costs and maintains serviceability by allowing historical structures to be stabilized without having to be rebuilt. The soil nailing process is 30% less expensive than traditional slope stabilization. Moreover, the ease of use, dependability, absence of vibration, and low noise levels during nailing are noteworthy. The author's conclusion highlighted the numerous benefits of soil nailing, making it an exceptional method for safeguarding historically significant buildings.

Ayazi et al. (2020) examined slope failure and soil nail stabilization techniques. The study revealed that soil-nailed slopes exhibited greater stability and less deformation compared to unnailed slopes. Among the crucial factors influencing slope stability in soil nailing, the inclination of the nail played a significant role, with an inclination of 10 degrees showing excellent performance. Moreover, the soil nailing approach proved to be more cost-effective, with a 30% lower cost and was particularly suitable for older slopes. The findings from the finite element analysis indicated

that the soil nailing process performed admirably in cases with a 60° inclination, outperforming those with a 45° inclination.

Sharma et al. (2019c) have investigated the benefits and limitations of the soil stabilization technique, particularly soil nailing. The major components of soil nailing are soil nails, centralizers, couplers, grout, connectors, and a drainage system. Because of its simplicity and minimal environmental impact, the construction of a fast soil-nailed wall is achievable. Soil nailing considers three categories of failure modes: internal failure modes, external failure modes, and facing failure modes. The growth of soil nail pull-out capacity is significantly influenced by the installation technique as well. The primary requirements for designing soil-nailed structures are external, internal, and facing stability. For soil-nailed structure construction, kinematical multi-check design approaches are generally used.

Chan and Raman (2017) stabilized the slope with the help of a soil nail and investigated the failure of the nail. The demo modal screw-type soil nail was used to stabilize the slope at different geometric levels. At the end of the experiment, the author notes that the newly formed soil nail improved both the natural slope and the artificially created slope. Full-scale simulations are advised for developing the installation technique and validating its efficacy.

2.3. Evolution of Soil Nailing

The interface shear stress-strain performance of newly created soil nails was investigated by Xu et al. (2018). The soil nail is constructed using glass fiber-reinforced polymer and soil nail performance evaluation is done by a strain-transfer model using an optical fiber sensor. The finite element model is used to validate an analytical strain-transfer model. Similarly, the interface shear stress was tested in the field at various excavation depths.

Dai et al. (2016) conducted a study to assess the effectiveness of a soil anchoring system using moso bamboo with branches. The performance of these novel bamboo soil nails was evaluated through both numerical simulations and practical experiments in the field. To compare their effectiveness, measurements from the bamboo soil nails were juxtaposed with those from

conventional soil nails constructed using steel pipes. The choice of bamboo as the material for soil nailing was motivated by its ready availability and renewable nature.

The strength of the bamboo soil nails was subjected to tensile tests, which were carried out both experimentally and in real-world conditions. The results from the field tests demonstrated that the pull-out performance of the bamboo nails, especially those equipped with branches, exhibited a significant improvement, ranging from 2.5 to 2.8 times better performance, particularly in soft clay or soil areas.

Pei et al. (2013) studied the stress-strain and shear resistance performance of glass fiber-reinforced polymer soil nails experimentally. The pull-out test in a laboratory setting was tested on a fully decomposed granite soil mass. The fiber bragg grating sensing system was used to measure the pull-out performance. The mechanical behaviour was measured using the strain result, while the glass fiber-reinforced soil nail pull-out performance was great in numerical analysis. By comparing the standard grouted soil nail to the glass fiber-reinforced nail, the test results were identical.

The study conducted by Tokhi et al. (2018) focused on evaluating the effectiveness of a screw soil nail system compared to grouted soil nails. The researchers performed tests using residual soil in a large pullout box under controlled laboratory conditions. The results demonstrate that the screw nail surpasses the conventional grouted soil nail concerning pullout load-displacement behavior and interface shear mechanism. The authors note that the screw nail system's peak tensile forces gather at approximately 49 mm, which is believed to simulate field testing conditions.

Rabie (2016) investigated the hybrid earth stabilization process through numerical and limit equilibrium approaches. Both soil nailing and MSE systems are used in combination to stabilize sloping soils. The purpose of the evaluation test was to compare the experimental, finite element, and limited equilibrium models. The hybrid soil stabilization method's performance was measured separately in two sections. Compared to other results, limit equilibrium approaches measured values were found to achieve higher tensile strength. The three types of measurement values are different from each other.

Ayazi and Tangri (2022) have investigated the performance of different flexible-facing materials used in the soil nailing process. Under various load conditions, calculations and comparisons were made for the settlement and displacement of facing materials. The study incorporated three types of flexible-facing materials, namely Geocomposite, HDPE Geomembrane Sheet, and Biaxial Geogrid. The obtained results were then contrasted between conditions with and without a facing slope. The test results demonstrate that the geocomposite-based fared well in terms of tensile and shear strength. The author highlighted that the flexible material can bear a maximum stress of 1.23 N/mm^2 based on the test results.

Zhang et al. (2015) investigated the performance of soil nailing, and the load-deformation of soil nails was evaluated. The glass-fiber-reinforced polymer-based soil nail was used on the slope stabilization. Due to the pull-out condition, the soil-nail interaction was taken into account in the evaluation. The pull-out data was used on the time-dependent effect on evaluation. The test result showed that simulation and experimental stress levels are more similar. The author noticed the interaction between the soil and nail placement that created the performance loss. The creep displacement of the soil nail significantly affects the mechanical parameters of the soil nail.

Spagnoli et al. (2020) have investigated the installation power of large helical piles in dry cohesionless soil. The parametric evaluation was conducted on the helical pile; the helix diameter was 0.6 and 0.45 mm, and the shaft diameter was 0.3 mm. the laboratory condition piles were tested in different loading conditions and the test result was compared. With rising soil unit weight, soil friction angle, and increasing RPM values, power increases for all three models. The power improved by around 40% when the wing ratio was increased from 1.5 to 2.

2.4. Studies on Conventional Soil Nail

Azzam and Basha (2017) investigated the improvement of geotechnical parameters of cohesive soil vertical soil nails. The assessment extended to examining the shear strength performance of a novel composite material concerning factors like embedment depth, the number of vertical inclusions, and alignment radius. The study revealed that both clay and vertical bars or inclusions experienced vertically applied stress together. Increasing the number of vertical inclusions led to

significant enhancements in shear strength and stiffness, accompanied by a notable reduction in settling. The results from direct shear tests further confirmed that the presence of these vertical inclusions contributed to increased shear strength and reduced horizontal deformation.

Tokhi et al. (2016) investigated the traditional nail's performance and decided to improve it by using new nails. As a result, an investigation was conducted using a screw nail, and the pull-out capacity and friction coefficients were calculated in the laboratory condition. The findings showed that the failure of the screw nail system followed the Mohr-Coulomb failure condition, which aligns with the behavior observed in traditional soil nail tests.

Liu et al. (2021) conducted a review and analysis for the facilitation of soil nailing implementation, in the design and construction of transportation infrastructure. The freezing and thawing cycles on soil nail walls are presented using numerical simulations and the collected data are used in the wall constructions. The heat transfer in the soil is also studied using the numerical simulations. The findings from the study state that, due to differences in the thermal conductivities, the soil zone between the nails freezes slower than the nails. In the nails located in the middle of a wall, the peak stress increase is found, because of the two-dimensional front penetration from both the top and the front and more restraints at the lower portion of the wall.

Bhuiyan et al. (2022) analyzed the pressure-grouted soil nail system with the help of newly developed soil nail testing apparatuses. The experimental apparatus was suitable for injecting grout at various injection rates. The pure water and cement combination was used to prepare the soil nail installation grout (w/c = 0.5). A custom-made screw jack pump system was designed to control the grout injection velocity and monitor the injected grout volume continuously. Automation and instrumentation were incorporated into the pump system. Additionally, an overburden pressure system utilizing a water-filled rubber bag was developed to apply surcharge pressure. The test outcomes revealed that the pull-out resistance of the pressure-grouted soil nail increases with higher injection rates.

2.5. Studies on Helical Soil Nail

Sharma et al. (2021c) studied a helical soil nail consisting of a helical disc attached to a hollow steel rod, and two types of structural nails were used. A total of nine ribbed soil shafts were installed at a uniform distance in an experimental setup to evaluate the soil nail efficiency. The investigation was carried out to quantify the variations in compressive and pullout properties. Similarly, the helical soil nail vertical and axial stresses were calculated experimentally. The author faces failure due to some limitations in the analysis of individual and group helical nails, such as high loads and nail tip designing errors.

Sharma et al. (2021d) investigated the pull-out behaviour of a helical soil nail made of an open-end hollow tube. Analyze how the soil fill affects the torque installation and pull-out performance evaluation. The author noticed that nail length, which depends on diameter, increases the installation torque and pull-out, not depending on the helices' number increasing. The soil plug's length contributes 12% to the total pull-out resistance, while the remaining 88% is derived from external shaft friction and bearing provided by the helical plates.

Sharma et al. (2022) used an open-ended, helical-pipe soil nail to improve the performance of the slope stabilization system. The test was conducted on cohesionless soil, and installation and displacement-controlled pull-out tests were used to make assessments. The testing of soil nail formation takes into account various factors, including the influence of internal skin friction, soil plug, and bearing resistance. The results of the tests revealed that increasing the soil nail diameter and the number of helices, as well as the installation torque, had a positive impact on the pull-out performance. The different loading conditions open-end helical tension values varied from 2.12 m^{-1} to 53.33 m^{-1} and compressive strength varied from 27 m^{-1} to 55 m^{-1}. The authors conclude that the experimental values were similar to the theoretical performance estimate.

Mollaei et al. (2022) have studied the performance of helical soil nailed walls under seismic conditions. The helical soil nailed wall performance was evaluated experimentally and the seismic effect was attained with the help of the shaking table. The test results indicate that implementing a uniform increase in nail length along the wall leads to a notable enhancement in the seismic

performance of the helical soil nail wall. Inclined nails demonstrate reduced lateral displacement compared to horizontal nails. Moreover, increasing nail length and inclination contribute to larger dimensions of potential failure surfaces.

Sharma et al. (2017) have investigated the performance of new soil nails in incoherent soils under laboratory conditions. They evaluated the performance obtained by using a helical soil nail in dry dense sand under laboratory conditions. Seven different types of helical nails were tested in displacement control mode to determine the precise performance of soil nails. The assessment revealed a notable correlation between the hardness of the nail shaft and the peak pull-off efficiency of the helical soil nail. In the diverse HN tests conducted, the results consistently met the Mohr-Coulomb failure Criteria. Furthermore, it was observed that the unequal helical soil nail outperformed the equal diameter HN in terms of performance.

Incoherent soils were the focus of Sharma et al. (2021) investigation of the performance of hollow and solid shaft helical soil nails. By altering the shaft type and nail arrangement, the researchers assessed the impact of soil nail parameters on performance through pull-out tests. Installation torque and relative soil nail pull-out capacity were measured using the torque correlation factor. The test findings revealed that the helical nail pitch within the range of 24.5 to 35.5 mm exhibited superior performance. Moreover, hollow shaft nails exhibit higher axial stresses, which change as the number of helices increases. When compared to a solid helical nail, the hollow steel helical nail achieved nearly equal interaction friction angle. The conventional and helical soil nailing testing soil and nail material with concluded observations are summarized in table 2.1

Table 2.1. State-of-the-art method in soil nailing

Author	**Type of nailing**	**Material**	**Observation**
Azzam and Basha (2017)	Vertical soil nailing	Soil: cohesive soil	After the inclusion of six soil nails in the selected area, a 231% increase in shear strength is

		Nail: steel rod	observed at a 0.85 depth ratio. The vertical inclusion of soil nail lowers the chances of horizontal deformation. A 5.7 times improved surface stiffness is achieved after the reinforcement of cohesive soil.
Tokhi et al. (2016)	Screw-type soil nailing	Soil: sand Nail: NA	Unlike conventional soil nailing, screw nails do not display any residual values. Their strong adherence makes them particularly suitable for use in earthquake-prone regions or areas with the potential for significant displacements.
Sharma et al. (2021d)	Helical soil nailing	Soil: cohesion less frictional Soil Nail: open-ended hollow pipe	When examining the pullout resistance, the soil plug length accounts for 12% of the contribution, while the remaining 88% is attributed to external shaft friction and bearing provided by the helical plates. Analysis of the torsional strain data revealed that open-ended helical nails undergo

			partial rotation along with horizontal displacement.
Sharma et al. (2021c)	Helical soil nailing	Soil: free-falling pulverized soil Nail: ribbed solid and hollow plain shafts	The study focuses on investigating the shear stress-displacement behavior of various types of helical soil nails (HSN) subjected to different overburden pressures and monotonic pullout loading. It was observed that after reaching the peak stress value, the stress gradually reduces until reaching the residual stress level, resulting in a non-linear behavior in the stress-displacement response of the helical nails.
Sharma et al. (2022)	Helical soil nailing	Soil: cohesion less frictional Soil Nail: open-ended pipe	The effectiveness of open-ended pipe installation, particularly regarding installation torque and pullout stress, is significantly influenced by the pipe diameter and the number of helices used. Moreover, the plug length experiences a noteworthy increase with the penetration depth ratio up to a value of five, after which it stabilizes. This

			phenomenon is attributed to the heightened adhesion and friction between the soil and the interfaces of the helical nails. Consequently, the pullout strength of the system shows a direct correlation with the plug length, further enhancing its overall performance.
Mollaei et al. (2022)	Helical soil nailing	Soil: wall reinforcement Nail: steel shaft	A thorough examination of the seismic performance of helical soil-nailed walls was conducted through rigorous shaking table tests. The introduction of inclined soil nails, as opposed to the horizontal variety, proves to be highly effective in mitigating lateral displacement, minimizing acceleration amplification, and lowering the fundamental frequency of the nailed walls.
Sharma et al. (2017)	Helical soil nailing	Soil: dry dense sand Nail: solid steel shaft	From the experiment, it is found that when pitch length is increased to 57 % the peak pullout capacity is also increased.

Sharma (2021)	Helical soil nailing	Soil: cohesion less Soil Nail: solid and hollow steel shaft	As the shaft and helix diameter, helices count, and overburden pressure (ranging from 5 to 12.5 kPa) increase, the installation torque experiences a corresponding rise. However, beyond 50 kPa, the torque gradually declines. The optimal pullout capacity is achieved with a pitch of 30 mm. Notably, helical soil nails demonstrate significantly reduced stress fluctuations during both installation and pullout phases when compared to conventional soil nails.
Hong et al. (2017)	Pressure-grouted soil nailing	Soil: decomposed granite Nail: steel shaft	The coefficient of friction exhibits a linear rise with the escalation of grouting pressure. Nevertheless, when subjected to constant grouting pressure, the coefficient of friction diminishes with the increase in overburden pressure.
Wu and Zhang (2009)	Grouted soil nailing	Soil: silty clayey fine sand	Due to the effect of soil dilatancy, there is a variation in

		Nail: steel shaft	the cohesion results obtained from the field and laboratory. But in both tests pullout shear strength increased concerning the normal stress.
Mickovski et al. (2016)	Self-drilled soil nailing	Soil: NA Nail: hollow steel shaft	An experimental and case study is conducted before stabilizing the slope in the Scotland highway. It is found that hollow bars are easy to install when compared to solid bars
Su et al. (2007)	Grouted soil nailing	Soil: decomposed granite fill Nail: steel bar	To maintain constant test length and soil nail stress conditions during pull-out testing, specific modifications were made to the conventional testing apparatus. As the degree of soil saturation increased, a notable migration of the shearing plane was observed, shifting from the interface between the nail surface and the surrounding soil further into the soil itself.

Zhou (2015)	Pressure-grouted soil nailing	Soil: decomposed granite fill Nail: steel bar	The Bayesian model class selection approach serves as a valuable tool for achieving a well-balanced trade-off between data-fitting capability and noise-modeling error. In the context of soil nail pullout resistance determination, crucial factors to consider include the degree of saturation and the combined influence of grouting pressure and overburden pressure. By employing this approach, researchers can effectively navigate the complexities of the problem, enhancing their ability to accurately estimate soil nail pullout resistance while accounting for various sources of uncertainty.

2.5.1. Pull-out behaviour

Rawat and Gupta(2017a) investigated the pull-out response of a helical soil nail using the finite element subroutine Plaxis 2D. The traction response is achieved using horizontal loading conditions and axisymmetric in the numerical modelling method. The author noted that the helical plate gradually increases the resistance; especially, increasing the quantity of the helical plate increases the resistance.

Hong et al. (2017) thoroughly investigated the peak pull-out resistance and influencing parameters using laboratory and field tests on decomposed granite or sand. Eight soil nail pull-out tests were conducted in the field to evaluate pull-out resistance at overburden pressure and grouting pressure. When comparing field and laboratory investigations, the author notices many differences, particularly full saturation soil's lower pull-out resistance compared to saturation soil.

Oliaei et al. (2019) have investigated the pull-out resistance and soil-nail interaction of soil nailing process using a new approach of mesh-free soil nailing analysis using a finite element analysis simulation method. In the study of soil-nail interaction, a novel approach is employed, incorporating a small thickness layer interface to capture the slipping behavior between the soil and nail surface. This innovative method enables the simulation of the elastoplastic response of the soil nail through the development of a custom computer code. Surpassing the conventional finite element analysis, the mesh-free analysis demonstrates enhanced accuracy. Intriguingly, the research reveals that constrained dilatancy has limitations concerning soil nailing, with the peak pull-out shear stress exhibiting a decreased rate of increase as the dilation angle rises.

In their study, Kim et al. (2013) conducted a comprehensive assessment of the pull-out performance of pressure-grouted soil nails and gravity-grouted soil nails using advanced three-dimensional finite element analysis. The nailing process was executed using the shear strength reduction method. Interestingly, the findings revealed that pressurized soil nails exhibited a notable increase in the factor of safety compared to gravity-based ones, indicating superior pull-out resistance. Moreover, the researchers embarked on a series of numerical slope stability analyses focused on a weathered soil slope to explore the impact of grouting pressure. The results of these numerical investigations unequivocally highlighted the paramount importance of the soil nail's pullout resistance in stabilizing slopes, outweighing the significance of the nail's shear resistance.

Ye et al. (2019b) experimented on compaction-grouted soil nails to study the influence of the saturation degree of the soil on the grouting compaction and pull-out performance. The initial saturation degree of the soil has a considerable impact on grout injectability, resulting in the diameter of the grout bulb. The diameter of the grout bulb modifies the pull-out force, with a larger

grout bulb producing larger pull-out forces and displaying stronger hardening behaviour. Overall, six experiments were performed, with saturation degrees ranging from 5.0 to 46.2%.

Zhou et al. (2011) have tested the performance of the soil nail under overburden and grouting pressure conditions. A three-dimensional finite element modal was used to simulate the soil nail with a pullout box. A modified Drucker-Prager/cap model was used to describe the completely decomposed granite stress-stain behaviour. The coulomb friction mode was used to find the soil nail interface behaviour. Laboratory soil nail Back-analysis of pull-out data was used to evaluate the interface characteristics. The author denotes the laboratory and numerical pullout result was close in vertical slop condition.

Ye et al. (2019a) proposed the investigation of a new compaction soil nail and investigated the physical model. The soil nail pull-out performance was evaluated on the different grouting pressure conditions. The scale effect of the physical model soil nailed system was studied through numerical modelling. In addition, the interface shear test was performed using the same boundary conditions as the physical model test. The results of the physical method investigation indicated that the pull-out efficiency gradually increased as the pulp pressure increased. The traditional and compaction soil nails were compared, and the test results indicate the pull-out resistance was increased with pull-out displacement.

Sharma et al. (2019b) analyzed the pull-out force and displacement behaviour of the soil nail in laboratory conditions. The soil nail performance was investigated on dry cohesionless soil in the experimental setup. The author took into account the effects of relative density, overburden pressure, and surface roughness on the tensile response of the soil. The results demonstrate that increasing the roughness increased the mobilized maximum pull-out resistance of the soil nails by more than twice. The author concluded that the experimental result follows the Mohr-Coulomb failure criterion.

Zhang1a et al. (2014) presented a novel hyperbolic pullout model designed to investigate the pullout capacity of soil nails and the key factors influencing their behavior during the pullout process. The model's effectiveness was confirmed through rigorous validation against laboratory

experimental data. Notably, the study highlighted the crucial influence of two dimensionless parameters in determining the distribution pattern of tensile force along the length of the nail. Remarkably, this method can be easily implemented through computer spreadsheet tools, eliminating the need for costly and time-consuming analyses while still enabling reasonable and accurate predictions.

2.5.2. Internal soil stress

Wang et al. (2017) used a novel grouting technique to examine the performance of soil nails in an experimental scenario. An innovative grout-filling process was used to limit slurry leakage and penetration into the surrounding soil. A soil chamber, a loading and linear guiding system, a pull-out system, a pressure grouting device, and a data recording system were all part of the experimental setup. Soil vibration and soil nail displacement are accurately calculated by the installed sensor. The sensor data show that no movement was seen on the soil surface when grouting pressure was applied. The results of the experiments showed that the grout-filling procedure increased the density and strength of the surrounding soil. There were no yield forces recorded, indicating a considerable advantage for the new soil nail.

The effect of drilled hole hardness on pull-out resistance and nail pull-out resistance was investigated by Hong et al. (2016). In the test setup, several internal surface holes are made to assess the impact hardness of drill holes. The peak pull-out resistance and the pull-out resistance at specific displacement levels for T-type soil nails exhibit an approximately linear increase with the roughness angle, ranging from 0 to 37°.

Horn et al. (2004) studied the consequences of utilizing mechanized harvesting vehicles, in the physical properties of the soil. The impacts of stresses in the soil structure are found by determining the internal soil stress through pre-compression stress measurements. The experiment on the soil compaction was conducted using different harvesting vehicles and found that almost all vehicles increased the pre-compression stress in the soil. The maximum stress of 90 kPa is noted on every driving lane. The determination of internal soil strength through pre-compression values separates the range of stress by making no changes in pore volume. From the study, it is concluded that

change in stress can affect the soil functions so sustainable wheeling is not possible in the harvesting soil areas. The authors recommended utilization of smaller machines, having less mass, to complete the harvesting may minimize the compaction of soil.

2.5.3. Factor of safety

In their study, Alsubal et al. (2017) focused on determining the optimum factor of safety for a soil nail system with variations in soil nail inclination, length, and spacing. The researchers conducted tests on a homogeneous soil slope, considering inclinations of 30°, 40°, 45°, 60°, 70°, and 90°. To investigate the impact of soil nails on the soil slope, Slope/W software was employed, and the results were compared between scenarios with and without nails. The findings revealed that the stability of the soil slope was significantly influenced by the inclination, spacing, and length of the soil nails. As the gap between soil nails increased, the slope's stability decreased. The highest factor of safety, 1.668, was attained at a nail inclination of 30°, while the lowest factor of safety was observed at a nail inclination of 15°.

In their study, Azzam and Sobhey (2019) focused on stabilizing sandy soil slopes using soil nails under seismic loading conditions and determined the safety factor. To analyze the soil nailing model, they employed an elastic-plastic finite element program. The study evaluated various characteristics, including the shear strength of the slope, slope angle, number of soil nails, soil nailing length, and soil nailing stiffness. The findings demonstrated that the implementation of soil nailing on sandy slopes subjected to cyclic loads had a significant positive impact on improving the slope's factor of safety and reducing slope deformation.

In their study, Sharma et al. (2020b) delved into investigating the static and seismic behavior of a soil-nailed wall constructed in a dry, cohesionless medium. The researchers began by conducting laboratory pull-out tests, from which they derived a pull-out capacity equation to be utilized in the subsequent stability analysis of the helical soil-nailed wall. Through a comprehensive parametric investigation, they assessed the impact of various factors on the wall's stability, including the nail inclination, angle of internal friction of the soil, vertical spacing of nails, helix size, number of nails, number of helices, and the face angle. To validate their findings, the authors compared the

results with existing approaches in the literature. The outcomes revealed that, for the provided input parameters, the factor of safety values obtained from their technique were lower than the pseudo-static and pseudo-dynamic values.

Elahi et al. (2022) conducted a comprehensive study on the stability analysis of slopes strengthened with soil nailing. Their research focused on evaluating the influence of slope geometry on the stability of the nailed slope, considering four distinct slope angles and three different backslope angles. The findings revealed that as both the slope angle and backslope angle increased, the factor of safety decreased. The study also explored the impact of various nail factors, such as nail inclination, length, and spacing. It was observed that the factor of safety improved with reduced vertical spacing of the soil nails, reaching its maximum value at a spacing of 1.25 m. However, even though smaller spacing enhanced the factor of safety, the difference in stability between 1.25 m and 2.0 m spacing ranged from 9% to 17%. A detailed summary of the parameters used in the efficiency analysis of the soil nails is given in Table 2.2.

Table 2.2. Parameters analyzed in the nailing process

Authors	**Input parameters**	**Output parameters**	**Observations**
Benayoun et al. (2021b)	Nail length, inclination angle, and vertical spacing between nails	Safety factor, cost	Lengthening the nails leads to an augmentation of the safety factor, primarily attributed to heightened axial nail force, shearing force, and bending moments, which collectively bolster the capacity to withstand loading and deformation.

Kotake and Sato (2021)	Bending stiffness and dimensions of the bearing plate	Deformation and bearing capacity of bearing plate	The footing flexibility reduced the ultimate bearing capacity by 10-20% under experimental conditions. This reduction is considered negligible because of the extremely large rigidity between the rigid and flexible footings.
Zhou et al. (2009)	Surcharge pressure loading	water content redistribution in the soil, internal deformation, and the performance of the soil nails	For the applied loading conditions increasing the overall stability of a loose fill slope is possible, using the soil nails.
Garg et al. (2014)	cohesion, frictional angle, nail inclination angle, nail length, slope height, and slope angle	Factor of safety	The analysis revealed that the frictional angle exerts the most significant influence on the Factor of Safety (FOS), followed by cohesion, nail length, slope angle, nail inclination angle, and slope height.
Hao et al. (2014)	Soil cohesive strength, soil friction angle, pre-stress of anchor cable,	maximum lateral displacement of the composite soil-nailed wall	In the sensitivity analysis performed on the factors impacting the maximum displacement of the excavation side, the order of influence was revealed in a

	soil-nail diameter, soil-nail spacing, soil-nail length		descending manner. The prestress of the anchor cable emerged as the most significant factor, followed by the soil cohesive strength, soil friction angle, soil-nail length, soil-nail spacing, and soil-nail diameter. These various parameters were examined to better understand their contributions to the displacement of the excavation side.
Pradhan et al. (2006)	overburden pressure	Peak pullout force and the load-displacement	Enhanced overburden pressure leads to a notable enhancement in the pullout resistance of soil nails. Interestingly, the results closely align for soil strength parameters derived from direct shear box tests and the interface parameters of grouted nails obtained through pullout tests.
Su et al. (2010)	Soil dilation and Overburden pressure	Soil nail pull-out resistance	The correlation between the simulated peak pull-out resistance and the overburden pressure appeared to be negligible, mirroring the findings from laboratory pull-out tests. Surprisingly, the simulated pull-out resistance displayed a noteworthy augmentation as the

			dilation angle of the shearing zone increased.
Yin et al. (2009)	Overburden Stress and Grouting Pressure	Interface Resistance	The study revealed a noteworthy interactional effect on the soil-nail pullout resistance, influenced by both the grouting pressure and overburden stress. Remarkably, when the grouting pressure is low, the soil-nail pullout resistance exhibits minimal dependence on the overburden stress. However, an intriguing trend emerges as the grouting pressure increases, with the soil-nail pullout resistance displaying a clear increase with higher overburden stress.

2.6. Theoretical Studies on Soil Nailing

Seo et al. (2019) experimented to investigate the mechanical characteristics of slope reinforcement through a combination of soil nailing and soil anchoring systems. The study utilized pre-stressed soil nails made of steel bars and PC strands. To optimize the design load (capacity) of pre-stressed soil nails, it was essential to match the yield displacements of these two components. The pre-stressing of PC strands before applying the pullout load proved to be effective in maximizing the design load. Load transfer in both soil nails and pre-stressed soil nails was determined using skin friction theory and load transfer theory, and the results were validated against field tests. The study demonstrated that exceeding a certain upper bound level of pre-stressing values led to earlier yielding of PC strands than steel bars, resulting in a reduction in the total yield load.

In a separate study by Goyal and Shrivastava (2022), the performance of helical and conventional soil nails was evaluated using theoretical equations and finite element analysis. The factor of safety was calculated for both types of nails using the finite element approach and the limit equilibrium method. The experimental, analytical, and computational results revealed that helical soil nails exhibited less deformation and higher factors of safety compared to traditional soil nails under similar loads and soil conditions. Helical soil nails provided approximately 19% more safety and caused 5% less soil distortion at identical pressure and soil conditions. Experimental findings also indicated that helical soil nails outperformed traditional soil nails by 42% in terms of pull-out capacity at various additional charge pressures.

Hong et al. (2012) have proposed the investigation of the progressive pull-out performance of the soil nail system. A comparative study was conducted between experimental and calculated data to predict the sensitivity of the mode. In addition, a comprehensive parametric investigation was conducted to help find the important parameter of pull-out performance. Soil nail length and diameter, plastic zone length, and soil nail elastic modulus were all considered for pull-out performance. Nail length appears to significantly reduce the normal pull-out force of a hard soil nail. The author only calculated the pull-out of the soil nail passive zone and did not consider the bending and shearing effect of the soil nail.

2.7. Numerical Modelling and Analysis of Soil Nailing

Rawat et al. (2017b) investigated the soil nail performance with the help of FEA. The soil nail was made of circular discs attached to the shaft, with circular disc numbers varying from 1-4. In the evaluation of soil nailing, the characteristics of the pull-out load displacement, the mechanism of failure during pull-out, and pressure around the soil are considered. Finite element analysis was used to run 67 simulations with various parameter settings. The author observed that the nail disc spacing ratio and disc diameter ratio had a substantial impact on the pull-out behaviour.

Farrokhzad et al. (2021) investigated the soil nail length and soil nail installation angle using Plaxis 2D finite-element software. The optimum mesh was used to analyze the soil nailing. The soil nail improves the unstable soil, rock, and slope's overall shear strength and dynamic properties. After

nailing, the dynamic properties of excavation systems were enhanced. Raising the length of the nails enhances the foundation's resilience and reduces excavation deformations.

Ghareh (2015) investigated the impact of nailing structures on cohesive and cohesion less soil. To assess the influence of soil-nail cuts' shear strength and the behavior of nailed buildings, the researchers employed the Plaxis finite element modeling software. The outcomes indicate that the soil's physical properties and the impact of soil surcharge directly affect the behavior and stability of soil-nailing structures. The numerical simulation indicates that nails enhance the safety of excavation walls.

Moniuddin et al. (2016) conducted a study on soil nail wall performance in deep vertical ground excavations with different nail inclinations to horizontal. The impact of varying nail lengths on a soil nail wall system was assessed through PLAXIS 2D finite element analysis. This analysis enabled the calculation of the wall and nail displacement, maximum shear, axial force, and bending moment. The results revealed that the length of the nail significantly affects the overall behavior of the system. The Global Factor of Safety (FSG) will increase to some degree as nail length increases.

Maleki and Mir Mohammad Hosseini(2022). Numerical analysis (finite element) was used to evaluate soil-nail walls under artificially stable seismic conditions. The nailed reinforced walls took deformation and stability into account. Nail placement angles of 10 and 15 degrees have the least amount of displacement and the highest safety factor.

Ebrahimi and Asakereh (2016) Used the finite element approach and the PLAXIS program, to examine how the stability of slopes was affected by changes in angle, nail length, and the horizontal and vertical spacing between them. Results showed that nail positioning should be close to 30 degrees for the highest level of safety. The nails' influence on slope stability is drastically reduced when the angle increases beyond 30. The most ideal distances between nails are around 1 to 2 meters.

Chavan et al. (2017) used OpenSees 2D finite element to generate a conventional nailed soil slope with seismic conditions. For the analysis, a set of five soil nails was employed, each with a 15mm

length and a 25mm diameter. The nails were spaced horizontally at 1 m intervals and vertically at 2.4 m intervals. Notably, the modeling of the soil-nail interface significantly impacted the persistent deformation of the slope after experiencing a seismic event. Additionally, the failure surface observed in this study bears a striking resemblance to the bi-linear failure surface that is believed to be present in the German technique.

Majidian and Panah (2020) investigate the performance of nailing in soil under artificial seismic conditions using hybrid experimental and numerical approaches. Different earthquake levels are generated by special equipment, while vibration levels and soil nail displacement measurements are collected and the data is compared. The physical model configuration was assessed using the push-down device and shaking table tests. The author found that 80-cm-high soil nails performed better compared to others in soil shack tests. Same time as push-down tests fail.

Rawat and Gupta(2016a) evaluate the performance of a soil-nailed slope and an unreinforced slope with the help of the finite element method. Two types of slopes are considered in the evaluation, and the test load level increases gradually. The soil nails were put at three different inclinations: 0°, 15°, and 30° degrees. In the test findings, the most significant load-bearing increase was observed in a soil slope with a 45° inclination and a nail inclination of 0°. However, during the mode testing and analysis, a higher percentage increase in the load-bearing capacity was noted for a 60° slope compared to a 45° slope.

Ye et al. (2017) evaluated the mechanical behaviour of the newly developed soil nail through numerical and experimental analysis. The experimental results are compared with the method of 3D finite element simulation for higher accuracy. Differences in pull-out force between model test and simulation were attributed to friction coefficients and shape angle. The overall soil nail's pull-out force is affected by both the friction coefficient and the shape angle, leading to a gradual increase in the pull-out force as the soil nail's length and diameter are enlarged.

Tavakoli et al. (2021) have used numerical and experimental testing to investigate the mechanical parameters of soil nailing. In the test system, the soil nailing pull-out behaviour was evaluated with

the help of a pull-out box. The height length, and width of the pullout box setup are 120, 100, and 120 cm, respectively.

Rawat and Gupta (2018) have evaluated the performance of screw-type soil nails using numerical testing methods. The soil slop at 45° and 90° was stabilized with six soil nails at 0° inclination with horizontal. The author examined the failure surface, failure load, and slope's volumetric deformation reinforced with screw soil nails. The investigation utilized two numerical approaches: the LEM and FEA. According to the test results, the screw soil nails implementation contributed to a consistent increase in the soil slope's FOS.

Mohammed et al. (2023) evaluated the step-by-step process method of soil nailing using the finite element approach. The soil nail performance evaluation was conducted using experimental and numerical software. Based on the evaluation, the hardening-soil model was used to calculate the stress-strain relationship. The soil nail final performance result was compared for numerical and experimental processes. The test was carried out in six stages, from top to bottom, with the depth measured between 140 and 700 mm. The author concluded that the finite element analysis test result is clear and highly efficient.

Halabian et al. (2012) conducted a comprehensive evaluation of the soil nail system's performance under steady-state conditions. The research focused on examining the distribution of earth pressure at the soil nail placement site and identifying various geometrical factors that influence the effectiveness of soil nails. The investigation encompassed crucial elements such as nail length, nail inclination, slope inclination, length pattern, and nail bar arrangement to assess their impact on the soil-nailed structures' performance. The soil's characteristics were assessed by an Elastic-Perfectly-Plastic constitutive model with the Mohr-Coulomb failure criterion. Notably, the study found that soil nail length and length patterns significantly contribute to enhancing the stability of retaining walls. Detailed findings from the numerical analysis of soil nail performance can be found in Table 2.3 of the literature.

Table 2.3. State of art soil-nailing numerical approaches

Numerical and analysis approaches	**Considering factors**	**Observations**	**Reference**
Finite element (PLAXIS)	Construction stages and overburden pressure stages	The simulated soil nail model has similar capabilities to the actual soil nail model.	Mohamed et al. (2023)
SLOPE/W	Soil nail inclinations, Factor of Safety	The numerical test result indicated that the soil nail inclination was significantly affecting the factor of safety.	Dewedree, and Jusoh (2019)
Finite element method	Wall geometry and soil parameters	Based on the numerical findings, it is observed that an increase in the step width leads to a decrease in wall deformation and nail forces.	Ahmadi, and Borghei (2018)
PLAXIS 2D finite element analysis	maximum horizontal nail and wall displacement, nail's maximum shear & axial force	As per the test findings, the soil nail's length is notably impacted by the factor of safety. On the other hand, the results of the numerical analysis suggest that employing a soil nail wall to ensure stability in retaining systems was a favorable option.	Moniuddin et al. (2016)

PLAXIS 3D	Failure mechanism of soil nail	Through finite element analysis, it is evident that the slopes exhibit distinct variations in their maximum load-bearing capacity and settlement at the crest under the applied surcharge load.	Rawat and Gupta (2016a)
limit equilibrium theory framework	Stability of soil nail, Soil shear failure	The test result moreover equal to the traditional limit equilibrium methods	Deng et al. (2017)
fast lagrangian analysis of continua (FLAC3D)	Excavation stability	The numerical calculations align well with the observed monitoring data, showing a high level of consistency.	Liu et al. (2016)
PLAXIS 2D and SLIDE	Safety factors	FEM software program data was compared to mathematical expressions	Ramkrishnan et al (2019)
LEM and FEM	critical slip surfaces FOS and nail forces	Both approaches 'failure surfaces are found to differ considerably In all slop conditions, the large nail force was observed at 45^{O}on limited equilibrium method. Similarly, 60^{O} condition slop angle was increased on the finite element method	Rawat, S. and Gupta et al. (2016b)
Finite element method	Slope stability	The study results show that the soil cohesion and friction	Sharma et al. (2019a)

		angle increase as the slope safety factor increases.	
Finite Element Method	Safety factor	From the static and unstable soil analyzes it appears that the soil nail displacement is low.	Mohammad Zaki et al. (2015)
strength reduction method (SRM) and the LEM	FOS and Failure mode	According to this investigation, the FOS obtained from the SRM and the LEM exhibit close similarity in the majority of cases.	Wei and Cheng (2010)
LEM, FEM strength reduction factor	FOS	For soil nail designs on islands, it is advisable to opt for finite element methods over limit equilibrium methods.	Villalobos and Villalobos (2021)
limit-equilibrium method (LEM) and three-dimensional (3D) rigid-body rotational failure mechanism	FOS	The results of the 3D analysis demonstrated consistently higher FS values in all scenarios compared to the FS values obtained from the 2D analysis.	Basudhar et al. (2017)
PLAXIS 2D	Slope geometry and nail parameters	The optimal nail inclination at a horizontal angle was shown to range between 0 and 25°.	Elahi et al. (2022)

2.8. Soil Nailing Optimization

In a study conducted by Benayoun et al. (2021a), the stability of a vertically cut soil nail was analyzed using PLAXIS 2D through finite element analysis. The researchers aimed to enhance soil nailing stability by optimizing three input parameters. To achieve this, they employed three different optimization techniques and compared the resulting data to ensure accurate outcomes and identify the most effective optimization approach. The analysis revealed that the minimum factor of safety was attained with a structure length of 9 m, vertical span of 2 m, and inclination of 10°.

Sharma and Ramkrishnan (2020) used finite element analysis to study the possible parametric optimization in soil nailing by incorporating soil-nail interaction and the nail's pull-out strength. PLAXIS 2D and GEO5 represent two widely utilized numerical analysis software tools in the field of geotechnical engineering. They serve for conducting FEA and LEA. The parameters taken into account during FEA involve nail diameter, nail length, nail axial stiffness, nail bending stiffness, facing axial stiffness, and bending stiffness. Meanwhile, soil nail parametric optimization considers factors like pull-out strength using nail length pattern and soil nail interaction as well as limit equilibrium analysis.

Babu and Singh (2009) conducted a detailed investigation of the performance of a soil-nailed wall utilizing regularly used analytical and design techniques. The author compared the lateral displacement, a factor of safety ratings, and several design parameters of soil nail walls obtained using traditional design procedures and numerical simulations. Concerning the overall stability of the soil nail wall system, the influence of shear and bending stiffnesses of the nails seems to be relatively minor. Based on experimental findings, this technique shows promise as an effective, economical, and feasible option for reinforcing vertical or nearly vertical excavations in soil for various slope stability requirements in the field of geotechnical engineering.

Benayoun et al. (2021b) optimized the parameters of soil nailing using the computational optimizing process. By utilizing response surface methods (RSM), this study explored the impact of nail geometric parameters on the analysis of soil-nailed walls, identifying the key factors that significantly influence their stability and cost. The soil nailing process optimization considers three

main criteria: soil nail length, soil nail installation inclination, and vertical spacing between nails. RSM is used to determine the best optimal combination and safety factors. RSM box-behnken design was adopted following finite element analysis optimization.

Goyal and Shrivastava (2023) conducted experimentation on design parameters of soil nails using Box Behnken design (BBD) of response surface methodology (RSM), performed in design expert software. In the experimentation phase, a total of 25 runs were conducted to assess the significance of the developed quadratic model, which was analyzed using the analysis of variance (ANOVA) test. They indicated that the optimal results of DBN-CO were greater than RSM, DBN, and artificial neural network (ANN) methods. Based on prediction approaches the proposed hybrid DBN-CO results were in perfect agreement with experimental values and are additionally superior to the RSM, DBN, and ANN.

Mohamed et al. (2019) utilized Limit Equilibrium software (SLOPE/W) to optimize the design of soil-nailed walls. The optimization process considered three main criteria: soil nail length, inclination, and spacing. The soil nail length was found to significantly impact the soil nailing performance, as shorter soil nails gradually reduced the factor of safety. Similarly, lower inclination angles of the soil nail were observed to increase the safety factor. Through the optimized soil nail specifications, the cost was reduced by 18% to 53%.

Dhakal and Acharya (2019) improved the stability of steep cut slopes with the help of soil nailing. The soil-nailed steep-cut slop structure was optimized using numerical simulation. The failure mode and factor of safety were considered in the soil nail performance evaluation section. Experimental and numerical methods were used to calculate performance, and PLAXIS 2D was used for numerical simulation. The soil parameters and shear parameter bead test were conducted in a laboratory setting.40 simulations were employed in the analysis due to enhanced soil nail parameter computation. The optimal soil nail lengths were 5 m, 5.5 m, 6 m, and 7 m, respectively. The soil nail's safety factor was increased by 10^{O} to 60^{O} and gradually decreased by 30^{O} to 60^{O}. The soil nailing bead's different types of optimization technic and optimized factors of literature are shown in Table 2.4.

Table 2.4. State of art soil nailing optimization approaches

Reference	Optimization techniques	Optimized factor	Observations
Benayoun et al. (2020)	Genetic algorithm method	Soil nail parameter	The optimum method was used to find the optimum soil nail inclination, length, and spacing.
Benayoun et al. (2021b)	Response surface methodology (RSM)	vertical spacing between nails, inclination, and Nail length,	Based on the ANOVA data, it is evident that altering the nail length has a more significant impact on both soil nailing stability and cost.
Benayoun et al. (2021a)	Genetic Algorithm (GA), Taguchi's Design of Experiment (DOE), and Particle Swarm Optimization (PSO).	Nail inclination angle, ratio of nail length to wall height, and vertical spacing between the nails.	The optimization techniques optimized value to minimize the safety factor All three-optimization result values are equal
Liu et al. (2021)	support vector machine (SVM), Artificial neural network (ANN), and random forest (RF)	Soil nail horizontal displacement	The promising result was obtained through machine learning approaches.
Imani and Babaei (2021)	Genetic algorithm genetic algorithm (MATLAB)	Factor of safety	To achieve the most favorable (minimum) factor of safety value, an optimization approach

			is employed to compute the unknown parameters.
Shirgir et al. (2023)	Metaheuristic and reliability-based design optimization	Soil nail mechanical and geometrical property	The analysis of reliability-based design optimization suggests the potential development of a nailing system with predicted reliability and failure probability. The research findings highlight the significance of soil mechanical characteristics' uncertainties on the dependability of the ideally designed soil nail system.
Nowroozi et al. (2021)	FLAC3D finite difference software	Lateral pressure behind the wall, safety factor, and soil nail horizontal displacement	The result shows that installing two rows of nails significantly reduces the maximum wall displacement compared to 5 and 3 rows
Arvin et al. (2021)	Limit equilibrium based Prevalent Limit Equilibrium Method	Optimum nail inclination angle and safety factor	The results show that increasing the nail diameter causes an increase in both the safety factor and optimum nail Inclination angle. Additionally, an increase in soil friction improves the safety factor while just slightly increasing the optimum nail Inclination angle.

2.9. Research Gap

After conducting an extensive literature review on CN and HN several research gaps were identified, which have led to the establishment of the objectives for this present study.

Research Gap 1: Study of conventional and helical soil nails in cohesive soil

The existing literature primarily focuses on laboratory and numerical studies related to CN and HN, but the emphasis has been on cohesionless soil. Moreover, there is a lack of pull-out studies on different model nails specifically in cohesive soils.

Research Gap 2: Slope stability analysis of helical soil nail in cohesive soil

The literature review reveals that FEA and LEM are commonly employed for soil nail analysis. However, there is limited research that directly compares these two methods, particularly concerning the application of helical soil nails in cohesive soil.

Research Gap 3: Requirement of optimization and prediction approaches for helical soil nail parameters

From the existing literature on soil nailing research, very little work has been done for the optimization of conventional soil nails, and no work has been done for the optimization of helical soil nail parameters to avoid installation issues. Moreover, various studies have used only constant shaft diameter and variations in surcharge stresses as input parameters. No work has been performed using different shaft diameters, helix pitches, surcharge pressure, and inclination angles as input parameters for measuring the safety factor and pull-out resistance of helical soil nailing. To fill this research gap, this study investigates soil nailing behaviors and validates the helical soil nailing outcomes using RSM and a hybrid NN.

2.10. Summary

The literature done by various authors related to this thesis is summarized in this chapter. Various methods for soil nailing and affecting factors of system operation are elaborately discussed. The

soil nail system and performance and its types are reviewed; the soil nail system is studied in depth. The helical soil nailing and its different type of approaches is studied and traditional soil nail efficiency are studied. The different soil nail performance affecting factors are studied in this literature survey. In addition, the study of soil nailing and different types of performance evaluation methods in numerical and computer-based studies has been discussed. The computer simulation software utilized by various researches to determine the efficiency of materials and design in the soil nail components is also discussed briefly. Similarly, for the soil nail system, different variants of optimization approaches are thoroughly investigated in this chapter.

CHAPTER 3

EXPERIMENTAL DESIGN

3.1. General

The experimental setup, materials, and methods used in the current investigation are described in depth in this chapter. The materials used for the experiment as well as measurement procedures and standards used to determine their properties are briefly discussed. The chapter also includes the fabrication of testing instruments and nails. Besides, the installation and displacement-controlled pullout test protocols are provided. The pullout testing apparatus and its components are also studied in this chapter. The following subsection provides a brief description of the backfill material and its properties, soil nails and its installation as well as components used in the current investigation.

3.2. Backfill material

The soil was obtained from the surrounding area of the Ajay Kumar Garg Engineering College in Ghaziabad, India. To determine the qualities of the backfill, preliminary soil identification tests are conducted in the laboratory. The soil sample was subjected to sieve and hydrometer analysis by IS: 2720, Part-4 (IS 1985). The measurement procedures of various properties of the backfill material sample and the standards used for the measurement of properties are summarized as follows.

3.2.1. Soil sample characterization

The grain size analysis test is conducted to determine the distribution of different grain sizes present in a soil sample. This information is essential for classifying the soil and predicting its behavior. The test involves sieving the soil through a combination of 4.75 mm IS sieve and 0.075 mm IS sieve, followed by hydrometer analysis. The results indicate that the soil is predominantly composed of coarse-grained particles, primarily sand. Half of the soil particles passed through the 4.75 mm sieve, while 80% of the soil was retained on the 0.075 mm sieve. According to the test results, Cu and Cc were 18.61 and 2.37, respectively. Figure 3.1 indicates the soil sample's particle size distribution. Natural water content was recoded as 12% as per IS2720-2:2020. Based on the

results of the Atterberg test according to IS 2720-5:2020, the soil exhibits a Liquid Limit (WL) of 30, Plastic Limit (WP) of 15.6, and Plasticity Index (IP) of 14.4. Accordingly, following the Indian Standard Soil Classification System, the soil is classified as clayey sand (SC). Soil's maximum dry unit weight was determined to be 16.87 kN/m^3 through a light compaction test conducted by IS 2720-7:2021 guidelines. The specific gravity of the soil was measured using the Pycnometer method as per IS 2720-3(1):2021 standard, resulting in a calculated value of 2.65. Additionally, the relative density of the soil was determined using the IS 2720-14:2020 standard, yielding a relative density of 65%.

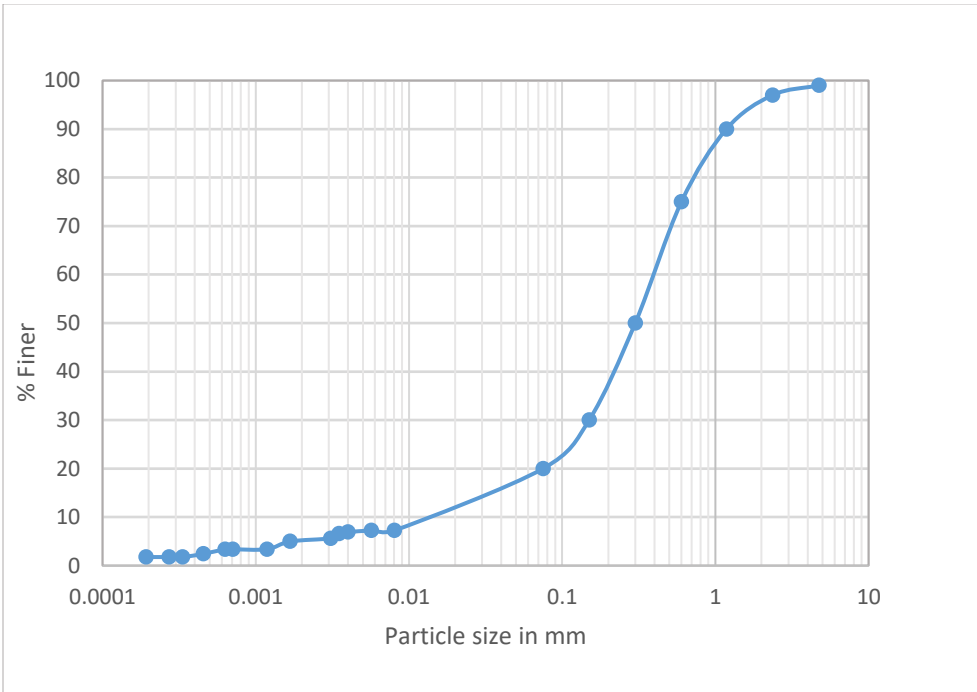

Figure 3.1. A soil sample's particle size distribution

3.2.2. Cohesion and friction angle

The soil's physical characteristics, namely the frictional angle, and cohesion, play a significant role in determining factors like rupture angle, shear strength, factor of safety, and slope stability in soil. The friction angle is the angle resulting from the interaction between normal reaction and friction limitations. It reflects the soil's shear strength. On the other hand, cohesion refers to the ability of soil particles to bind together. Cohesive soils, such as silts, clays, or fine-grained soils, exhibit

strong binding properties. Higher cohesion reduces the likelihood of soil crumbling, making vertical slope excavation feasible in areas with such soils. The Mohr-Coulomb failure analysis is commonly employed to determine cohesion and friction angle in soil samples. This analysis relies on a set of linear equations to describe the failure conditions of isotropic materials. The Mohr-Coulomb failure criterion defines the soil material's shear stress as the product of normal stress, the tangent of the friction angle, and the added cohesion. These shear stress parameters can be accurately determined through the triaxial test, which applies to all types of soils. The test offers significant advantages as it allows for control of various soil conditions such as drainage, pore water pressure, and volume, leading to more efficient and precise measurements of the parameters.

The triaxial test is performed following the IS 2720-11: 2021 standard. Figure 3.2 illustrates the schematic of the triaxial test apparatus. Within the apparatus, a de-aired coarse porous disc is positioned on the pedestal, and on top of it, a disc-shaped filter paper is placed. The cohesive soil specimen is then positioned over the filter paper, and another porous disc is placed on top of the specimen. The entire sample is enclosed in a rubber membrane and securely sealed with a ring. Over the base of the apparatus, the triaxial cell is placed and tightened through nuts. The specimen is then consolidated by applying pressure through water filling method. The applied pressure is continued till the change in specimen volume stops. After consolidation, the load and pressure measuring devices are attached to the specimen, and shearing is conducted by applying load. The readings for the corresponding loads are collected till failure in the specimen occurs. From the load and change in volume, the stress values are calculated. The Mohr Envelopes are drawn for over-consolidated clay in terms of effective stresses, and the test for at least three samples should be carried out by altering the load cells. Even though the initial envelop is curved, it is approximated to a straight line to reduce the complexity. The cohesion and friction angle were calculated from the envelope using equation 3.1, resulting in values of 31º and 22 kN/m^2 for the internal friction angle and cohesion, respectively. Table 3.1 provides a comprehensive listing of the assessed geotechnical characteristics of the soil material.

$$s = c + \sigma \tan \phi \tag{3.1}$$

Where c is the soil cohesion and ϕ is the friction angle

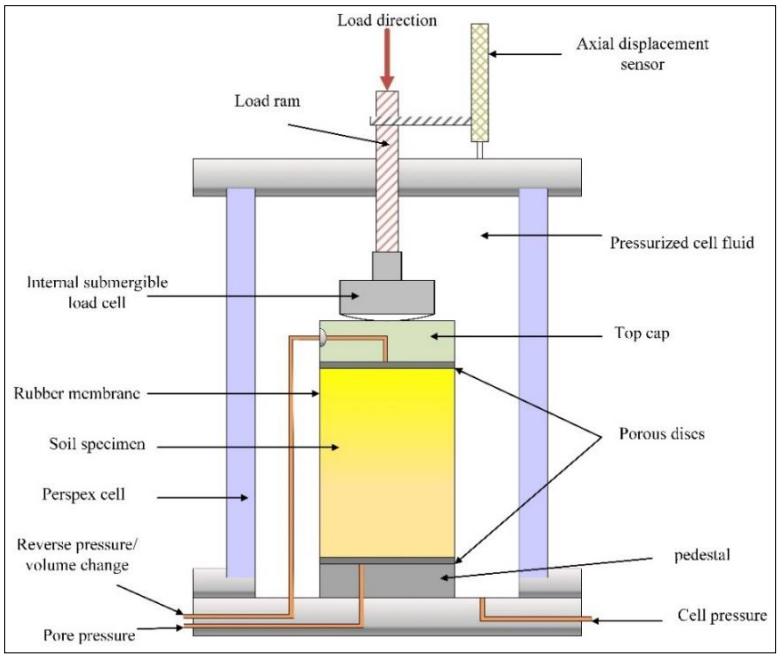

Figure 3.2. Triaxial test apparatus

Table 3.1. Soil sample's geotechnical characteristics

Properties	**Value**
Specific Gravity, Gs	2.65
D10(mm)	0.023
D30(mm)	0.15
D60(mm)	0.42
D50(mm)	0.30
Coefficient of curvature, C_c	2.37
Coefficient of uniformity, C_u	18.61
Friction angle, Φ (°)	31
Cohesion, c (kN/m^2)	22
Relative density (R_D)	65%

Yd(min)(kN/m3)	13.13
Yd(max)(kN/m3)	16.87
Gravel percentage	1.0
Sand percentage	79.0
Silt percentage	14.88
Clay percentage	5.12
Liquid Limit	30
Plastic Limit	15.6
Plasticity Index	14.4
Soil classification	Clayey Sand

3.3. Soil nail

The conventional and helical soil nail specimens seen in figures 3.3 (a) and 3.3 (b) were made of mild steel. The conventional soil nail has a solid shaft with small patterns for obtaining better grip and cohesion with the soil. The HN is the improved form of the conventional soil nail where the mild steel shaft of the soil nail is welded with helical discs of a certain diameter. The helical discs are expected to be providing better cohesion behaviour with the soil. The soil nail interaction is also expected to be improved due to the helical disc.

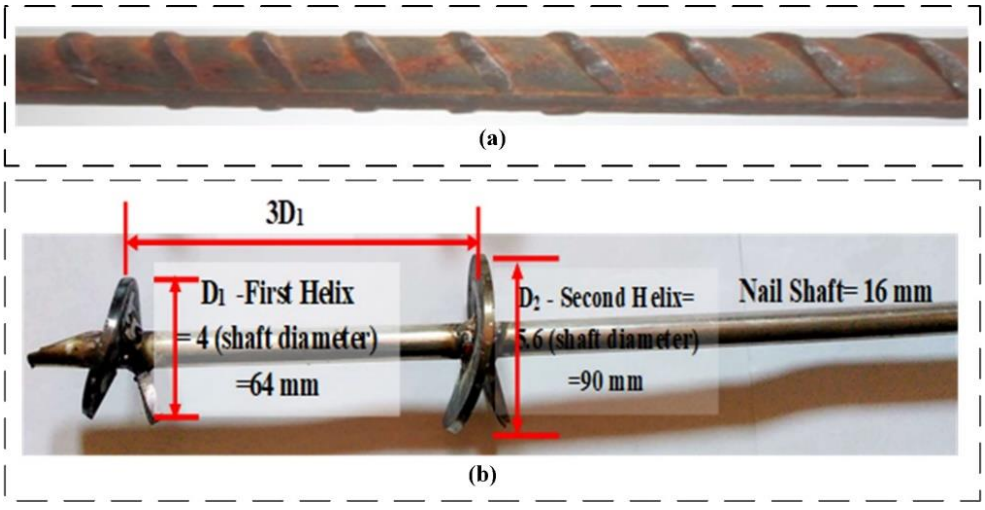

Figure 3.3. (a) Conventional soil nail (ribbed steel bar); (b) Helical soil nail

3.3.1 Scaling and fabrication of soil nails

While the helical diameter is 4 to 6 times larger than the shaft diameter depicted in Figures 3.3(a) and 3.3(b), both conventional and helical soil nails have a 16 mm diameter shaft. The length of the nail samples in this investigation was 1 m, while the nail's effective length was engaged into consideration to be 0.7 m. The scale effect phenomenon may have an adverse impact on the helical soil nail laboratory test findings in cohesive soil. The scale effect is explored through two methods:

i. Analyzing the impact of mean particle size on the helical bearing.

ii. Investigating the effects of mean particle size on nail shaft behavior.

If the ratio of the smallest shaft diameter (d_s) to the mean soil grain size (D_{50}) satisfies the given equation 3.2 then there is no scale effect on the nail shaft.

$$\frac{d_s}{D_{50}} > 30 - 50 \tag{3.2}$$

On the other hand, concerning the helical plate, scale effects are commonly associated with the effective radius of a helix (E_r), which can be determined using equation 3.3.

$$E_r = \frac{D_h - d_s}{2} \tag{3.3}$$

Equation 3.4 be used to calculate the ratio of a helix's effective radius (E_r) to its mean grain size (D_{50}) when there is no scale impact on the helical plate.

$$\frac{E_r}{D_{50}} > 58 \tag{3.4}$$

If equation 3.2 and equation 3.4 are satisfied, no scaling effect is seen for helical elements.

In the current investigation minimum shaft diameter (d_s) is equal to 16 mm, the soil's mean grain size (D_{50}) is equal to 0.3 and the helix's effective radius (E_r) is calculated by equation 3.3. From the values d_s/D_{50} and E_r/D_{50} are calculated as 53.33 and 123.3, respectively. So, the present study satisfies both the norms according to equation 3.2 and equation 3.4. The model test results indicate no significant scale effect.

To meet the no-scale effect criteria, the present study's scale factor was set at 5.55. Hence, the scale effect won't have an impact on the lab results. The diameter of the model nail specimen was chosen after the original diameter was scaled down using equation 3.5.

$$M_d = \frac{P_d}{k} \tag{3.5}$$

Where, M_d = Diameter of the model nail

k = Scaling factor

P_d = Prototype nail's diameter.

3.3.2. Fabrication of model test tank and soil nailed slopes

In this study, an investigation was conducted using a tank measuring 2000 mm in length, 1100 mm in width, and 1100 mm in height. The tank size was designed to be ten times larger than the largest helical diameter, combined with the smallest tank dimension, to entirely avoid the border effect in the sample tank. The soil sample was compacted into ten layers, each 100 mm thick, forming a total height of 1000 mm. To further investigate the behavior of nails under varying pressures, the sample was placed beneath an 8 mm thick steel plate and subjected to three different overburden pressures: 10kPa, 20kPa, and 40kPa, respectively.

The pullout resistance is significantly influenced by the overburden pressure. Soil nails are installed in environments with similar overburden pressure. Large soil slopes are divided into smaller segments to prevent the build-up of excessive overburden pressure, which can lead to an arching effect and a subsequent reduction in pullout resistance. Based on this suggestion, other studies used a different range of surcharge pressure, which is shown in Table 3.2. As a result, a hydraulic jack was used in the current investigation to apply low confining pressure ranges of 10kPa, 20kPa, and 40kPa.

Table 3.2. Researchers employed a variety of overburden pressure ranges in their experiments

S. No	Overburden pressure	References
1.	0 to 150kPa	Pradhan et al. (2006)
2.	5.6 to 22.7kPa	Milligan GWE and Tei K (1998)
3	5 to 50kPa	Sharma et al. (2021e)

3.4. Experimental procedure

3.4.1. Soil nail installation process

The distinction of this study is that the techniques utilized for installing CN and HN are the same as those employed to put these nails in the field. Using a drilling machine, the trench was created for conventional soil nails towards the middle, 0.5 m from the base. According to the Federal Highway Administration in Washington, DC, in 2015, a soil nail can be installed at an angle between 0° and 20°, with 15° being the ideal angle. However, one may choose any angle between 0 and 20º depending on the simplicity of installation or the site conditions. After inserting the conventional nail to a depth of 700 mm, the grouting procedure was carried out using gravity flow. As a result, following the grouting procedure, pressure is unchanged. In the grouting process, CN employed a w/c ratio of 0.55. The nail was placed for the installation of HN at a 10 RPM revolution rate and a 10 mm/min regulated displacement rate.

The soil nail installation is a critical phase due to the disturbances it causes in the soil mass. To monitor this process, earth pressure cells were positioned around the soil nail. For calibrating the earth pressure cells and load cells, a perspex cylinder occupied by water and wrapped with a pressure controller was employed. The data logger recorded the earth pressure/load cell response during each increment of water pressure, varying from 0 kPa to 100 kPa in the cylinder. The disruption caused by the installation operation of soil nails makes this step of execution one of the most crucial. As seen in Figure 3.4, earth pressure (EP) cells around the soil nail were used to monitor the installation process. EP cells have a 3 MPa capacity and a 0.01 MPa sensitivity, respectively. A drill chuck was used to drill the soil nail cell for the placement of standard soil

nails. Significant variations in internal stresses were observed during drilling. Figure 3.5 and 3.6 shows the various forces acting on HN and CN.

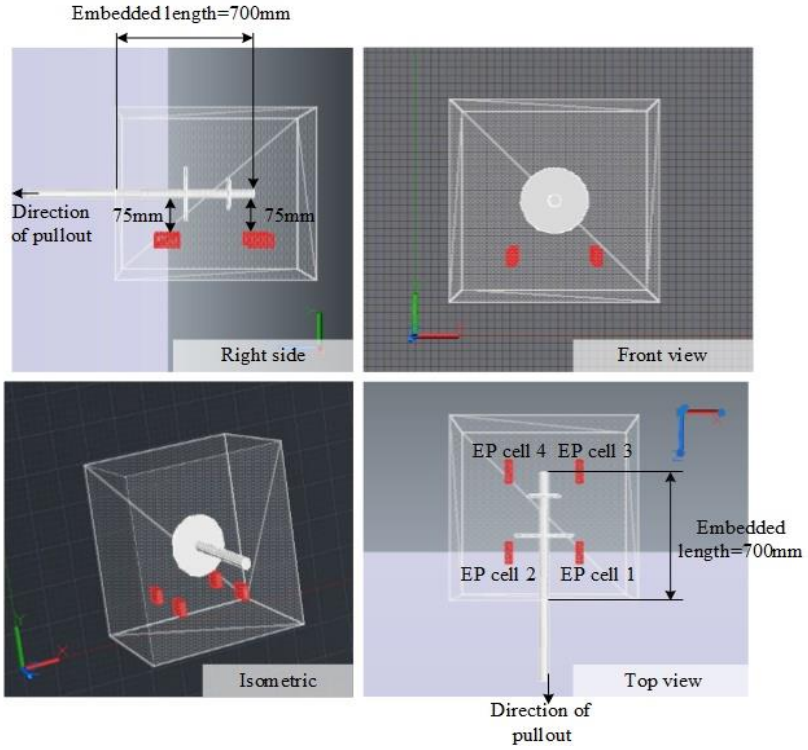

Figure 3.4. A pictorial representation of earth pressure cell placement

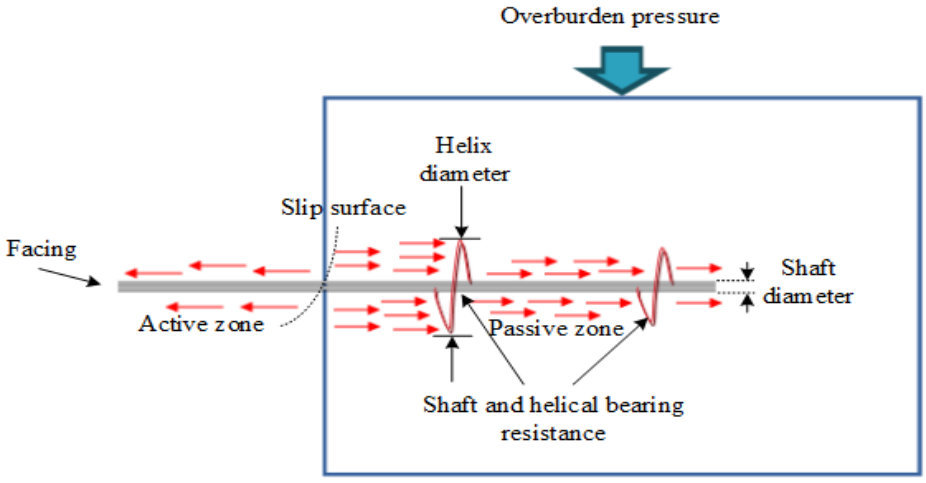

Figure 3.5. Diverse forces that impact a HN (Goyal and Shrivastava 2023)

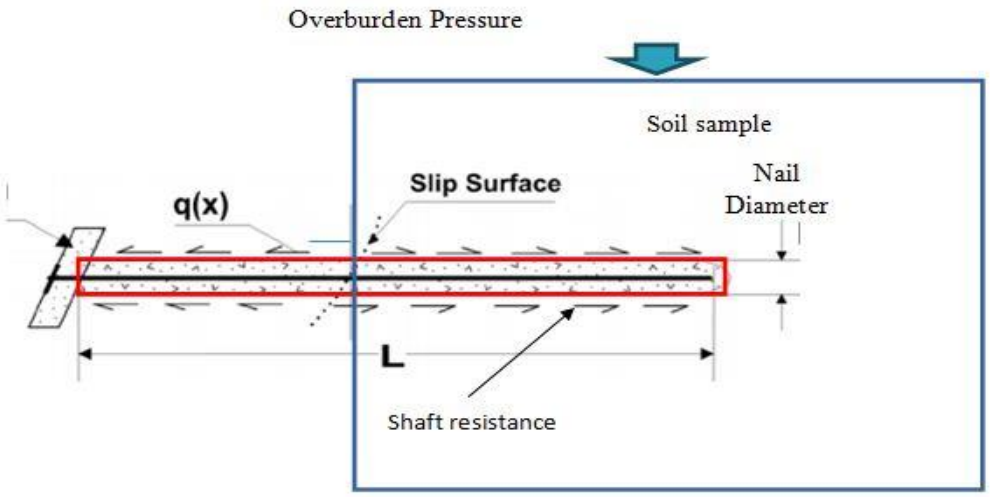

Figure 3.6. Diverse forces that impact a CN (Goyal and Shrivastava 2023)

3.4.2. Pullout testing process

The displacement-controlled apparatus with a pullout capacity of 50 kN was used to test the pullout of both the CN and the HN (Niroumand and Saaly 2019; Sharma et al. 2020a). Both of the nail types used in the investigation had a 10 mm/minute pullout displacement rate (Lazarte et al. 2015). When the resistive force increases by less than 1% for every 1 mm of displacement or when the displacement surpasses 30 mm, the bond failure value is determined (Zhang et al. 2009; Anil and Chen 2004).

The author has designed and fabricated the apparatus specifically for pullout testing and has also applied for a patent under the Office of the Controller General of Patents, Design & Trade Marks, Government of India. As per the detailed conditions provided under Chapter VI of the Indian Patent Act (Section 29-34), the actual apparatus applied for the patent should not be published before receiving the final patent. Hence, only a line diagram is an only schematic diagram of the laboratory pull-out device given in figure 3.7.

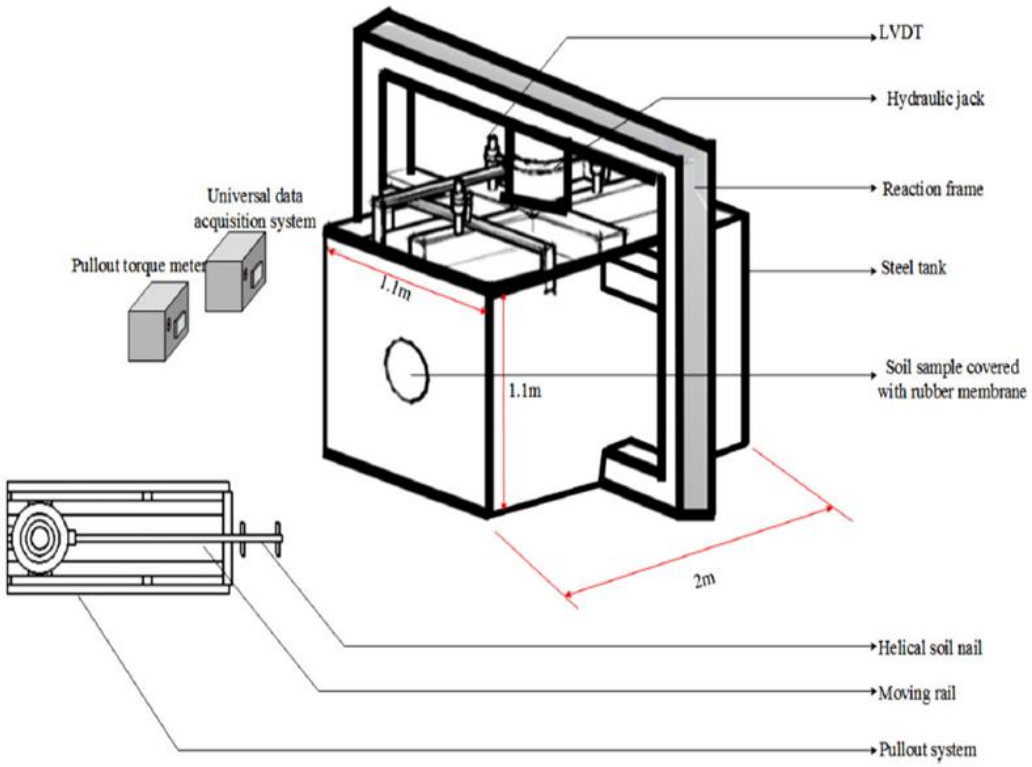

Figure 3.7. Pullout device test apparatus

3.5. Components of pullout testing apparatus

Soil nail pullout testing apparatus typically consists of the following components:

- Linear Variable Differential Transformer (LVDT)
- Hydraulic jack
- Reaction frame
- Steel tank
- Rubber membrane
- Pullout system
- Pullout torque meter
- Universal data acquisition system
- Moving rail

3.5.1. Linear Variable Differential Transformer (LVDT)

The Linear Variable Differential Transformer is abbreviated as LVDT. It is an electromechanical transducer that is used in the conversion of the linear motion of an object into a corresponding electrical signal. Through these electrical signals, the displacement of an object can be determined. The LVDT sensor works on the principle of inductance in transformers. This sensor contains a primary coil and a secondary coil which are winded around a movable core. When a power supply is given to the primary coil, the magnetic inductance is developed between the primary and secondary coil. As per the movement of the core, the inductance varies, which provides the displacement value of the core as shown in Figure 3.8. The available range of measurement in this sensor is from ±0.01 cm to ±25 cm. For current research, the LVDT sensor with a range of 0.1 mm to 100mm is utilized. The linear movement results in a voltage output ranging from 1 V to 24 V rms, with frequencies spanning from 50 Hz to 20 kHz. LVDT sensors are offered in options for both AC and DC current. AC-type sensors require no internal electronics, carrier amplifier, external oscillator, or demodulators and filters to function, distinguishing them from DC-type LVDT sensors. However, DC sensors need a carrier generator or signal conditioning module. The major merits of this sensor are the contactless core and coil, which eliminates the wear of parts due to friction. This improves the mechanical life of the sensor.

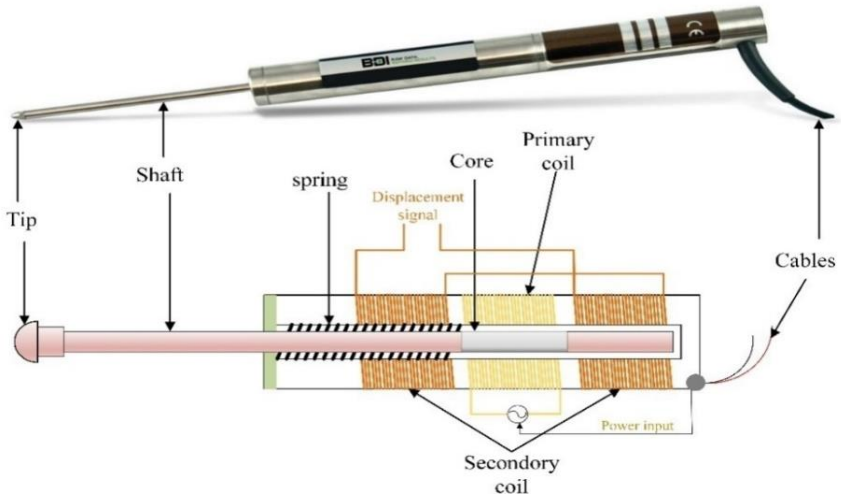

Figure 3.8. LVDT sensor

3.5.2. Hydraulic jack

A hydraulic jack is a device used to carry large loads with the use of less amount of force. In the lifting process of heavy loads, hydraulic jacks are employed. They are extremely useful mechanical device, that uses hydro pressure energy to lift heavy loads over a large distance. The major applications of hydraulic jacks are in the automotive, industrial, and construction industries. The functioning of a hydraulic jack is based on Pascal's law, which dictates that any pressure exerted on a fluid within a sealed container will be equally transmitted to all parts of the fluid and the container walls without any alteration in its intensity. To operate the hydraulic jack, a hand pump is employed to pressurize the fluid chamber, and this pressure is subsequently transmitted to the jack, adhering to the principles of Pascal's law. The hydraulic jack and the pump are used to pressurize which is shown in Figure 3.9. A hydraulic cylinder is linked to the hand pump via both the inlet and outlet connections. When the hand pump is operated the fluid enters into the cylinder which raises the piston, which in turn elevates the jack. When the pressure lever is released the fluid inside the cylinder is sent back to the storage under the hand pump, so that the jack returns to its normal position. A pressure gauge is connected to the hand pump to monitor the pressure of the fluid inside the cylinder.

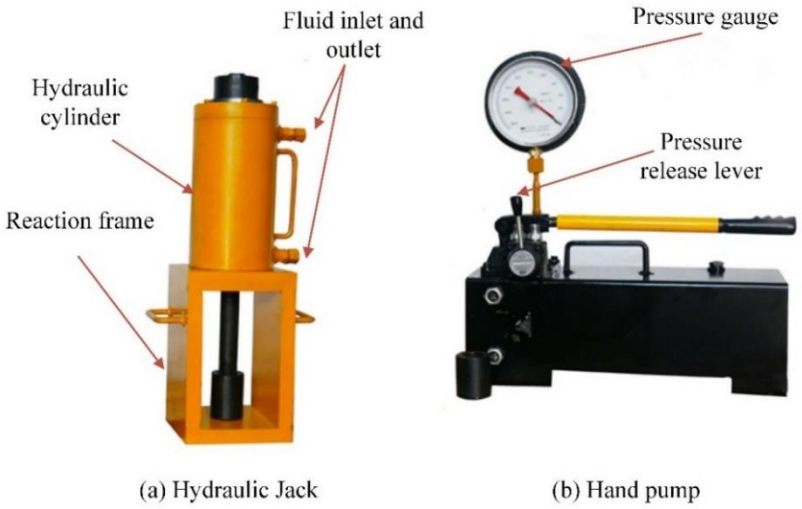

Figure 3.9. Hydraulic jack and pump

3.5.3. Reaction frame

The frame used to withstand the reaction force arising due to the input force given during the static pull-out test is known as a reaction frame. The frame used must have high load-withstanding capacity. The dimension of the frame should not interrupt the pullout testing, so it is designed in different shapes as per the requirements. Some pull-out testing machines contain solid cylindrical rods as the reaction frame. In the current experiment rectangular-shaped frame is used. Without the reaction frame, the force given to pull the nail cannot be transmitted towards the nail.

3.5.4. Steel tank

A steel tank is used to conduct a sample soil nailing process where the pullout test is conducted. To mitigate the boundary effect, the tank's dimensions are set at ten times greater than the highest helical plate diameter. To account for each dimension's boundary condition, the tank's size is specified as 2 meters in length, 1.1 meters in width, and 1.1 meters in height, as depicted in Figure 3.10. To facilitate the installation and pullout process of the HN, a spherical opening of 160 mm is positioned on one side of the tank. On the top side, the sensor and compacting apparatus are placed, for loading and testing of soil sample. The reaction plate is supported on the steel tank.

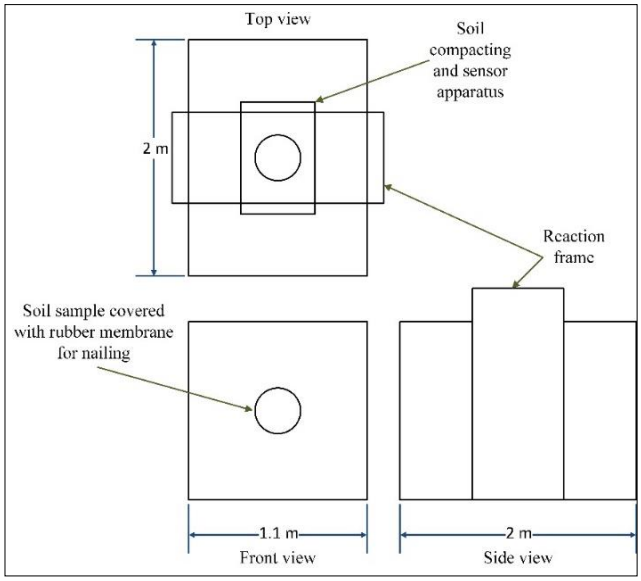

Figure 3.10. Steel tank in pullout testing apparatus

3.5.5. Rubber membrane

To fill and compact the soil inside the test tank, a hole is placed at one side of the tank, which is closed with a rubber membrane for soil nailing. The rubber membrane acts as an enclosure for the compacted soil samples inside the testing tank. The soil nails are inserted through the rubber membrane using the nailing apparatus.

3.5.6. Pullout system

The pullout system is the major part of the pullout testing. It contains the different types of power tools to pullout the nail from, under the soil. The most used pullout systems are hydraulic or electrical-based. In a hydraulic-based pullout system, the force from a hydraulic pump is used to pullout the nail. In the electrical system, the torque obtained from the electric motor is used to pull the nail from the soil. The pullout system contains two three-phase motors, one for installation and the other for pullout. Both motors are connected to the displacement sensor to detect the movement of the soil nail. A nail placement system and an angle adjustment system are present in the pullout system, which helps in the installation of nails at the desired angle.

3.5.7. Pullout torque meter

In the helical soil nailing process, a torque meter is employed to measure both the real-time nail installation torque and the pullout torque. A transducer is present in the pullout apparatus which is connected to the measuring unit shown in figure 3.11. The transducer converts torque into electrical output and the torque is measured as per the output voltage. During the helical soil nailing process, the torque meter was utilized to record and display both the installation torque and the pullout force. The results are collected and stored for the entire pullout testing process for later analysis. Furthermore, strain gauges are also placed in the nail shaft to determine the torque effect in the soil nail.

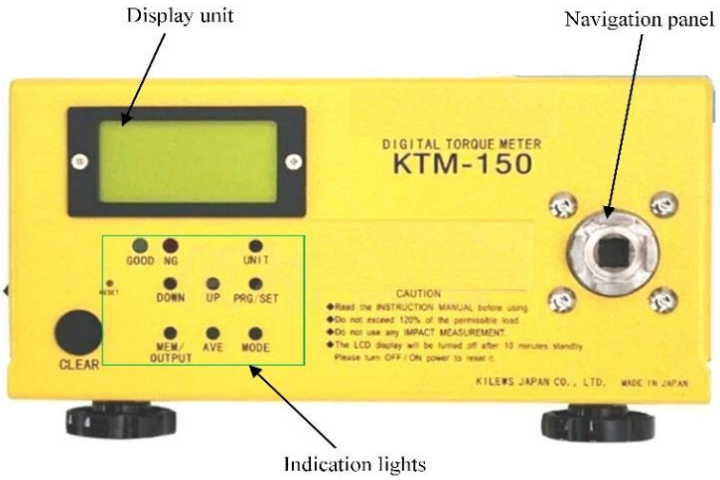

Figure 3.11. Torque meter in pullout test

3.5.8. Universal data acquisition system

To collect the multiple real-time data, a sixteen-channel universal data acquisition system is utilized in this experiment shown in figure 3.12. This system continuously records the data of horizontal and vertical displacement from the LVDT sensors. Furthermore, the surcharge pressure and pullout force data from the load cells are also simultaneously recorded in the data logger system. This data collection happens for the entire experiment and is shown in any type of digital display unit. The data can be stored for later analysis in a USB storage device, through the USB port in the front panel.

Figure 3.12. Data logger system

3.5.9. Moving rail

The moving rail is used in the movement of the pullout and installation setup of the nail. It is a shaft that has a sliding or threaded movement setup over the surface. The shaft used in the moving rail mechanism must have resistance against varying stress and strain produced during the soil nailing process. The moving rail is more important for the nail installation process because the nail should be in constant movement toward the soil according to the rotational torque given to the nail. This provides a better installation of nails in the soil with better soil-nail interaction.

3.6. Summary

The backfill material's characteristics samples utilized for the present experiment are determined using the international standard process. The procedure for properties determination such as friction angle, relative density, specific gravity, cohesion, and coefficient of curvature is summarized in this chapter. The types of soil nails used and their scaling and fabrication processes are also analyzed. The installation and pullout behavior determination are conducted and the components of the pullout apparatus are discussed.

CHAPTER 4

MATHEMATICAL AND NUMERICAL MODELLING

4.1. General

In geotechnical engineering, soil nails play a vital role as a means of ground reinforcement, and mathematical and numerical modeling serve as essential tools for comprehending their behavior. These soil nails are primarily utilized for providing lateral support to excavated slopes or stabilizing vulnerable existing slopes and embankments. By employing mathematical and numerical modeling techniques, one can make predictions about the behavior of soil nails under diverse loading conditions, including fluctuations in soil moisture, variations in ground conditions, and alterations in the applied load. This modelling can help engineers design more efficient and effective soil nail systems, reducing costs and improving safety. Conventional soil nails are typically straight, while helical soil nails have a twisted shape that allows them to provide additional reinforcement against lateral forces. Mathematical and numerical modelling can be used to analyse the behaviour of both types of soil nails, including their deformation, stress distribution, and load-carrying capacity. Overall, mathematical and numerical modelling are powerful tools for understanding the behaviour of soil nails and designing more effective ground reinforcement systems.

4.2. Mathematical modelling

The process of mathematically modeling soil nails encompasses studying how both nails and surrounding soil respond to different loads and boundary conditions. This procedure applies to CN and HN, wherein analyzes the behavior of the nail and the surrounding soil under a diverse set of loads and boundary conditions. The following steps are typically followed in the mathematical modelling of CN and HN: characterize the soil properties, determine nail properties, develop the soil nail model, apply load and boundary conditions, and analyse soil nail behaviour.

The bond strength of the soil nail wall system may be verified or ascertained with the use of mathematical modelling of soil nail load-displacement behaviour. The equilibrium forces serve as the foundation for the hyperbolic model of soil nails under external force. The curve is split into

pre-peak and post-peak behaviour. Sharma et al. (2021e) developed mathematical models for soil nails exposed to external force. In the context of CN and HN, distinct expressions define the pre-peak and post-peak stages. The pullout force pre-peak stage (F) relies on the soil nail's surface area, whereas interface friction between the soil and nail influences the same stage for HN. The equilibrium equation of various forces serves as the basis for the load-displacement equation. The pullout force equation that was obtained from the equilibrium equation is presented in equations (4.1) and (4.2).

$$F(y) = \frac{\pi}{4} D_{sc}^2 E\varepsilon(y) \tag{4.1}$$

$$F(y) = \frac{\pi}{4} D_{hh}^2 E\varepsilon(y) \tag{4.2}$$

Where,

$F(y)$ =External pressure exerted on a soil nail

D_{hh} =HN helical diameter

D_{sc} =CN shaft diameter

E =Soil-nail’s elasticity modulus

$\varepsilon(y)$ = Axial strain at point y

The correlation between displacement and pullout force in equations (4.3) and (4.4) is expressed by a second-order differential equation.

$$\frac{\partial^2 F(y)}{\partial y^2} = \frac{4KF(Y)}{\pi^2 E {D^3}_{hh} {\tau^2}_{ul}} \left[\frac{dF(y)}{d(y)} + \pi D_h \tau_{ul} \right]^2 \tag{4.3}$$

$$\frac{\partial^2 F(y)}{\partial y^2} = \frac{4KF(Y)}{\pi^2 E D^3{}_{sc} \tau^2{}_{ul}} \left[\frac{dF(y)}{d(y)} + \pi D_h \tau_{ul} \right]^2 \tag{4.4}$$

The theoretical information for this study was taken from Sharma et al. (2021a), and it was solved using Wolfram Mathematica 7.0 (Wolfram 1992) by using appropriate boundary conditions as stated in equations (4.5) and (4.6).

$$F_0 = F(y = 0) \tag{4.5}$$

$$F(y = L) = 0 \tag{4.6}$$

Where,

L = Length of the nail

F_0 = The null force at zero displacement

The residual factor was estimated for CN and HN in the post-peak stage using equation (4.7) (Sharma et al. 2021e, Sharma et al. 2021a).

$$f = \frac{\tau_s - \tau}{\tau_s - \tau_p} \tag{4.7}$$

Where,

τ = Primary shear stress

τ_s = Peak shear stress,

τ_p = Residual shear stress.

During the post-peak stage, equation (4.8) describes the relationship between the change in residual factor and displacement. (Sharma .2021a).

$$f = 0.97\ln[u(y)] - 3.12 \quad (4.8)$$

Equations (4.9) and (4.10) give the relationship to predict pullout force and pullout shear stress under different overburden for CN and HN, using experimental and theoretical data.

While using CN:

$$\text{Shear stress or peak pullout capacity} = 1.3q+28 \quad (4.9)$$

While using HN:

$$\text{Shear stress or peak pullout capacity} = 2.32q+29 \quad (4.10)$$

Where,

q= Overburden pressure

4.2.1. Factor of safety of CN and HN

The FOS is a crucial metric that represents the safety margin or the ratio between the extreme capacity of a soil nail and the applied load. FOS equations dictate that the value must be greater than 1 to ensure the soil nail system can safely withstand the applied load. The soil shear strength parameters, geometry, and nail material all affect the (FOS) in a soil-nailing system. The LEM is a secure approach to designing soil slopes using equation (4.11), FHWA (Lazarte et al. 2015).

$$FOS = \left(\frac{\left(F_r \cos(\psi - i) + \{(w+q)\cos\psi + F_r \sin(\psi - i)\}\tan\phi\right)}{(w+q)\sin\psi} \right) \quad (4.11)$$

Where,

w = Soil mass weight (γh)

γ = Soil's unit weight

F_r = Equivalent nail force = $0.75\gamma_s S_h K_a z S_v$

S =Vertical spacing

S_h = Horizontal spacing

K_a = The active earth pressure coefficient = $\frac{1-\sin\phi}{1+\sin\phi}$

ψ = A failed inclination plane = $45^\circ + \frac{\phi}{2}$

q = Overburden pressure (For example, 10kPa, 20kPa, and 40kPa in the current study)

i = Inclination of Nail (i=0 for this case)

Equation (4.11) has the drawback of calculating an equivalent safety factor for various specimen types of nails. To put it another way, the FHWA's equation (Lazarte et al. 2015) is only appropriate for typical soil nails and cannot predict accurately the FOS for soil nails with a different profile or different geometry. Also, the equation is inadequate for calculating the FOS for HN since it may replicate the lateral pressure, installation effect, and 3D effect of preferred soil. The authors of the current work have lessened their originality by using the concept of a helical pile or anchor to calculate the FOS of HN.

The following equation (4.12) is used to calculate the FOS for various kinds of soil nail structures.

$$F_s = \frac{F_u}{FOS} \tag{4.12}$$

Where,

F_s =Pullout load, kN

FOS =factor of safety

F_u =the maximum strength of the helical soil nail, KN

As the ratio of helical's spacing to diameter was chosen to be 3 in the study, cylindrical shear failure will be the mode of failure. When there occurs a cylindrical shear failure, the maximum pullout capacity for HN is given in equation (4.13).

$$F_u = 2\pi R h_s (c + K_0 q \tan\phi) + A_h (cN_c + qN_q) \quad (4.13)$$

Where,

h_s = Helical spacing

K_0 = Earth pressure coefficient at rest $(1 - \sin\phi)$

A_h = Bigger helix area

R = Helics average area

c = Cohesion

N_q and N_c =The Dimensionless Bearing Capacity Factors for Meyerhof determined using equations (4.14) and (4.15)

$$N_q = 1 + 0.56(12\phi)^{\phi/54} \quad (4.14)$$

$$N_c = (N_q - 1)\cot\phi \quad (4.15)$$

Equation (4.16) shows the ultimate pullout capacity for CN,

$$F_u = \pi L_N \tan\delta d_s \sigma_{avg} \quad (4.16)$$

Where,

σ_{avg} = Average normal stress which is calculated using equation (4.17) (Sharma et al. 2020b, Sharma et al. 2021e, Sharma et al. 2019b, Rotte and Viswanadham 2013, Sharma et al. 2021b, IS 1985, Milligan GWE and Tei K 1998)

$$\sigma_{ang} = \frac{\sigma_h + \sigma_v}{2} = \frac{\sigma_v(1+K_0)}{2} = \frac{\sigma_v(2-\sin\phi)}{2} \quad (4.17)$$

Where,

σ_v = Vertical stress

σ_h = Horizontal stress

4.3. Numerical modelling

Computer software is used to simulate the behaviour of CN and HN reinforcement systems in numerical modelling. This type of modelling is frequently employed to anticipate system performance in various soil types and loading conditions. The initial step in CN and HN numerical modelling is to create a detailed 3D model of the soil, reinforcement system, and support structure, using specialized software like PLAXIS, ANSYS, or ABAQUS. Soil properties can be obtained from laboratory testing or empirical correlations based on soil type, while reinforcement system properties can be obtained from manufacturer specifications or testing. Once the model is set up and its properties are defined, various numerical analysis methods like FEA, boundary element method (BEM), or finite difference method (FDM) can be employed. This process involves the application of loads to the structure and simulating the soil's response and reinforcement system. The results of the numerical analysis provide valuable insights into factors like stress and displacement distribution within the soil, the deformation and reinforcement's load-carrying capacity, and the overall stability of the structure. Utilizing numerical modeling for conventional nails (CN) and helical nails (HN) proves to be a highly effective approach for optimizing soil reinforcement system designs, reducing costs, and ensuring the safety and stability of structures.

In this study, the laboratory model was replicated through the application of the FEM software, specifically PLAXIS 2D. The software allowed the simulation of the tank's laboratory-like dimensions, the soil nails' geometry, and the soil properties. For the simulation, the Mohr-Coulomb (MC) model was employed, which combines Hooke's and Coulomb's failure theories. To represent the behavior of soil and nails accurately, an elastoplastic model based on deformation was utilized. Table 4.1 provides a comprehensive list of the various parameters employed in the MC model.

Table 4.1. Characteristics for soil and nails used in PLAXIS 2D

Parameters	**Values**
Modelling element	Plate
Axial stiffness	5.024×10^{-05} kN/m
Diameter of plate	16mm
Nail's elastic modulus (E_h)	160 GPa (From Experimental load-displacement)
Geotechnical properties	Table 3.1
Bending stiffness	1.7×10^{-09} kN-m^2
Type of model	Elasto-plastic

An undrained plane strain state serves as the model's foundation. Using a consolidated undrained test, the soil sample's shear strength parameters (ϕ' and c') were calculated (CU test). The plate components are used to model the soil nail element (Milligan GWE and Tei K 1998). On the plate element, the material's characteristics were achieved that are similar to the soil nail's flexural rigidity and axial stiffness. The soil nail's equivalent modulus of elasticity (E_{em}) is provided in Equation (4.18)

$$E_{em} = E_n\left(\frac{A_c}{A}\right) + E_g\left(\frac{A_{cc}}{A}\right) \quad (4.18)$$

Where,

E_g = Elastic modulus of grout

E_n = Elastic modulus of nail material

A_c = Cross-sectional area of helical nail

A = Gross area of soil nail

A_{cc} = Cross-section area of grouted soil nail

The components A_{cc} E_g are equivalent to zero for soil nails without grout. The bending stiffness (EI) and axial stiffness (EA) over which the FEM operates, are supplied as in equation (4.19) and equation (4.20).

$$EA = \frac{E_n}{S_u}\left(\frac{\pi D_{on}^2}{4}\right) \quad (4.19)$$

$$EI = \frac{E_n(\pi d_s^2)}{S_u 64} \quad (4.20)$$

Where,

S_u = Unit spacing

D_{on} = Overall nail diameter

d_s =Shaft diameter

In Plaxis 2D, the soil is mass's base constrained in the x-y direction, while its face remains free and unaffected by both directions. These boundary conditions are modeled as standard fixities. The Strength Reduction Factor (R_{ifs}) determines how soil and nails interact. To achieve adequate

soil-nail interaction, the virtual thickness factor (Δ) for mesh construction is set at 0.1. According to equations (4.21) and (4.22) for fine-grained soil and sandy soil, respectively, the R_{ifs} relates to the interface friction between the soil-nail:

$$R_{ifs} = \frac{\tan \phi_{if}}{\tan \phi_s} \tag{4.21}$$

$$R_{ifs} = \frac{c_{if}}{c_{so}} \tag{4.22}$$

Around the HN and CN, the analysis was conducted using medium-mesh over the PLAXIS 2D. The K_0-procedure, which replicates the ground pressure at rest, was then used to complete the initial stresses. Thus, FOS and deformation for both CN and HN are assessed for the model. The interface's shear strength is decreased until the critical or failure value (Milligan GWE and Tei K 1998). Plaxis 2D utilizes the strength-reduction approach to ascertain the FOS. The study employs the phi/c reduction technique, but it does not impact the strength of the CN and HN components. The total multiplier's mean ($\sum Msf$) is used to establish the safety factor as in equation (4.23)

$$\sum Msf = \frac{\tan \phi_{ip}}{\tan \phi_r} = \frac{c_{ip}}{c_r} \tag{4.23}$$

The factor of safety (FOS) can vary for CN and HN due to a variety of factors, including soil properties, slope geometry, and groundwater conditions. Ensuring that the FOS falls within an acceptable range is crucial for maintaining long-term slope stability.

4.4. Summary

Analyzing the behaviour of soil nails, mathematical and numerical modelling are important tools. In this chapter mathematical modelling of CN and HN is presented and also numerical modelling of CN and HN is discussed. Furthermore, the determination of FOS for both CN and HN in mathematical and numerical modelling is described. Optimization models such as the Response surface model and Hybrid Deep Belief Network- COOT Optimization are discussed in the next chapter.

CHAPTER 5

OPTIMIZATION MODELS

5.1. General

In this study, prediction and optimization of helical soil performance can be done using Response Surface Models (RSMs) and Hybrid Deep Belief Network-COOT Optimization. Response Surface Models are mathematical models used to predict the behaviour of a system in response to changes in input variables. In the case of helical soil nail performance, RSMs can be used to model the relationship between various input factors and the resulting performance metrics. Hybrid Deep Belief Network-COOT Optimization is a more advanced method for predicting and optimizing helical soil nail performance. This approach involves using a hybrid deep belief network (DBN) to model the complex relationships between input variables and performance metrics. The DBN is trained on a large dataset of helical soil anchor performance data to learn the underlying patterns and relationships. Once the DBN is trained, it can be used to predict the performance of helical soil anchors for any combination of input variables. COOT (Conformational Optimization on Target) is an optimization algorithm that can be used to refine the results obtained from the DBN. COOT works by using an iterative process to adjust the input variables to maximize the predicted performance metric. This iterative process continues until the predicted performance metric is optimized to a desired level. Overall, the combination of RSMs and Hybrid Deep Belief Network-COOT Optimization can provide a powerful approach for predicting and optimizing the performance of helical soil nails.

5.2. Response Surface Methodology

Response Surface Methodology (RSM) in statistics investigates the correlation among various descriptive factors and one/multiple response variables. This technique was presented by George E. P. Box and K. B. Wilson back in 1951. The primary objective of RSM is to achieve the optimal response by conducting a series of well-designed experiments. Specifically, it aims to:

- Generate valuable knowledge in the relevant experimental field.
- Precisely estimate the experimental variance (pure error).

- Ensure that the proposed model and the experimental data are sufficient to easily detect any lack of fit. Based on the outcomes, suggest sequential techniques for carrying out experiments with other possibilities.
- To streamline the identification of outlier data
- To minimize ambiguity, facilitating decision-making even in uncertain circumstances.

RSM technique is a mathematical and statistical method utilized to address optimization problems. Figure 5.1 depicts the RSM design workflow. The primary objective of employing the RSM approach is to establish the connection between the response and the variables being studied. This methodology offers numerous advantages and has proven successful in investigating and optimizing process parameters. By conducting a relatively small number of experiments, RSM yields valuable insights and enables the identification of interaction effects among independent factors influencing the response. The model clearly shows the impact of combining the independent process variables in binary form.

In addition, data is gathered using the empirical model that links the response to the independent variables. To suggest desirable responses and minimize the number of experiments, RSM has been extensively used in investigations into various processes, experiment design, model construction, evaluation of the impacts of various elements, and determination of optimal conditions. Following a comprehensive analysis of the experimental results, a mathematical model is formulated to demonstrate the relationship between the process variable and the response. Equation (5.1) is used to mathematically define RSM, which is a very useful tool for the optimization and enhancement of the response factors. (Mumtaz et al. 2017).

$$x = g(y_1, y_2) + e \tag{5.1}$$

Recent times have seen the adoption of first and second-order response surface models; a first-order model can utilize an approximation of a response-basis function based on the response represented by a linear function of variables that are normally independent. Equation (5.2) is used to represent the first-order model (Mumtaz et al. 2017).

$$x = \beta_0 + \beta_1 y_1 + \beta_2 y_2 + e \tag{5.2}$$

A second-order model denotes a function with two variables. It takes into account all quadratic and cross-product components in addition to the first-order correlation model terms. Equation (5.3) can be used to numerically represent a second-order model (Mumtaz et al. 2017).

$$x = \beta_0 + \beta_1 y_1 + \beta_2 y_2 + \beta_{11} y_1^{\,2} + \beta_{22} y_2^{\,2} + \beta_{12} y_1 y_2 + e \qquad (5.3)$$

Where, y_1 and y_2 are the independent variables, x is the response, ℓ is an experimental error, β_0, β_1 and β_2 are the regression coefficient respectively.

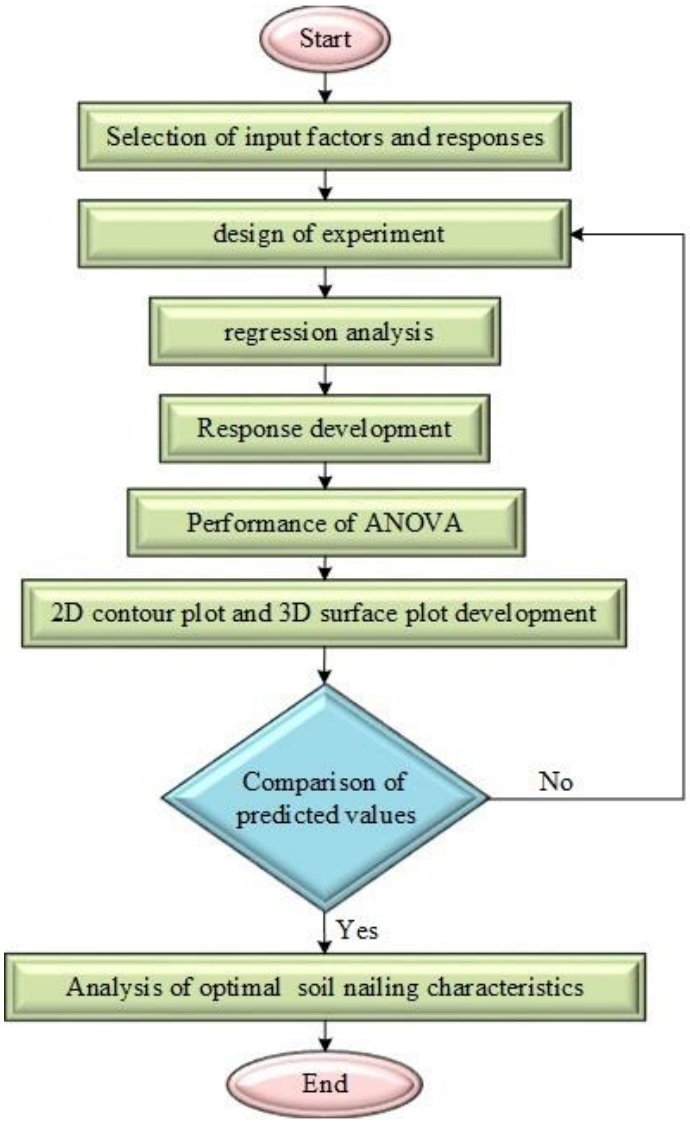

Figure 5.1. Work flow of RSM design

The well-known RSM approach is called Box Behnken Design (BBD). As compared to conventional factorial design methods, BBD reduces the number of experimental sets without compromising optimization accuracy. In this study, the input characteristics are denoted by three distinct codes: -1, 0, and 1. The coding system represents the highest value as (+1), the intermediate value as (0), and the minimum value as (-1). To ensure simplicity and minimize the number of experiments, the BBD-RSM design is utilized. The objective of this research is to achieve optimal soil nailing behavior, characterized by maximum pull-out capacity, lowest installation torque, and the lowest factor of safety. Table 5.1 provides a comprehensive overview of the specific input parameters and their corresponding levels.

Table 5.1. Input parameter's levels

Input parameters	**Levels**		
	High	**Intermediate**	**Low**
Surcharge pressure(kPa)	40	30	20
Shaft diameter(mm)	16	15	14
Helical pitch(mm)	35	30	25
Inclination angle(^{o})	20	15	10

5.2.1. Steps involved in response surface methodology

The following are the steps in RSM by using Design-Expert version 13 software which is a software package that can be used for response surface design.

Step 1: Open Design-Expert 13 software on the computer and click the "**New design**" icon.

Figure 5.2. Main Tab of Design-Expert software

Step 2: Click on the "**Response Surface**" icon and select "**Box-Behnken**" type design from the main menu to create a new response surface design.

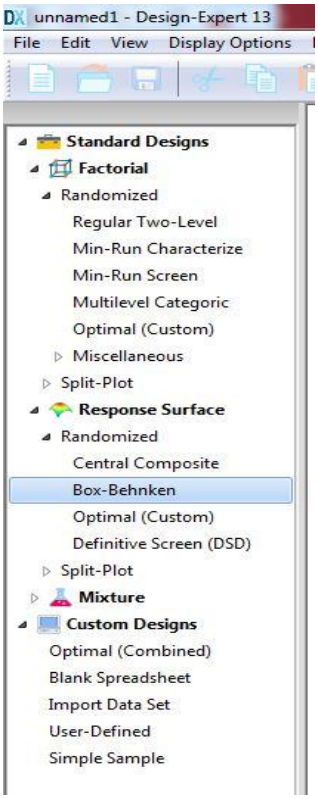

Figure 5.3. Selection BBD

Step 3: Enter the number of factors.

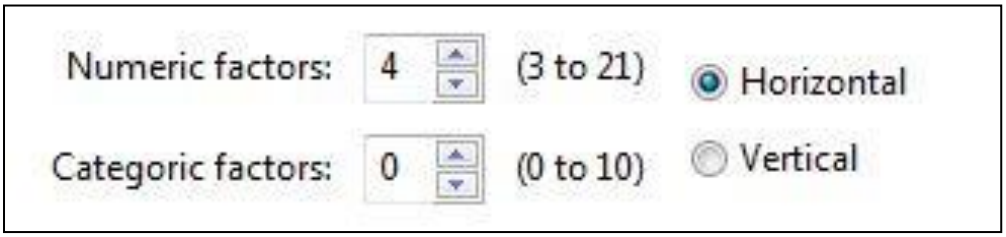

Figure 5.4. Numbers of factors

Step 4: Enter the names of factors and units; also specify the range or levels of factors.

	Name	Units	Low	High
A [Numeric]	Surcharge pr	kPa	20	40
B [Numeric]	Shaft diamet	mm	14	16
C [Numeric]	Helical pitch	mm	25	35
D [Numeric]	Inclination ar	°	10	20

Figure 5.5. Names and units of input factors

Step 5: Adjust the number of center points per block based on the requirement of experimental runs.

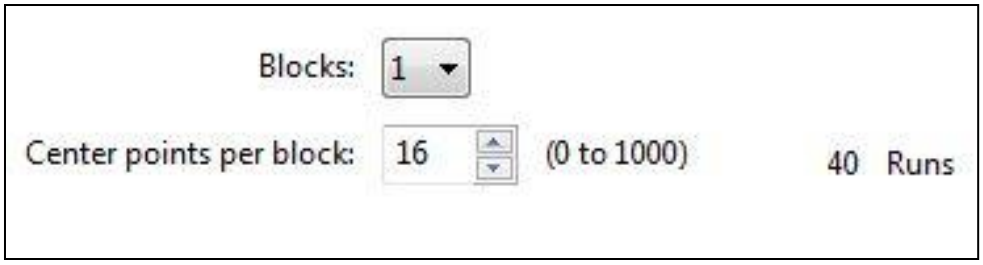

Figure 5.6. Numbers of experimental runs

Step 6: Click "**Next**" when entered all the factors and levels.

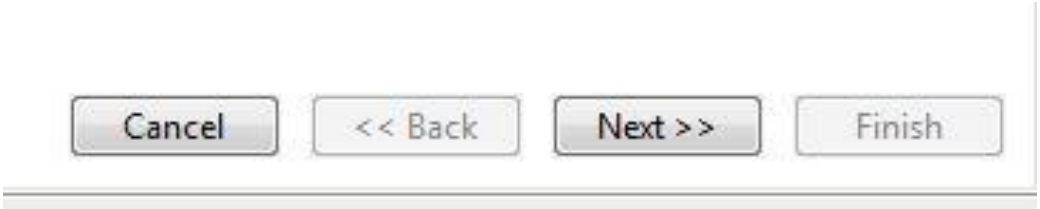

Figure 5.7. Next tab

Step 7: Enter the number of responses and enter response names and their units.

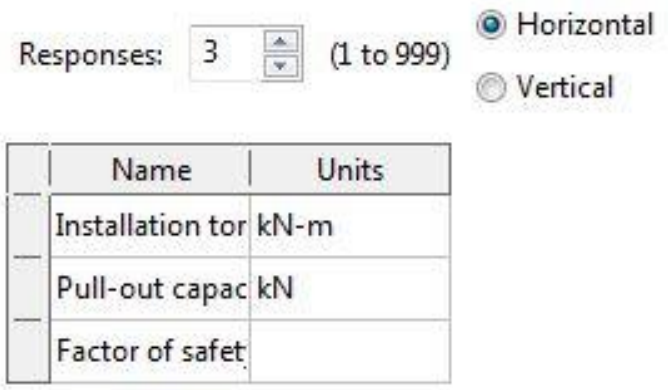

Figure 5.8. Responses numbers, names, and units

Step 8: Click "**Finish**" when entered all the responses and its units.

Figure 5.9. Finish tab

Step 9: Design-Expert will generate a "**design matrix**" based on the levels of input factors. Check the matrix and make any necessary adjustments.

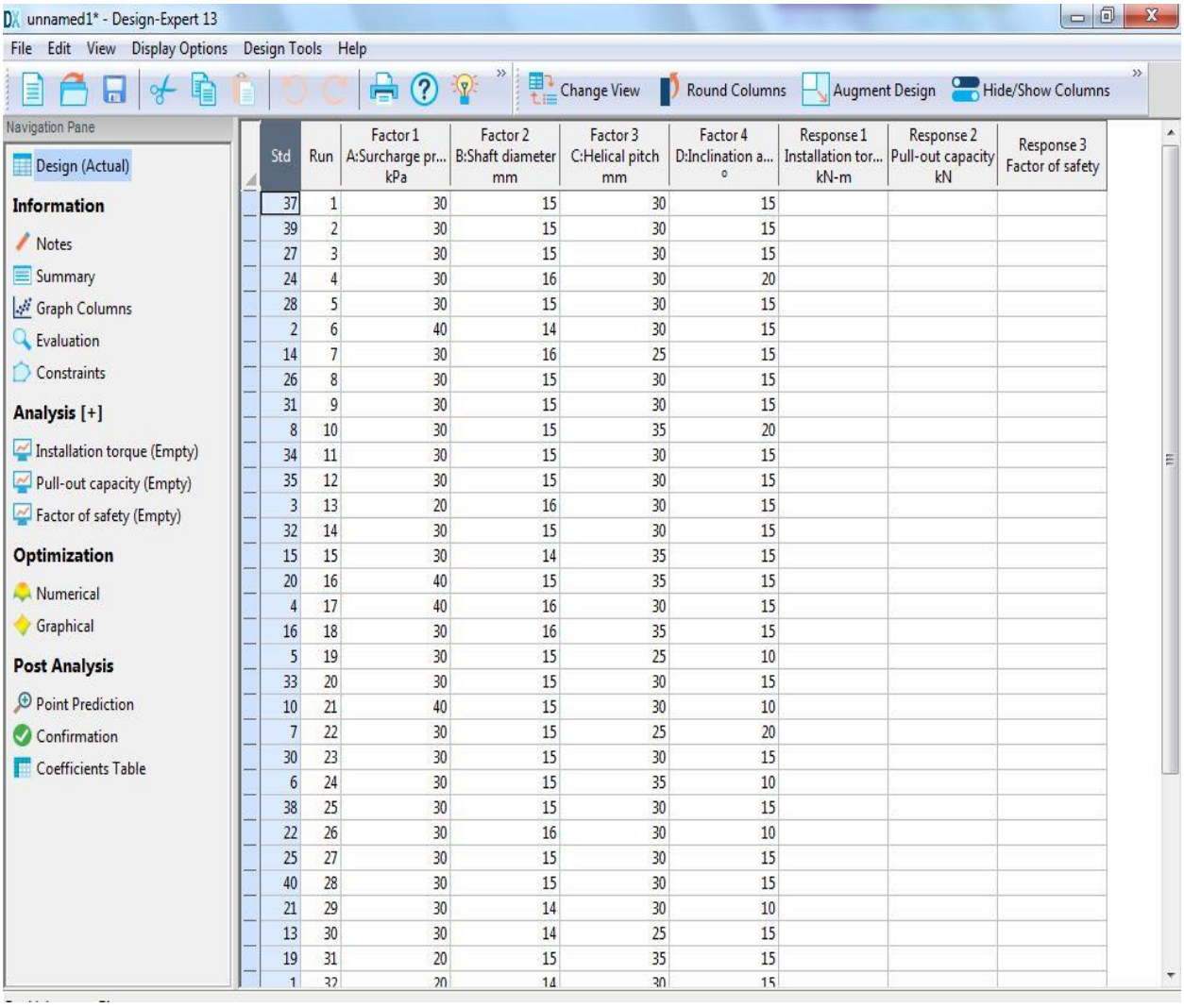

Std	Run	Factor 1 A:Surcharge pr... kPa	Factor 2 B:Shaft diameter mm	Factor 3 C:Helical pitch mm	Factor 4 D:Inclination a... °	Response 1 Installation tor... kN-m	Response 2 Pull-out capacity kN	Response 3 Factor of safety
37	1	30	15	30	15			
39	2	30	15	30	15			
27	3	30	15	30	15			
24	4	30	16	30	20			
28	5	30	15	30	15			
2	6	40	14	30	15			
14	7	30	16	25	15			
26	8	30	15	30	15			
31	9	30	15	30	15			
8	10	30	15	35	20			
34	11	30	15	30	15			
35	12	30	15	30	15			
3	13	20	16	30	15			
32	14	30	15	30	15			
15	15	30	14	35	15			
20	16	40	15	35	15			
4	17	40	16	30	15			
16	18	30	16	35	15			
5	19	30	15	25	10			
33	20	30	15	30	15			
10	21	40	15	30	10			
7	22	30	15	25	20			
30	23	30	15	30	15			
6	24	30	15	35	10			
38	25	30	15	30	15			
22	26	30	16	30	10			
25	27	30	15	30	15			
40	28	30	15	30	15			
21	29	30	14	30	10			
13	30	30	14	25	15			
19	31	20	15	35	15			
1	32	20	14	30	15			

Figure 5.10. Design matrix

Step 10: Enter the response data into Design-Expert. Click the "**Data**" tab and enter the response data in the appropriate cells.

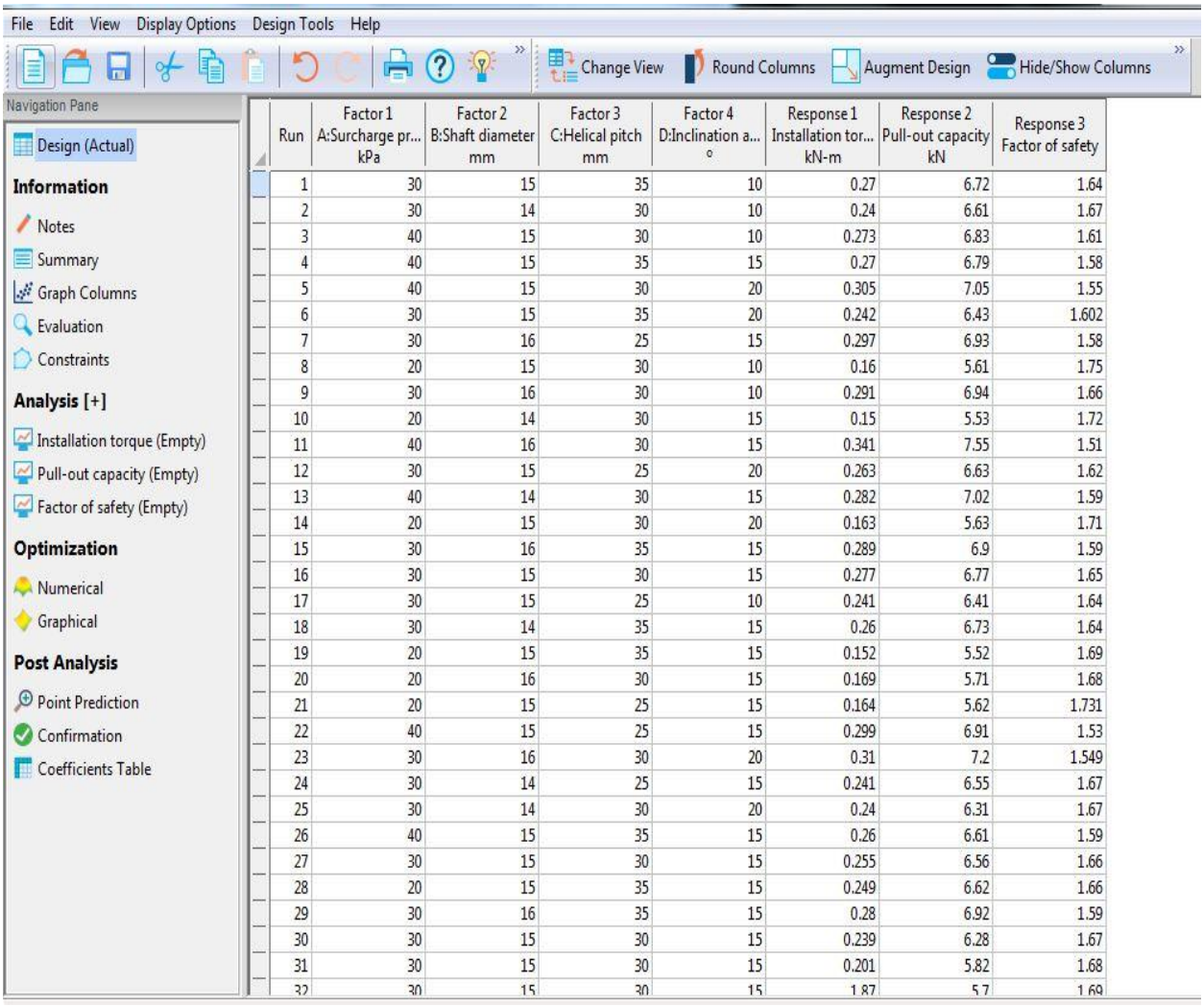

Run	Factor 1 A:Surcharge pr... kPa	Factor 2 B:Shaft diameter mm	Factor 3 C:Helical pitch mm	Factor 4 D:Inclination a... °	Response 1 Installation tor... kN-m	Response 2 Pull-out capacity kN	Response 3 Factor of safety
1	30	15	35	10	0.27	6.72	1.64
2	30	14	30	10	0.24	6.61	1.67
3	40	15	30	10	0.273	6.83	1.61
4	40	15	35	15	0.27	6.79	1.58
5	40	15	30	20	0.305	7.05	1.55
6	30	15	35	20	0.242	6.43	1.602
7	30	16	25	15	0.297	6.93	1.58
8	20	15	30	10	0.16	5.61	1.75
9	30	16	30	10	0.291	6.94	1.66
10	20	14	30	15	0.15	5.53	1.72
11	40	16	30	15	0.341	7.55	1.51
12	30	15	25	20	0.263	6.63	1.62
13	40	14	30	15	0.282	7.02	1.59
14	20	15	30	20	0.163	5.63	1.71
15	30	16	35	15	0.289	6.9	1.59
16	30	15	30	15	0.277	6.77	1.65
17	30	15	25	10	0.241	6.41	1.64
18	30	14	35	15	0.26	6.73	1.64
19	20	15	35	15	0.152	5.52	1.69
20	20	16	30	15	0.169	5.71	1.68
21	20	15	25	15	0.164	5.62	1.731
22	40	15	25	15	0.299	6.91	1.53
23	30	16	30	20	0.31	7.2	1.549
24	30	14	25	15	0.241	6.55	1.67
25	30	14	30	20	0.24	6.31	1.67
26	40	15	35	15	0.26	6.61	1.59
27	30	15	30	15	0.255	6.56	1.66
28	20	15	35	15	0.249	6.62	1.66
29	30	16	35	15	0.28	6.92	1.59
30	30	15	30	15	0.239	6.28	1.67
31	30	15	30	15	0.201	5.82	1.68
32	30	15	30	15	1.87	5.7	1.69

Figure 5.11. Response data for design matrix

Step 11: Analyze the responses by clicking "**start analysis**" in the Configure tab.

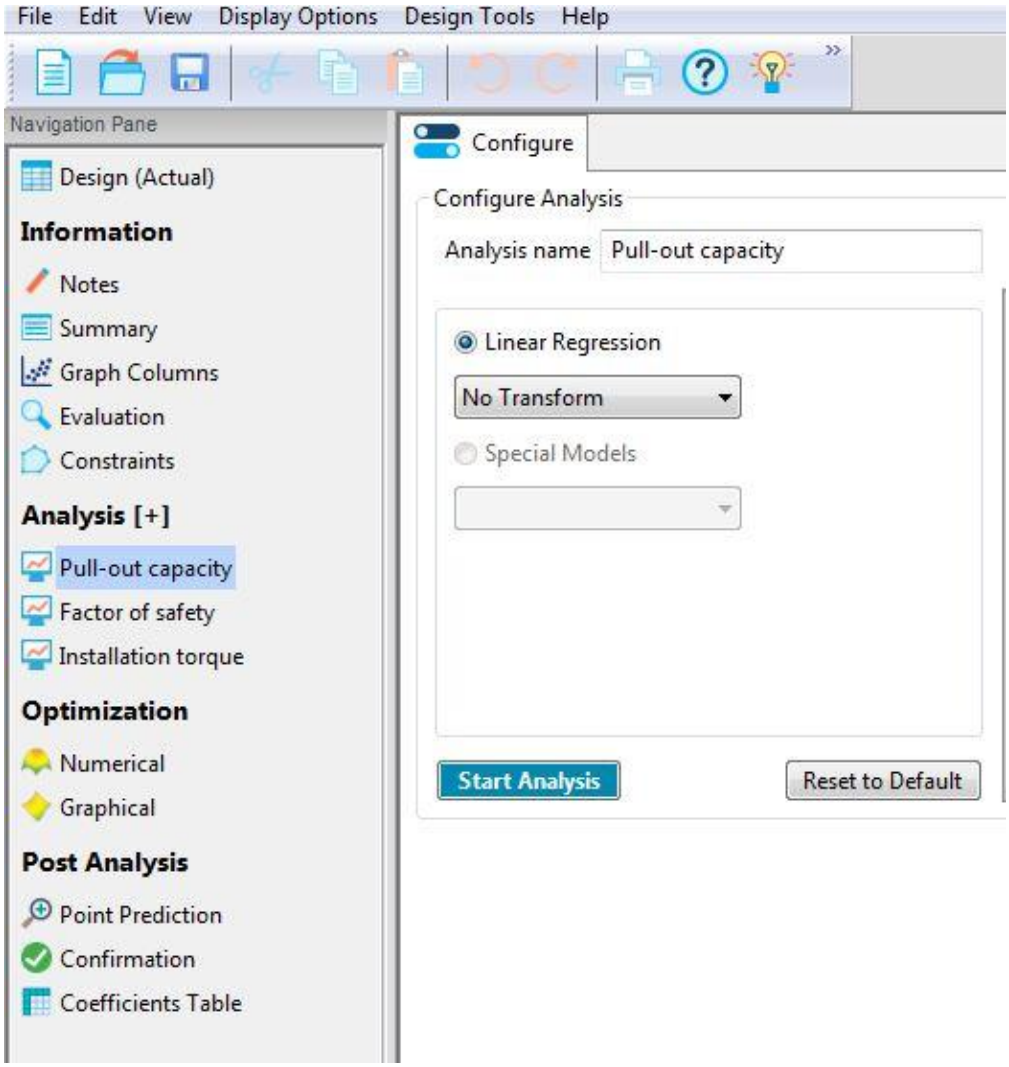

Figure 5.12. Configure tab

Step 12: Click the "**Fit summary**" tab; the design expert has fitted the response to two-factor interaction (2FI), linear, cubic polynomials, and quadratic. The cubic order terms will not considerably enhance the fit, but Design-Expert is now stating (by bold emphasis) that the quadratic model seems the best. These terms are significant: for Lack of Fit testing on the various model orders, scroll down to the "**Lack of Fit**" testing window. Relative error and "Pure Error" derived from replicated design points are compared in the "Lack of Fit Tests" window. The quadratic model, which was named as the most probable model, does not exhibit a major lack of fit; do not select the cubic model since it is aliased.

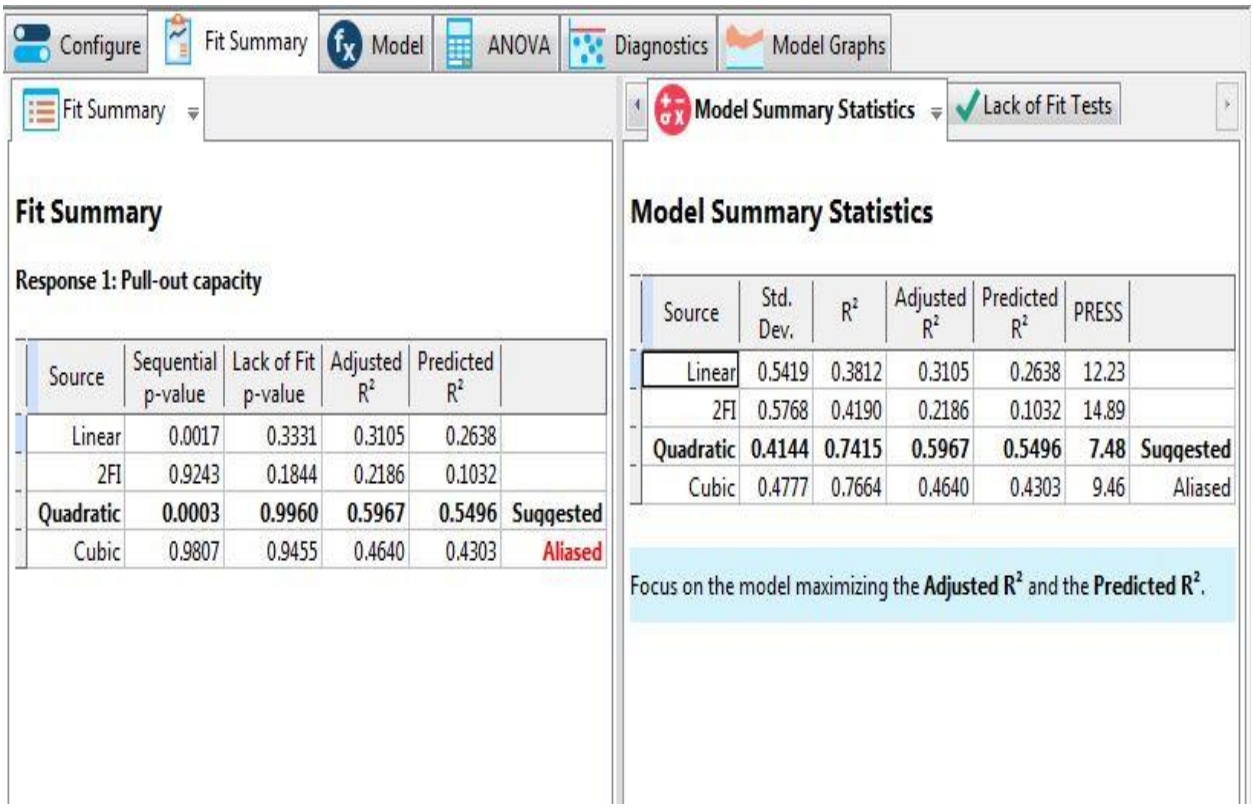

Figure 5.13. Fit summary results

Step 13: Choose the model for a comprehensive statistical analysis using Design-Expert. To view the terms in the model, at the top of the screen click the "**Model**" tab. The "**Suggested**" model that was previously presented in the Fit Summary table is the default model used by the program.

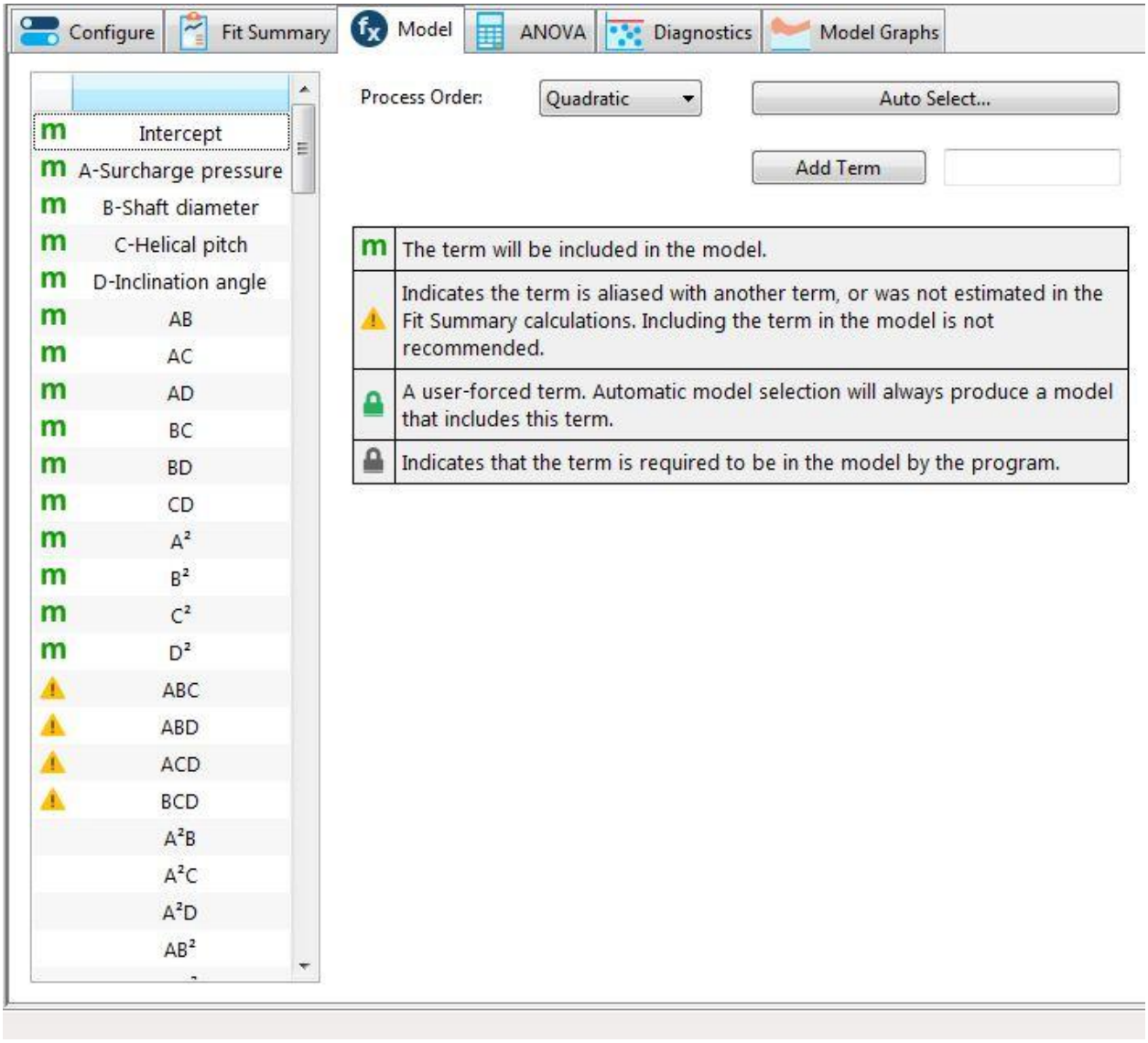

Figure 5.14. Process order

Step 14: To generate the analysis of variance, fit statistics, model comparison statistics, and final equation in terms of actual factors, coefficients, and coded equations in terms of coded factors for the chosen model, click the "**ANOVA**" tab.

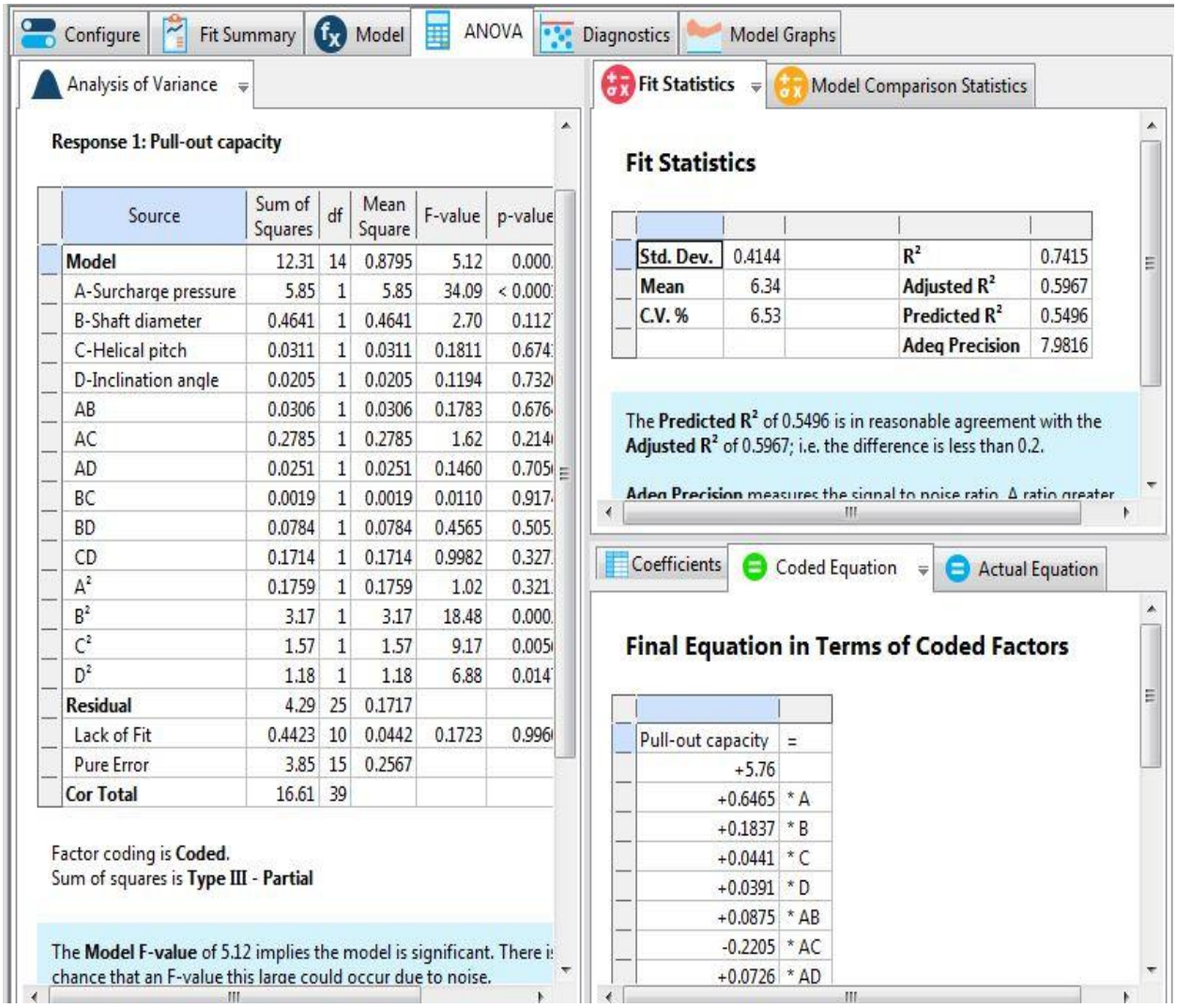

Figure 5.15. ANOVA results

Step 15: Plots made available via the "**Diagnostics**" tab are the best way to understand the diagnostic information offered by Design-Expert. The first pane displays the most crucial diagnosis, a normal probability map of the residuals. Also, Box-Cox plot, Pred. vs. Actual plot, Cook's distance plot, leverage plot, DFFITS plot, DFBETAS plot, and Residuals plots are the important diagnostic plots.

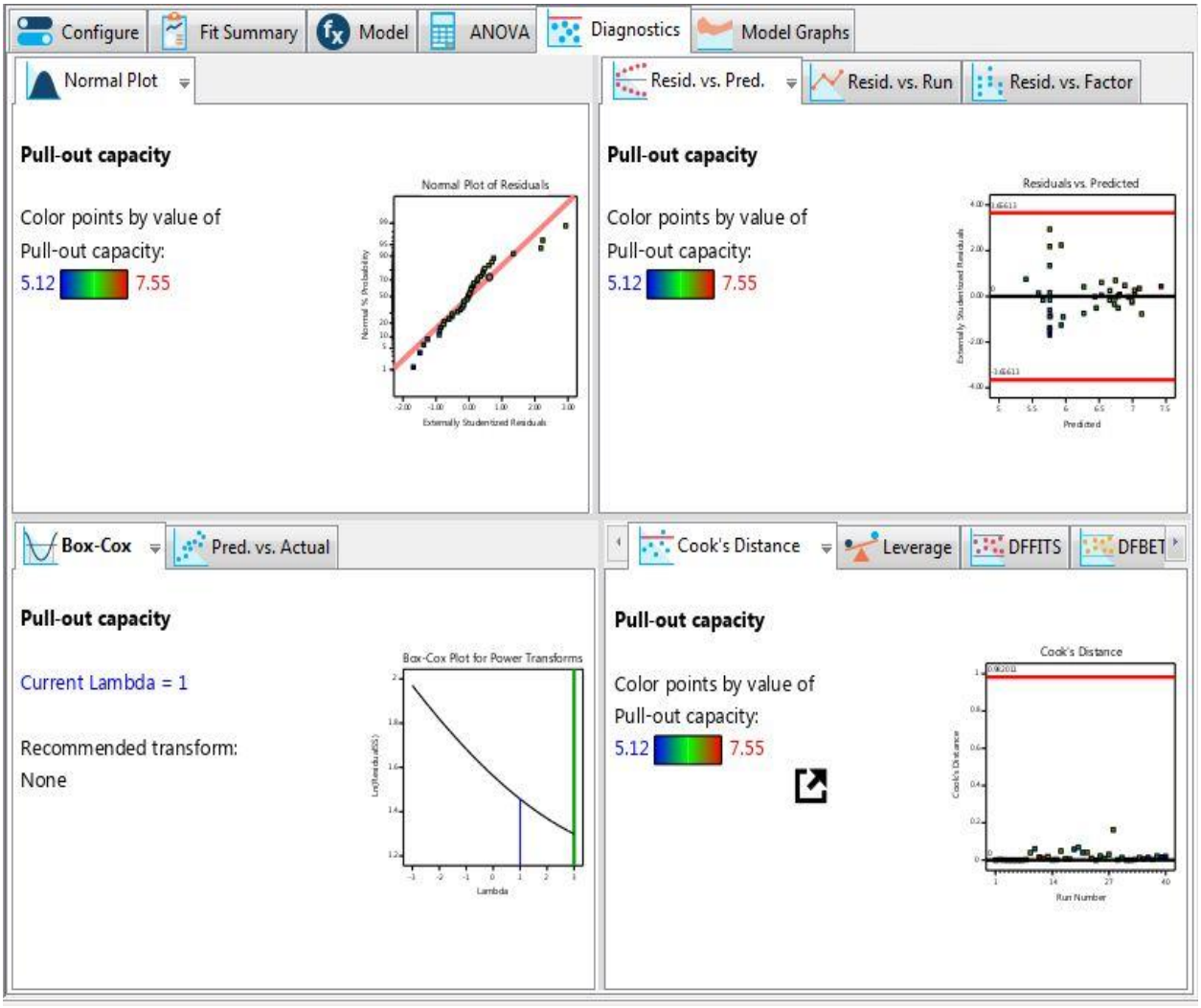

Figure 5.16. Diagnostics details

Step 16: Create response surface plots as the residuals diagnosis shows no statistical issues. Navigate to the "**Model Graphs**" tab. By default, graded color is used to display the 2D contour plot of variables A vs B. In this tab, also generate the other important graphs such as perturbation graph, one-factor graph, 3D surface graph, all factor graph, and interaction graph.

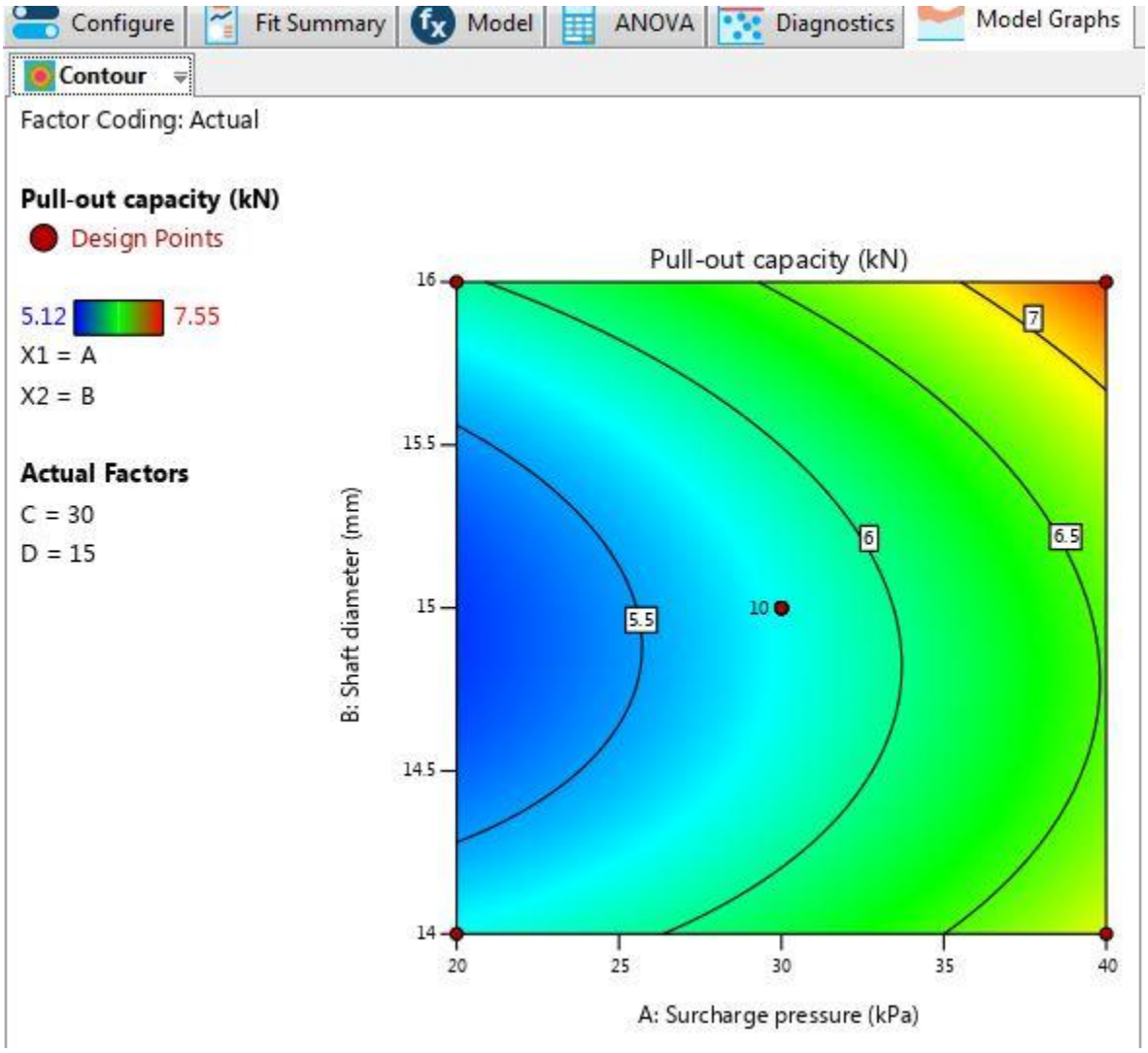

Figure 5.17. Model graphs

Step 17: Repeat Step 11- step 16 for analyzing second and third responses. Then move to optimization experiments. To begin, select the Numerical node from the "**Optimization**" branch on the left of the screen.

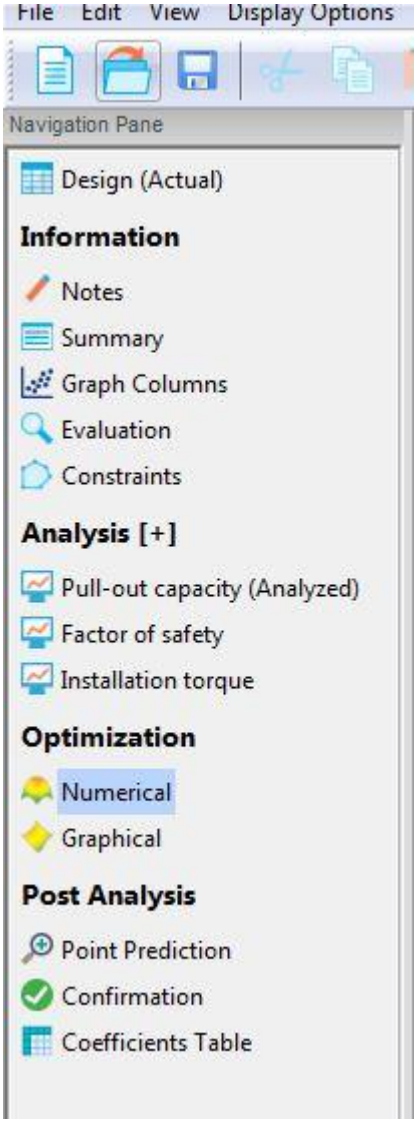

Figure 5.18. Numerical Optimization

Step 18: Define the "**criteria**" for any variable using Design-Expert. Desirability indices (di) are created by the program using the following five choices as a "**Goal**": Maximize, Minimize, Target, In range, and Equal to desired values. For every given response, desirability varies from 0 to 1. The program calculates the total desirability by adding together each individual desirability.

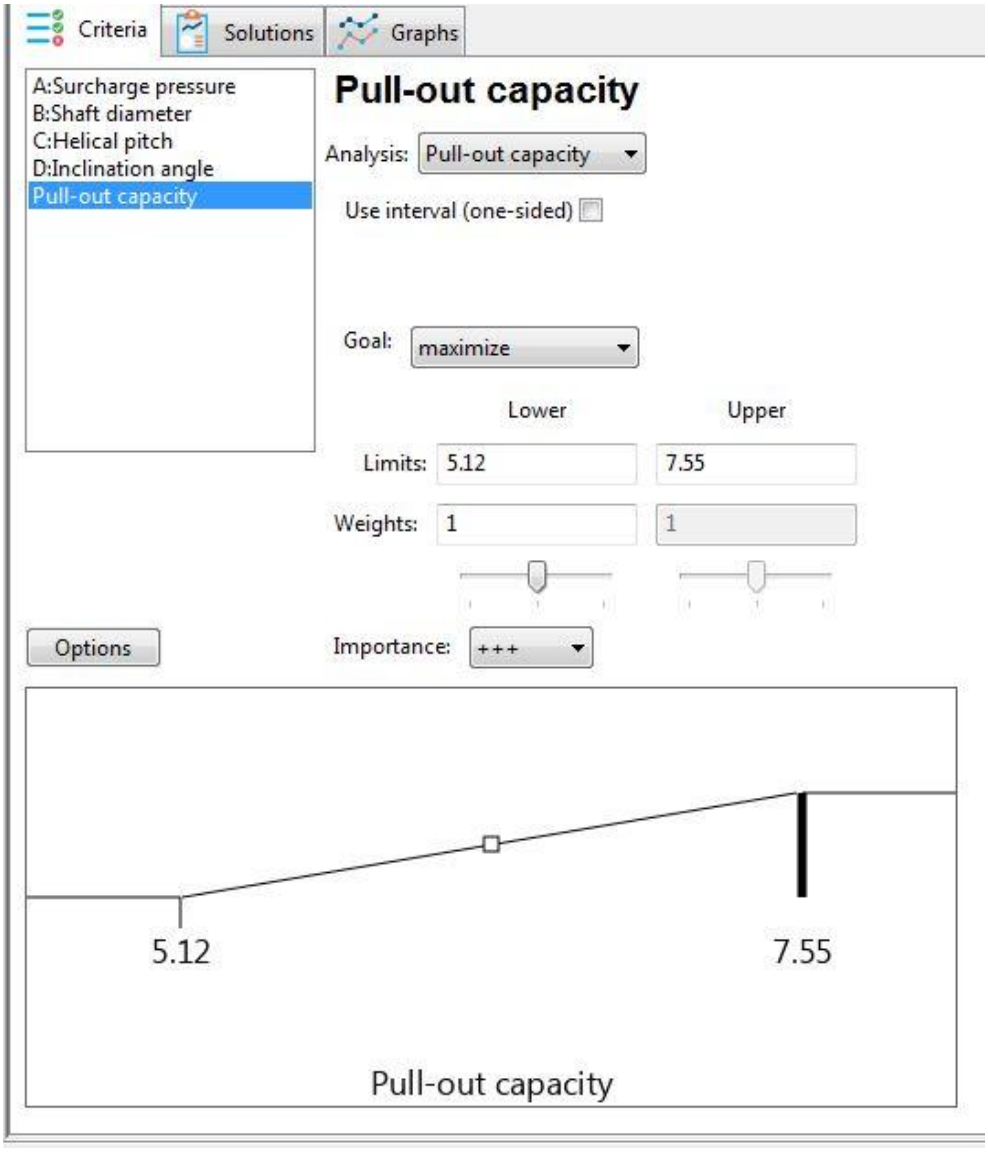

Figure 5.19. Numerical optimization criteria

Step 19: By selecting the "**Solutions**" option, begin the optimization which automatically switches to the Ramps view. So, the ideal factor settings and predicted responses desirability are clear visuals by Ramps view. The outcomes are then ranked by Design-Expert from most to least desired.

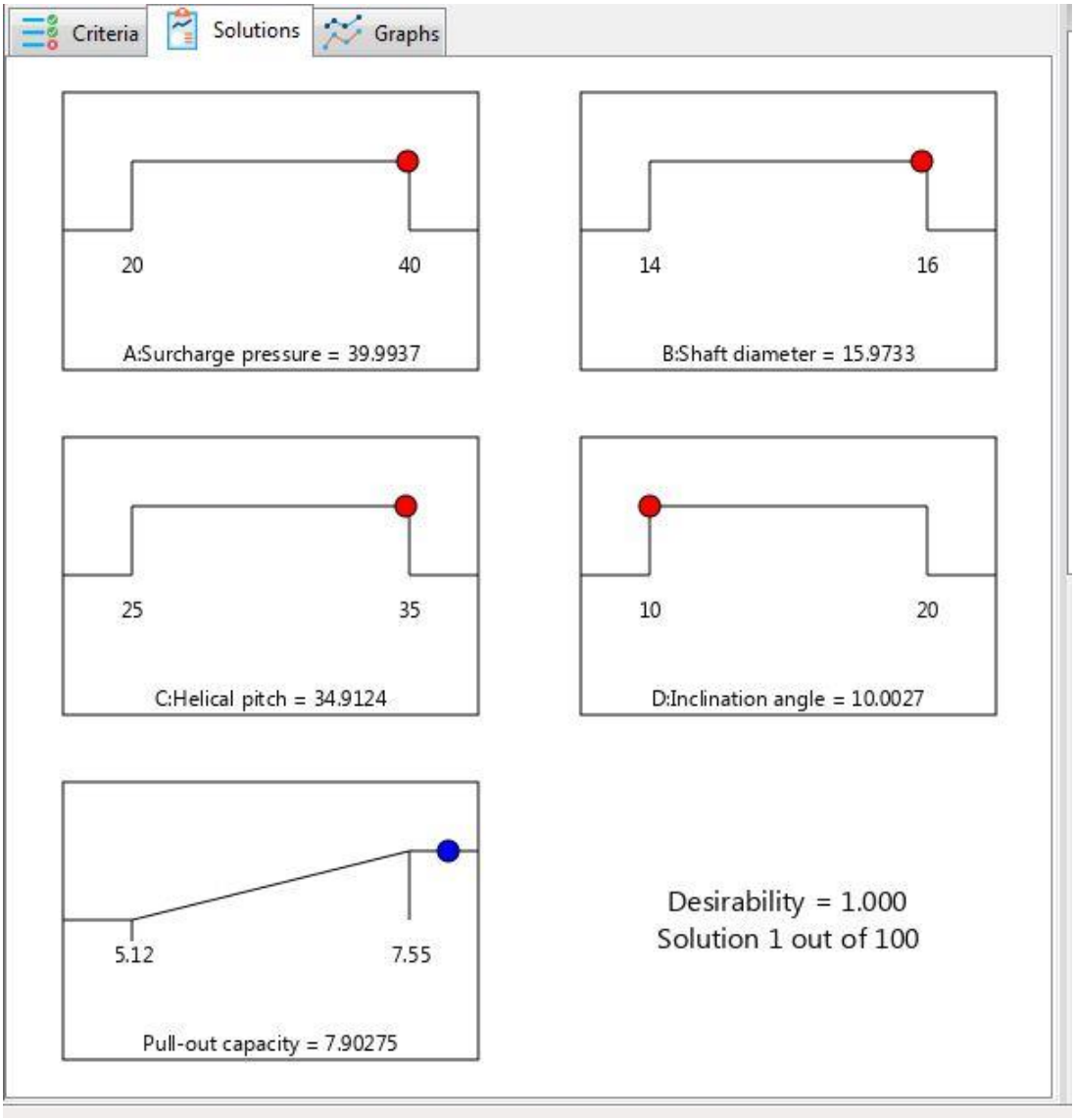

Figure 5.20. Solutions of numerical optimization

Step 20: A contour graph showing the overall desirability; Desirability of all responses viewed by selecting the "**Graphs**" tab. These same steps are repeated for factor of safety and installation torque for analyzing and optimization.

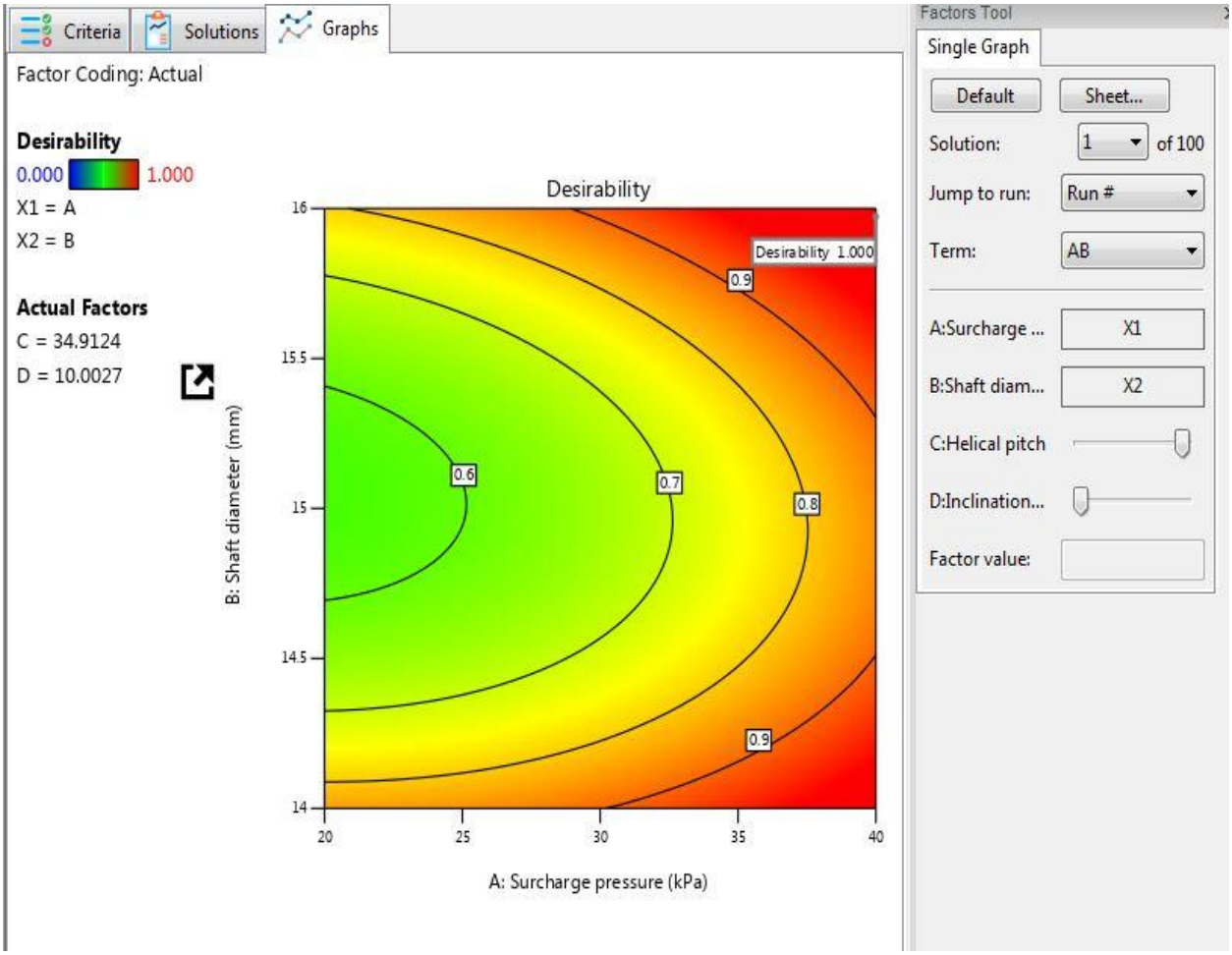

Figure 5.21. Desirability graph

Step 21: Choose "**Save As**" from the "**File menu**" by clicking on that item. The File name for Save as type "***.dxpx**" in the data folder for Design-Expert or other specified folder.

5.3. Deep Belief Network

A potent deep generative model known as the Deep Belief Network (DBN) consists of stochastic latent variables in several layers, where binary variables act as feature detectors or hidden units. These binary latent variables are sometimes referred to as feature detectors. Unlike traditional generative graphic models, DBNs do not have directed linkages in the upper two levels; however, they do possess direct connections to lower levels in the layer above. The essence of DBNs lies in their use of probabilistic deep learning without any need for supervision.

DBNs represent a distinct type of machine learning approach, which shares some similarities with deep neural networks, yet they have significant differences. These neural networks are feed-forward and exhibit a deep architecture with numerous hidden layers. On the other hand, DBNs consist of unsupervised networks such as Restricted Boltzmann Machines (RBMs), where each layer in the sub-hidden network also serves as the visible layer for the subsequent layer in the hierarchy.

5.3.1. DBN architecture

A Deep Belief Network (DBN) is a multi-layered neural network architecture constructed by chaining together several constrained Boltzmann machines. Each Boltzmann machine's output is fed as input to the subsequent Boltzmann machine in a cascading manner. During training, the network converges iteratively until it is fully constructed. The DBN exhibits associative memory due to the symmetric and undirected connections between its top two layers. Meanwhile, arrows indicating the direction towards the data's closest layer illustrate the relationships between the lower levels. At the bottom levels, directed acyclic connections transform associative memory into measurable variables.

To begin, the input data is directed to the visible unit’s lowest layer, which can accept binary or real data. It is important to note that DBN lacks intra-layer connections, much like the Restricted Boltzmann Machine (RBM). The hidden units in the network capture correlations in the data and serve as representative features. The connections between two layers in the DBN are governed by

a matrix of symmetric weights known as W, the new structure connects each unit in a layer to every other unit present in the layer above it. For a visual representation of the DBN's structure, refer to Figure 5.22.

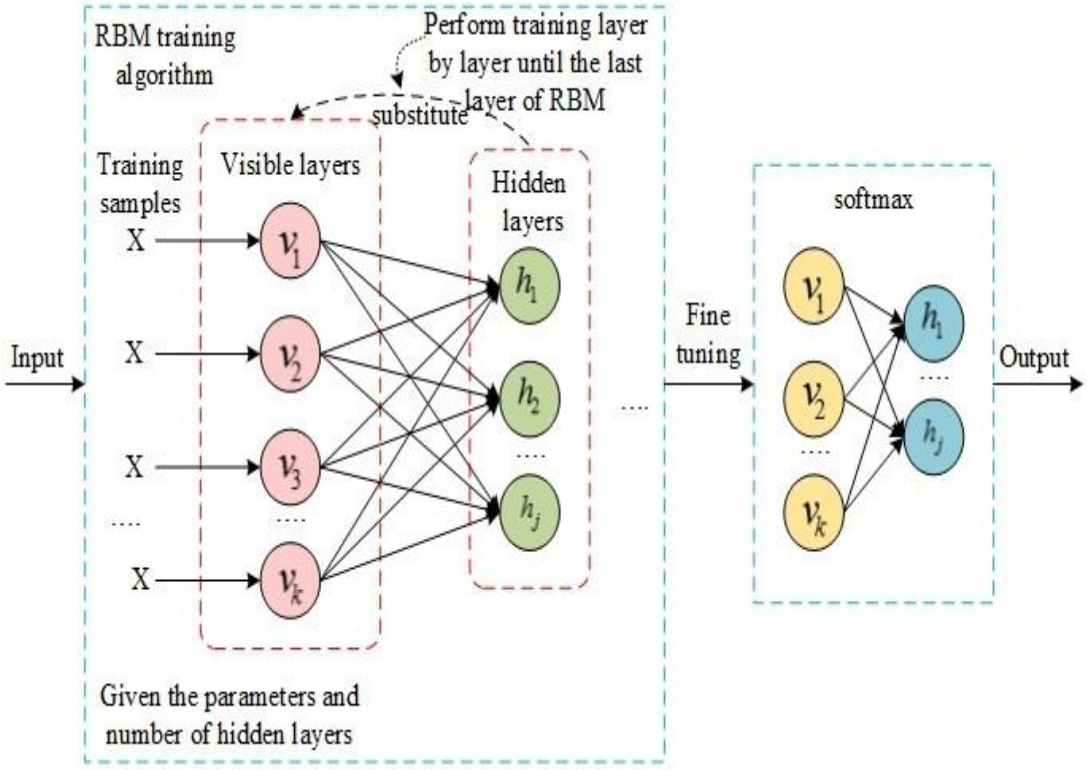

Figure 5.22. DBN Structure (Tao et al. 2020)

5.4. Hybrid Deep Belief Network-COOT Optimization

In hybrid DBN-COOT optimization, Both RBM layers initially occur in the bottom layer, which serves as the training stage. In this, the RBM functions as an energy function, and the parameters of the RBM weights between the bias of the visible (b), many neurons (w), and the hidden neuron (b_h). To adjust the DBN back propagation method is finally applied (Tao et al. 2020, Niu et al. 2020. Figures 5.23, 5.24, 5.25, and 5.26 illustrate four different movements of COOTs on the water's surface.

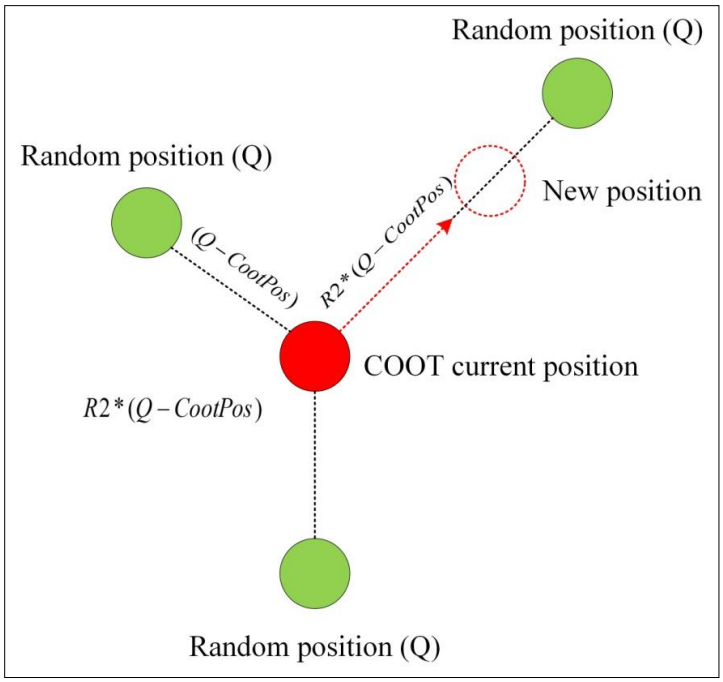

Figure 5.23. Random Movement in Multiple Directions (Naruei and Keynia 2021)

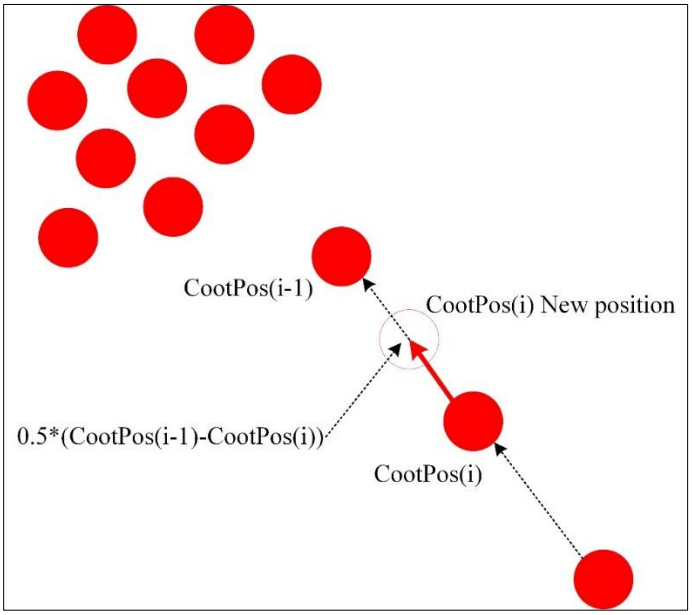

Figure 5.24. Coots Moving in a Chain Formation (Naruei and Keynia 2021)

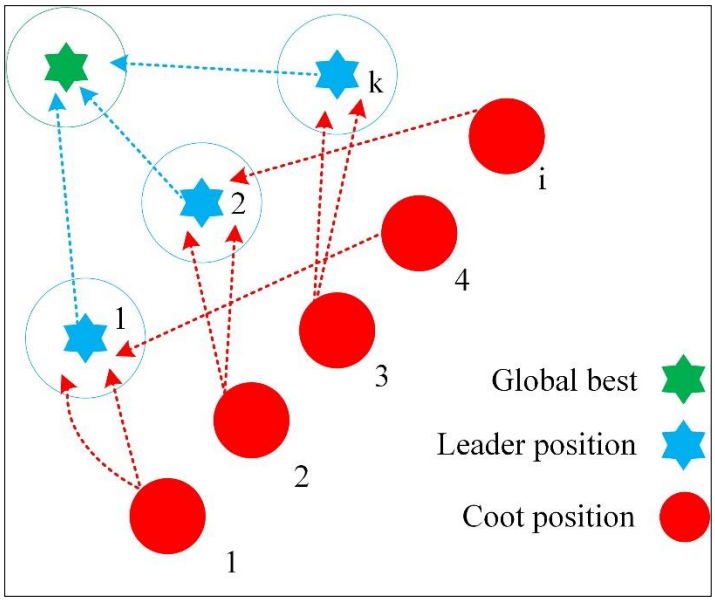

Figure 5.25. Selection of leader by coot (Naruei and Keynia 2021)

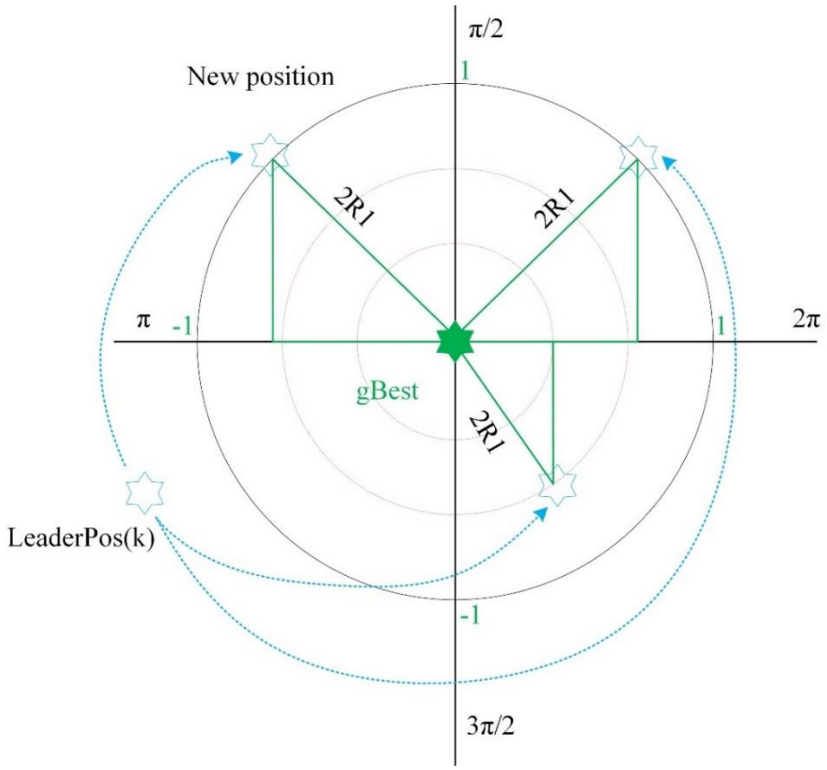

Figure 5.26. Leader Position Update Towards Optimal Position (Naruei and Keynia 2021)

The energy function (e) for the exposed and covered layers is as following equation (5.4):

$$e(a,h) = -\sum_{ij} w_{ij} a_i h_j - \sum_i b_i a_i - \sum_j b_{hj} h_j \quad (5.4)$$

Where,

h=vectors of the hidden layers

a =Vectors of the visible layers

w_{ij}=Weights connecting the neurons in the visible and hidden layers

h_j =The hidden units

b_i =Bias for visible layer neurons

b_{hj}=Bias for hidden layer neurons

The probability distribution (P) of the visible and hidden layer vectors is described as following equation (5.5) based on the partition function,

$$P\theta(a,h) = \exp(-e(a,h;\theta))/K(\theta) \quad (5.5)$$

The activation probability for both the hidden and the visible layers, according to the sigmoid activation function, is as following equation (5.6),

$$P_{aj} = \sigma\left(b_{hj} + \sum_i h_j w_{ij}\right) \quad (5.6)$$

Where,

θ =Three parametric set $\{W, b, b_{hj}\}$

σ = Sigmoid function

Moreover, the updated weight and bias formulae are written as equations (5.7) and (5.8),

$$\Delta w_{ij} = \varepsilon\left(< a_i h_i >_{data} - < a_i h_i >_{model}\right) \tag{5.7}$$

$$\Delta b_{hi} = \varepsilon\left(< a_i >_{data} - < a_i >_{model}\right) \tag{5.8}$$

Typically, DBN is used for the random weight update process. The Coot Optimization is used in this study to optimize the weight update process. When looking for food, crows are water birds categorized as members of the rail family. Hence, the primary goal of coot optimization is thought to be food hunting by the coot on the water's surface. To seek food, the coots are divided into leaders and followers. Whenever the fitness function is utilized in the optimization process as shown in equation (5.9),

$$f(x) = \frac{1}{rmse\left(\bar{l} - l\right)} \tag{5.9}$$

$$w_{pos}(i) = rand\left(a, d\right) * \left(ub - lb\right) + lb \tag{5.10}$$

$$q = rand(1, d) * \left(ub - lb\right) + lb \tag{5.11}$$

Equation (5.10) is used to start the population of weights (w_{pos}), and then equation (5.11) is used to compute the fitness of each solution.

Where,

l = Experimental values

$\bar{l}$ = Predicted values

w_{pos} = Weight population

q =The random position

d =The overall quantity of variables

ub = Upper bounds

lb = Lower bounds

Next, the most recent location is given as equations (5.12) and (5.13), depending on the random movement of weights.

$$w_{pos}(i) = w_{pos}(i) + x \times R2 \times \left(Q - w_{pos}(i)\right) \tag{5.12}$$

$$x = 1 - L\left(\frac{1}{I}\right) \tag{5.13}$$

The leaders' positions are then updated to reach the target using equation (5.14). Also, this equation (5.15) is utilized to identify the best approach for finding the targets.

$$Lead_{pos}(i) = \left\{y \times R3 \times \cos\left(2R\pi\right) \times gBest - lead_{pos}(i) + gbest\right\} \tag{5.14}$$

$$y = 2 - L\left(\frac{1}{I}\right) \tag{5.15}$$

Where,

L = Current Iteration

I = Maximum Iteration

Moreover, the random integer $R, R2 \, and \, R3$ falls between [-1, 1], [0, 1], and [0, 1].

5.4.1. Statistical Analysis of Models

An essential step in defining how well the model performs in its prediction is evaluating the model's accuracy. Metrics for evaluating problems might vary depending on their nature. For the constructed models RSM, DBN, and ANN in this work, statistical indicators R^2, Mean Square Error (MSE), R, Adjusted $R^{2,}$ and Root Mean Square Error (RMSE) are used. In regression analysis, statistical indicators are commonly utilized to evaluate prediction accuracy and model performance. These metrics help depict the model's efficacy by assessing how often it makes inaccurate predictions.

R^2: R^2 is also known as the coefficient of determination, measures how well the results align with the original values using the linear regression model. Its value ranges from 0 to 1, and it is a scale-free score.

MSE: It measures how much the predicted values differ from the actual values in the dataset, giving an idea of the residuals' extent.

R: Also known as a correlation coefficient, which measures the relationship between predicted and observed values of a variable.

Adjusted R^2: The modified version of R-square is known as Adjusted R-squared, which considers the number of independent variables in the model. It will always be less than or equal to R^2.

RMSE: Root Mean Squared Error provides a measure of the residuals' standard deviation.

Equations (5.16-5.20) are used to express the R^2, MSE, R, Adjusted R^2, and RMSE;

$$R^2 = \frac{\sum_{i=1}^{n}\left(y_{ev,i} - y_{v,i}\right)^2}{\sum_{i=1}^{n}\left(y_{v,i} - y_{emean}\right)^2} \tag{5.16}$$

$$MSE = \frac{1}{n}\sum_{i=1}^{n}\left(y_{v,i} - y_{e,i}\right)^2 \tag{5.17}$$

$$R = \frac{\sum_{i=1}^{n}\left(y_{v,i} - y_{vmean}\right)\left(y_{v,i} - y_{emean}\right)}{\sqrt{\left(\sum_{i=1}^{n}\left(y_{v,i} - y_{vmean}\right)^2\right)\left(\sum_{i=1}^{n}\left(y_{e,i} - y_{emean}\right)^2\right)}} \tag{5.18}$$

$$Adjusted\ \ R^2 = 1 - \left(\left(1 - R^2\right)\left(\frac{n-1}{n-q-1}\right)\right) \tag{5.19}$$

$$RMSE = \sqrt{\frac{1}{n}}\sum_{i=1}^{n}\left(y_{v,i} - y_{e,i}\right) \tag{5.20}$$

Where,

y_e = Actual values

y_v = Predicted values

y_{emean} =Average actual values

y_{vmean} = Average predicted values

q = Input numbers

n = Numbers of experimental values

5.5. Proposed methodology

The present study explores the soil nail behavior in cohesive soil through a combination of laboratory experiments, mathematical analyses, and numerical modeling. Additionally, the outcomes of helical soil nailing, encompassing installation torque, pull-out capacity, and safety factors, are validated using both RSM and hybrid DBN-COOT optimization approaches. Initially, select the soil and determiner the characteristics of the soil sample. Both conventional and helical soil nails are adopted for this study. Pullout load (KN), deformation (mm), and factor of safety are established for both CN and HN based on the laboratory, mathematical and numerical modelling. Based on theoretical and numerical research helical soil nails provide a greater level of safety than traditional soil nails. So, to validate and improve helical soil nailing results such as pull-out capacity, installation torque, and safety factor, RSM is used. Then hybrid DBN-COOT optimizations are utilized as the suggested model and are a successful tool for validating and improving the outcomes of HN. The proposed flow of the present work is shown in figure 5.27.

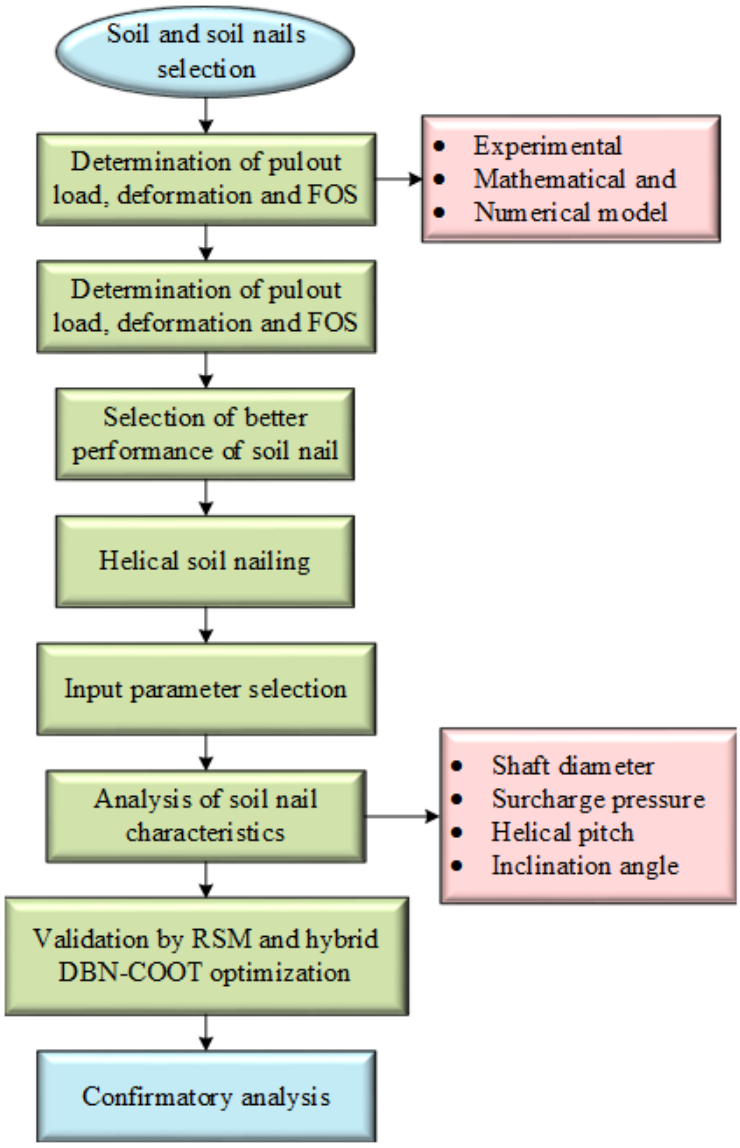

Figure 5.27. Proposed methodology

5.6. Summary

This chapter focused on the concept of RSM and its design steps; also introduced the hybrid model using DBN incorporating COOT for optimization. In additional, a statistical analysis of the models was discussed to evaluate their performance and accuracy. Finally, the proposed methodology is presented, which includes the step-by-step process of the study using RSM, and hybrid DBN-COOT optimization.

CHAPTER 6

RESULTS AND DISCUSSION

6.1. General

The results obtained through experiments and theoretical calculations for the parameters that are influenced by the CN and HN are analyzed in this chapter. The factor of safety analysis is also conducted to reduce the failure possibilities of the nailing process and stability of the nails. Furthermore, the validation and optimization of the collected outcomes are done numerically through Response Surface Methodology (RSM). In the RSM the Box-Bhenkan Design (BBD) model is used to validate and optimize the results. To enhance the accuracy of outcome predictions, the Coot optimization algorithm is employed and compared with both RSM and other machine learning methods.

6.2. Pull-out behaviour

The pullout displacement results collected during the experiment and mathematical calculations for conventional and helical soil nailing are shown in Figures 6.1 and 6.2, respectively. When pulling out the nail, initially, it resists strongly against the external force applied. After further increasing the force, till its peak withstanding capability, the resistance is reduced with increased pullout displacement. This phenomenon is observed for both CN and HN. The graphs demonstrate that an increase in overburden pressure results in additional pullout resistance for both CN and HN. The experimental findings show the pullout resistance is openly relative to overburden pressure. This relationship is likely attributed to enhanced soil-nail interaction and adhesion values caused by the increased surcharge pressure. The improved soil-nail interaction between the soil and nail appears to be influenced by the higher overburden pressure, contributing to the observed trends in pullout resistance.

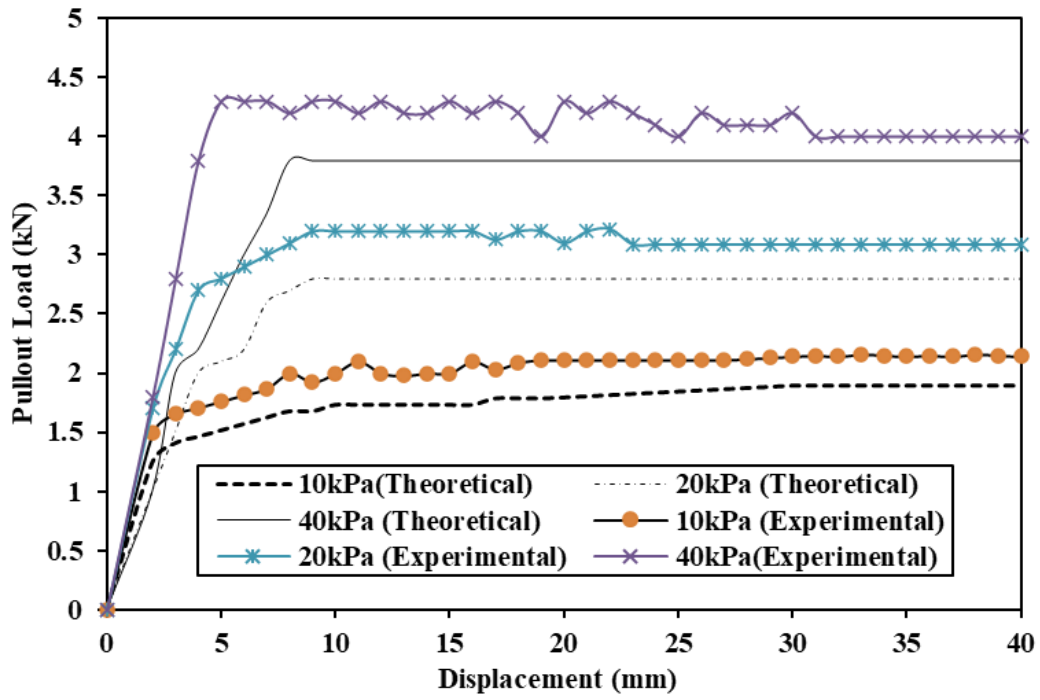

Figure 6.1. Load-displacement behavior of CN by experimental and simulated in cohesive soil

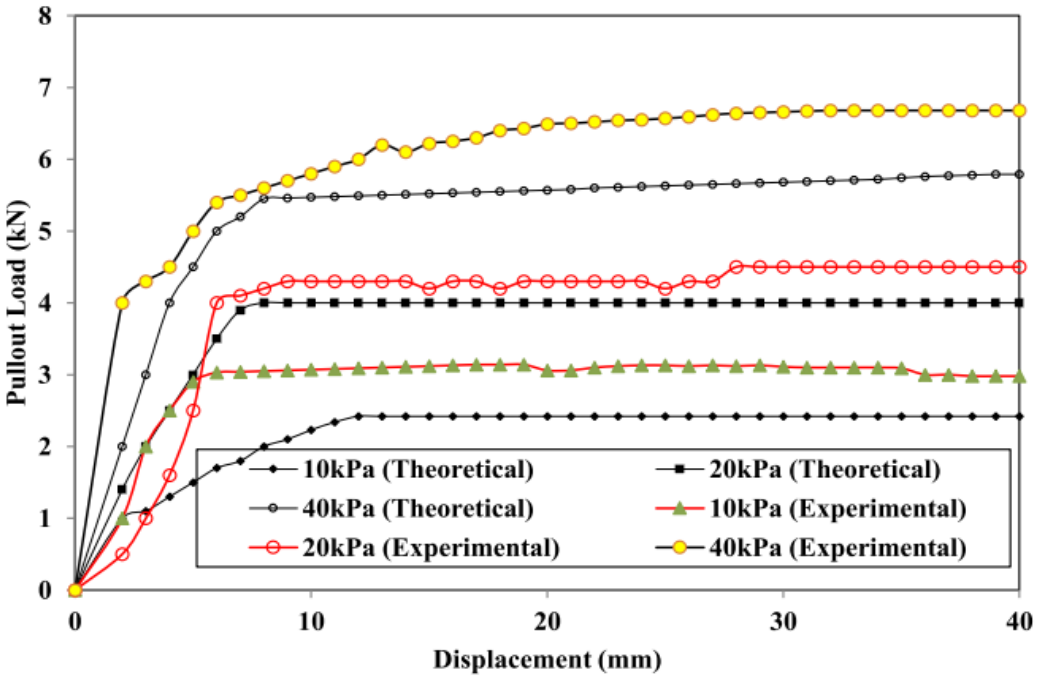

Figure 6.2. Load-displacement behavior of HN by experimental and simulated in cohesive soil

As the shear stress increases, the pullout capacity of the soil nail also increases. When compared to CN, HN showed 42% higher pullout capability under variable surcharge pressures. The installation effect and lateral pressure in the soil nailing are unable to be incorporated into the mathematical model. The variations in the design parameters also cause the difference in experimental and calculated pullout forces. Nail shaft type, shaft surface, friction angle, helix parameter, and shear strength of soil are considered for the pullout of soil nails. Soil dilatancy effect caused by soil nail pullout testing (Milligan et al. 1998; Pradhan et al. 2006; Zhang et al. 2009; Misra et al. 2004). The experimental results closely match the predicted values, indicating good agreement between the two.

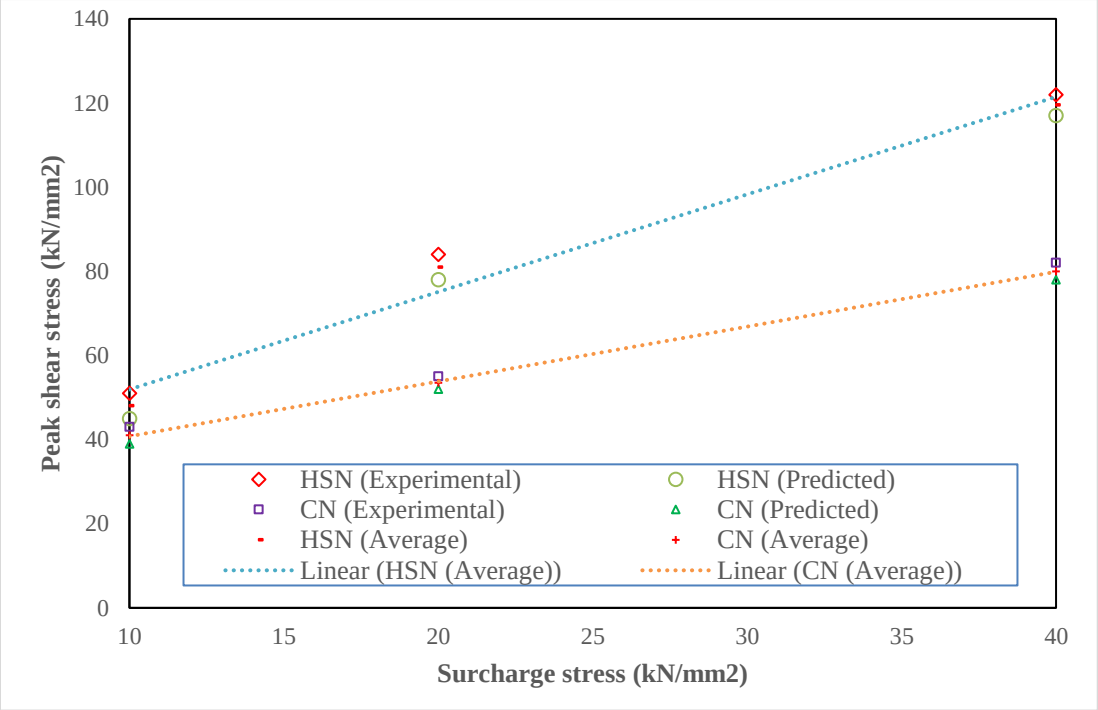

Figure 6.3. Experimental and Predicted shear stress

Under various surcharge pressures, the peak shear was designed. The same pattern was observed by both experimental and theoretical values. Figure 6.3 shows the pullout shear stress by experimental and predicted that shows that pullout force follows the Mohr-Coulomb trend.

6.3. Internal soil stresses

Figure 6.4 displays the earth pressure cell readings obtained during CN installation, while Figure 6.5 shows the readings collected during HN installation. Figure 6.4 indicates that the earth pressure experienced significant changes as the installation depth or embedded length increased for each set of cells. The difference in earth pressure causes a major shift in the amount of soil during CN installation. During CN installation, significant disturbances occur. Moreover, as the installation depth increases, the internal stresses continuously decrease. The internal stresses stay nearly the same even after CN is grouted. In figure 6.5, there was a continuous rise in earth pressure while installing the HN. This shows that the HN's advancement leads to a significant increase in confining pressure, resulting in higher soil density around the nail's perimeter. In the end, the soil exerts a stronger pullout force on the soil nail. The varying composition of the soil, ranging from coarse sand to clay, results in different earth pressures due to the unique unit weights of the particles (Sharma et al. 2020c; Rotte and Viswanadham 2013).

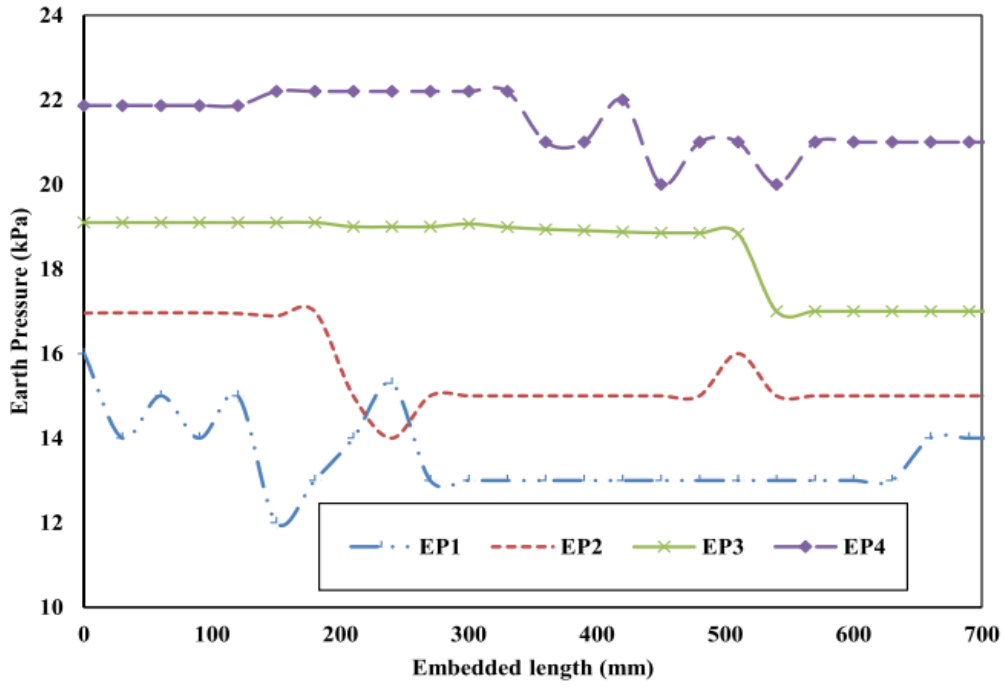

Figure 6.4. Earth pressure variations while installing the CN

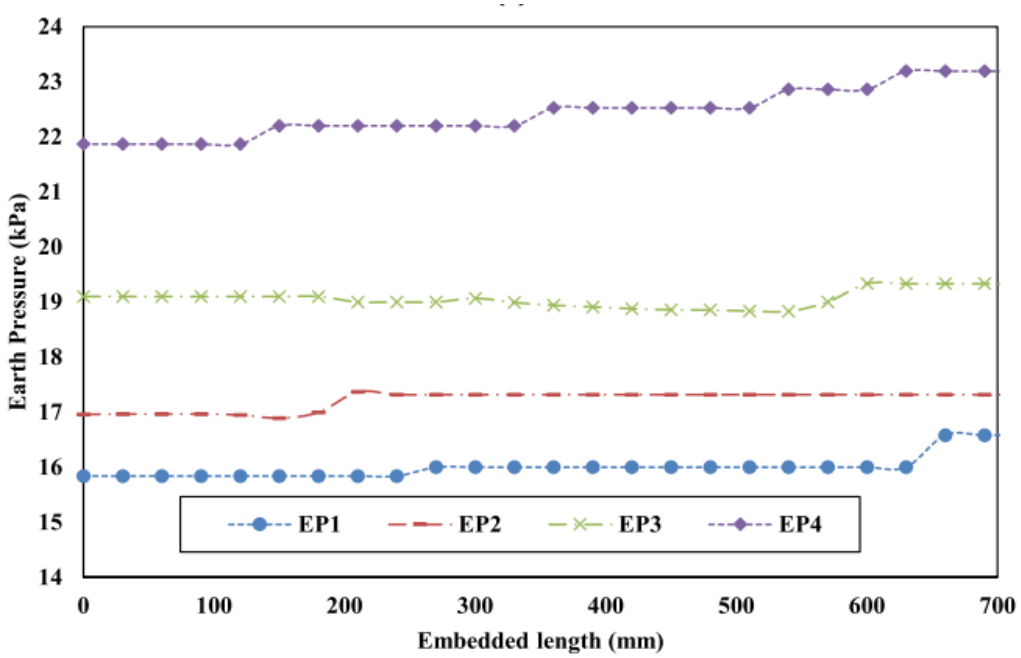

Figure 6.5. Earth pressure variations while installing the HN

6.4. Factor of safety of CN and HN

The safety factor (FOS) in a soil-nailing system depends on the soil's shape, its strength, and the nail material (Lazarte et al. (2015)). It can be determined by both mathematical method and numerical analysis methods. The mathematical methods are conducted through predetermined formulas, in the same time the numerical modelling is conducted through the FEA.

6.4.1. Mathematical modelling

The mathematical modeling analysis reveals that the FOS for CN is calculated as 1.19, 1.25, and 1.26 under surcharge pressures of 10kPa, 20kPa, and 40kPa correspondingly. Also, the FOS for helical soil nails was calculated as 1.2, 1.54, and 1.90 under the related surcharge pressure. Table 6.1 shows that HN provides significantly higher FOS than CN when exposed to similar surcharge pressure, soil condition, and installation depth. Even though the FOS of CN is slightly increased by increasing the overburden pressure, but FOS of HN is significantly increased by the improved overburden pressure. Through this outcome, it is ensured that the HN functions substantially better than CN in cohesive soil.

Table 6.1. Factors of safety for CN and HN

Overburden pressure (kPa)	FOS for CN	FOS for HN
10	1.19	1.24
20	1.25	1.54
40	1.26	1.70

6.4.2. Numerical modelling

By following the recommendation of PLAXIS guides, the FOS is characterized as $\sum Msf$ by soil mass displacement factor. From Figure 6.6 it is established that, under similar loading conditions the FOS of CN and HN was determined as 1.23 and 1.47 respectively. According to this graph, HN provides approximately 19% higher safety factor (FOS) compared to CN when subjected to comparable soil and loading conditions. This observation matches related to the previously conducted theoretical analysis.

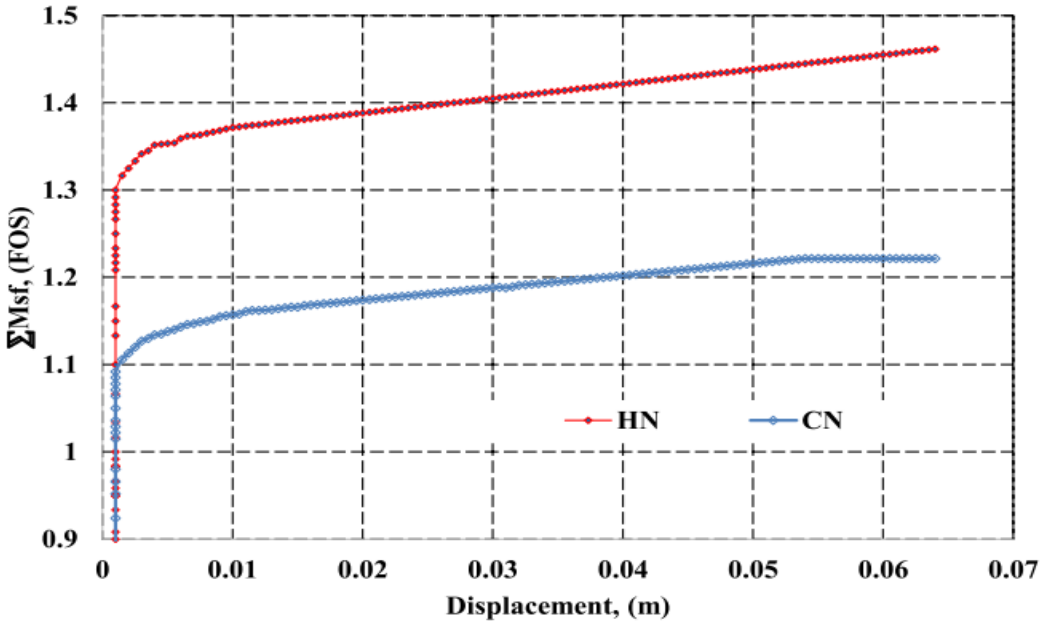

Figure 6.6. Factor of Safety for CN and HN

Furthermore, in Figures 6.7 and 6.8, it can be observed that HN experienced its maximum deformation at 0.15 m, while CN recorded it at 0.20 m, both under similar loading conditions. According to the results obtained, it is evident that HN leads to 5% lesser deformation compared to CN. This could be attributed to the additional bearing resistance provided by the HN's helices. In the soil nailing, lesser deformation indicates more strength. Both numerical and theoretical analyses demonstrate that HN offers a substantially higher safety factor than CN.

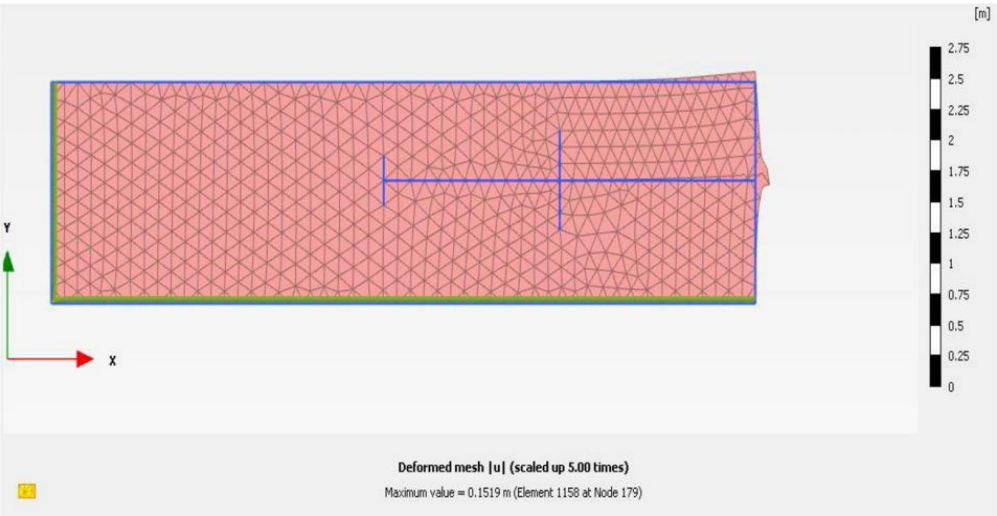

Figure 6.7. Maximum deformation for HN

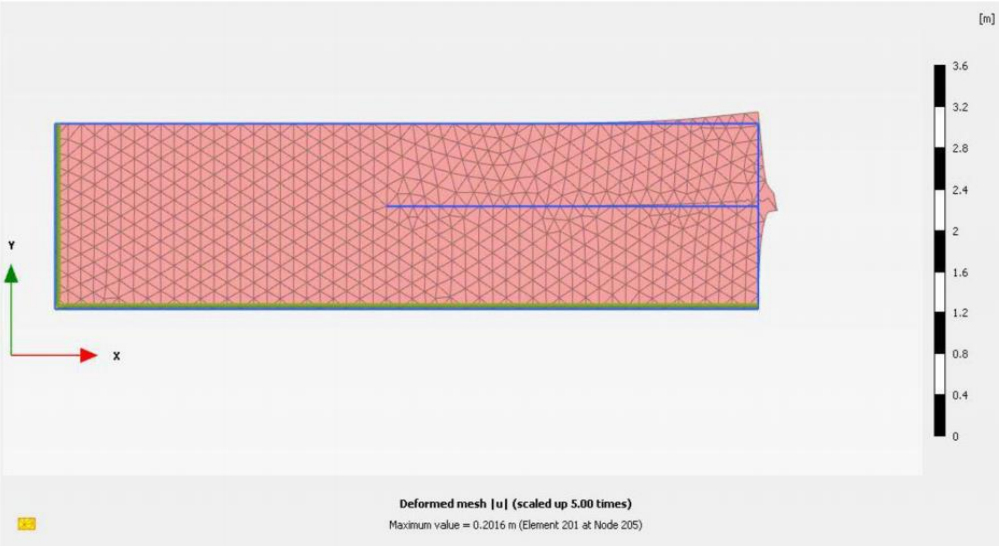

Figure 6.8. Maximum deformation for CN

6.5. Validation and optimization of helical soil nailing outcomes

Based on theoretical and numerical analysis HN provides higher safety and less soil deformation than CN. Particularly, HN provides the soil mass with 5% less distortion and 19% greater safety. To enhance and validate the characteristics of helical soil nailing, two approaches, namely RSM and Hybrid DBN-COOT optimization, are proposed. RSM is a statistical technique utilized to analyze and model the correlation between input variables and the response. On the other hand, Hybrid DBN-COOT optimization integrates artificial intelligence and optimization methods to optimize complex systems. These techniques are being used to better understanding and develop helical soil nailing systems. Validation and optimization by RSM and Hybrid DBN-COOT optimization led to a more effective and efficient system. MATLAB program 2020a was used to carry out the Hybrid DBN-COOT optimization method.

6.6. Performance of RSM-BBD approach

Based on the RSM-BBD approach, 40 experimental input combinations (i.e., experimental runs) are achieved in this study and are shown in Table 6.2. The soil nails are then inserted in the pull-out test tank according to the input variables. Following that, experimental calculations were made for the corresponding output characteristics, such as a factor of safety, installation torque, and pull-out capacity. RSM-BBD is then given the experimented output values to analyze the correlation between the input and output parameters and optimize them in accordance with the specification. The following is a summary of the outcomes attained:

Table 6.2.RSM-BBD design based on 40 input combinations

	Input factors				**Output responses**		
Run	**Surcharge pressure(A)**	**Shaft Diameter(B)**	**Helical pitch(C)**	**Inclination angle(D)**	**Installation torque**	**Pull-out capacity**	**factor of safety**
	kPa	**mm**	**mm**	**degree**	**kN-m**	**kN**	**-**
1	30	15	35	10	0.27	6.72	1.64
2	30	14	30	10	0.24	6.61	1.67
3	40	15	30	10	0.27	6.83	1.61

4	40	15	35	15	0.27	6.79	1.58
5	40	15	30	20	0.31	7.05	1.55
6	30	15	35	20	0.24	6.43	1.60
7	30	16	25	15	0.30	6.93	1.58
8	20	15	30	10	0.16	5.61	1.75
9	30	16	30	10	0.29	6.94	1.66
10	20	14	30	15	0.15	5.53	1.72
11	40	16	30	15	0.34	7.55	1.51
12	30	15	25	20	0.26	6.63	1.62
13	40	14	30	15	0.28	7.02	1.59
14	20	15	30	20	0.16	5.63	1.71
15	30	16	35	15	0.29	6.99	1.59
16	30	15	30	15	0.28	6.77	1.65
17	30	15	25	10	0.24	6.41	1.64
18	30	14	35	15	0.26	6.73	1.64
19	20	15	35	15	0.16	5.52	1.69
20	20	16	30	15	0.17	5.71	1.68
21	20	15	25	15	0.16	5.62	1.73
22	40	15	25	15	0.30	6.91	1.53
23	30	16	30	20	0.31	7.21	1.55
24	30	14	25	15	0.24	6.55	1.67
25	30	14	30	20	0.24	6.31	1.67
26	40	15	35	15	0.26	6.61	1.59
27	30	15	30	15	0.26	6.56	1.66
28	20	15	35	15	0.25	6.62	1.66
29	30	16	35	15	0.28	6.92	1.59
30	30	15	30	15	0.24	6.28	1.67
31	30	15	30	15	0.20	5.82	1.68

32	30	15	30	15	1.87	5.7	1.69
33	30	15	30	15	0.16	5.52	1.70
34	30	14	25	15	0.25	6.74	1.65
35	30	15	30	15	0.17	5.41	1.69
36	30	15	30	15	0.17	5.23	1.68
37	40	15	30	20	0.32	7.12	1.54
38	30	15	25	10	1.88	6.02	1.70
39	30	15	30	15	0.18	5.19	1.66
40	30	15	30	15	0.18	5.12	1.63

RSM-BBD is employed to analyze the correlation between input factors and output responses. This helps identify significant factors influencing the performance of the soil nail system. RSM-BBD is used to optimize the input factors for desired output responses. Engineers can identify the optimal combination of input parameters to achieve the best performance and stability. Each row in the table 6.2 represents a specific experimental run with unique input combinations. Analyzing the results helps in understanding how variations in input factors impact the performance of the soil nail system.

6.6.1. Regression Model Equations

In this research, the relationships between the independent variables and the output responses are modeled using a second-order polynomial equation. The installation torque, pull-out capacity, and safety factor are all parametric responses used in this study. Design-Expert will generate a "**design matrix**" based on the levels of input factors as shown in Figure 5.11 of step 11. After analyzing the input values and output responses, the RSM regression equations of installation torque, pullout capacity, and factor of safety were generated. After that design expert has fitted the response to two-factor interaction (2FI), linear, quadratic, and cubic polynomials. The cubic order terms will not considerably enhance the fit, but Design-Expert is now stating (by bold emphasis) that the quadratic model seems the best as given in Figure 5.13. The quadratic model is generated and then by ANOVA analysis the final equations in terms of actual factors, coefficients, and coded equations in terms of coded factors for the chosen model. The regression model equations (6.1),

(6.2), and (6.3) play a crucial role in understanding the relationships between the input factors (surcharge pressure, shaft diameter, helical pitch, and inclination angle) and the output responses (installation torque, pull-out capacity, and factor of safety). These equations are derived from the RSM and provide a quantitative representation of the impact of each input variable on the corresponding output response.

$$\begin{aligned} Installation\ torque &= 0.277 + 0.067A + 0.023B - 0.0018C + 0.004D \\ &+ 0.01AB - 0.0042AC + 0.0072AD - 0.0068BC + 0.0048BD - 0.012CD \\ &- 0.044A^2 + 0.004B^2 - 0.001C^2 - 0.0101D^2 \end{aligned} \quad (6.1)$$

$$\begin{aligned} Pullout\ capacity &= 6.77 + 0.71A + 0.207B + 0.03C + 0.011D + 0.088AB \\ &- 0.005AC + 0.05AD - 0.053BC + 0.14BD - 0.13CD - 0.42A^2 + 0.107B^2 \\ &- 1.122C^2 - 0.094D^2 \end{aligned} \quad (6.2)$$

$$\begin{aligned} Factor\ of\ safety &= 0.165 - 0.076A - 0.033B - 0.0025C - 0.022D - 0.01AB \\ &+ 0.023AC - 0.005AD + 0.01BC - 0.027BD - 0.0045CD - 0.0012A^2 \\ &- 0.017B^2 - 0.018C^2 + 0.001D^2 \end{aligned} \quad (6.3)$$

The installation torque regression equation is represented as (6.1) which indicates the relationship between input variables and installation torque. Where the coefficients of the equation represent the impact of each input variable on the installation torque. For instance, a rise in surcharge pressure (variable A) leads to an increase in installation torque with a coefficient of 0.067. While an increase in helical pitch (variable C) results in a decrease in installation torque with a coefficient of -0.0018.

The regression equation (6.2) indicates the impact of each input variable on the pullout capacity. The coefficient of B^2 which represents shaft diameter squared, is 0.107 which implies that pullout capacity is affected via the shaft diameter in a nonlinear manner. A rise in shaft diameter leads to a substantial improvement in the pullout capacity. In contrast, the coefficient of C^2, denoting the squared helical pitch, shows a value of -1.122, indicating a nonlinear impact of helical pitch on the pullout capacity. Furthermore, an augmentation in helical pitch results in a notable decrease in the pullout capacity.

In equation (6.3), the factor of safety is linked to the input variables. The coefficient of A corresponds to surcharge pressure and has a value of -0.076, suggesting that higher surcharge

pressure results in a lower factor of safety. On the other hand, the coefficient of AC, which reflects the interaction between surcharge pressure and helical pitch, is 0.023, indicating a positive impact on the safety factor.

With the aid of these equations, one can forecast the installation torque, pullout capacity, and factor of safety across different combinations of input variables. The default coding employs +1 for high levels and -1 for low levels of factors. Through the comparison of factor coefficients, the coded equations allow us to assess the impact of various factors. This not only enhances our understanding of the system behavior but also facilitates informed decision-making in the design and optimization processes.

6.6.2. ANOVA Analysis

The RSM approach employs ANOVA to gather statistical information about the model mean, standard deviation, and others. The model's significance is assessed by considering factors such as P-value, degree of freedom, F-value, and regression coefficient. The P-value in ANOVA represents the probability of obtaining results as extreme as the ones observed, assuming the null hypothesis is true. A smaller P-value indicates stronger evidence against the null hypothesis. The F-value is the ratio of the variance explained by the model to the variance not explained, and a higher F-value suggests a more significant model. A low P-value (typically ≤ 0.05) suggests that the observed effects are statistically significant (Kotadiya et al. 2016). If the P-value is less than 0.05 and the F-value is high, it indicates that the model or factor is statistically significant. If the P-value (significance probability value) exceeds 0.05, the model is deemed insignificant. Table 6.3, 6.4, and 6.5 presents the ANOVA result for installation torque, pull-out capacity, and factor of safety.

The sources of variance used in the analysis are listed in the “Source” column. The quantity of variance to each source is displayed in the “Sum of Squares” column. Each source's degrees of freedom are listed in the “df” column. The "Mean Square" column provides an estimate of the variance, calculated by dividing the SS by the df. On the other hand, the "F-value" column serves as a measure to evaluate the significance of each source, representing the ratio between the mean square for each source and the mean square for the residual. The “Model” row which incorporates

all the sources provided, displays the overall variation explained by the model in each ANOVA table. The unexplained variance is demonstrated in the “residual” row and the “Cor Total” row shows the total variation in the data.

The ANOVA tables reveal almost significant effects which suggesting that the input parameters have a significant impact on the responses. The model’s P-value and F-value which are less than 0.05 indicate the RSM model’s significance. The responses namely installation torque, factor of safety, and pull-out capacity are significantly influenced by shaft diameter and surcharge pressure. Thus, these parameters have a significant impact on the responses. The RSM’s empirical model equations demonstrate that the entire response’s R squared value is greater than 0.97 which indicates the model’s adequacy.

Table 6.3. ANOVA for Installation Torque

Source	**SS**	**df**	**MS**	**F-value**	**p-value**	
Model	0.0742	14	0.0053	38.31	< 0.0001	significant
A-Surcharge pressure	0.0549	1	0.0549	397.20	< 0.0001	significant
B-Shaft Diameter	0.0067	1	0.0067	48.59	< 0.0001	significant
C-Helical pitch	0.0000	1	0.0000	0.2916	0.6010	
D-Inclination angle	0.0002	1	0.0002	1.39	0.2660	
AB	0.0004	1	0.0004	2.89	0.1199	
AC	0.0001	1	0.0001	0.5223	0.4864	
AD	0.0002	1	0.0002	1.52	0.2458	
BC	0.0002	1	0.0002	1.32	0.2778	
BD	0.0001	1	0.0001	0.6524	0.4380	
CD	0.0006	1	0.0006	4.52	0.0595	
A^2	0.0054	1	0.0054	39.22	< 0.0001	significant
B^2	0.0000	1	0.0000	0.3131	0.5881	
C^2	0.0004	1	0.0004	2.62	0.1365	
D^2	0.0003	1	0.0003	2.08	0.1803	

Residual	0.0014	10	0.0001			
Cor Total	0.0756	24				

Table 6.4. ANOVA for Pullout capacity

Source	**SS**	**df**	**MS**	**F-value**	**p-value**	
Model	7.97	14	0.5692	29.46	< 0.0001	significant
A-Surcharge pressure	6.06	1	6.06	313.80	< 0.0001	significant
B-Shaft Diameter	0.5125	1	0.5125	26.53	0.0004	significant
C-Helical pitch	0.0001	1	0.0001	0.0069	0.9354	
D-Inclination angle	0.0014	1	0.0014	0.0729	0.7927	
AB	0.0306	1	0.0306	1.58	0.2366	
AC	0.0001	1	0.0001	0.0052	0.9441	
AD	0.0100	1	0.0100	0.5175	0.4884	
BC	0.0110	1	0.0110	0.5706	0.4674	
BD	0.0784	1	0.0784	4.06	0.0717	
CD	0.0650	1	0.0650	3.37	0.0965	
A^2	0.4961	1	0.4961	25.67	0.0005	significant
B^2	0.0324	1	0.0324	1.68	0.2246	
C^2	0.0427	1	0.0427	2.21	0.1681	
D^2	0.0250	1	0.0250	1.30	0.2815	
Residual	0.1932	10	0.0193			
Cor Total	8.16	24				

Table 6.5. ANOVA for Factor of safety

Source	**SS**	**df**	**MS**	**F-value**	**p-value**	
Model	0.0969	14	0.0069	54.81	< 0.0001	significant
A-Surcharge pressure	0.0692	1	0.0692	547.59	< 0.0001	significant

B-Shaft Diameter	0.0127	1	0.0127	100.87	< 0.0001	significant
C-Helical pitch	0.0001	1	0.0001	0.5549	0.4735	
D-Inclination angle	0.0060	1	0.0060	47.74	< 0.0001	significant
AB	0.0004	1	0.0004	3.17	0.1055	
AC	0.0021	1	0.0021	16.39	0.0023	significant
AD	0.0001	1	0.0001	0.7918	0.3945	
BC	0.0004	1	0.0004	3.17	0.1055	
BD	0.0031	1	0.0031	24.39	0.0006	significant
CD	0.0001	1	0.0001	0.6413	0.4418	
A^2	4.123E-06	1	4.123E-06	0.0326	0.8602	
B^2	0.0008	1	0.0008	6.06	0.0336	
C^2	0.0010	1	0.0010	7.62	0.0201	
D^2	4.711E-06	1	4.711E-06	0.0373	0.8507	
Residual	0.0013	10	0.0001			
Cor Total	0.0982	24				

SS- Sum of Squares, df-degrees of freedom, MS-Mean Square

6.6.3. Predicted vs. Actual plots

Figure 6.9, 6.10, and 6.11 shows a comparison between the RSM's predicted values and the actual values for installation torque, pull-out capacity, and factor of safety. The accuracy of the model's prediction was determined by these prediction plots. These plots compare the actual values of installation torque, pull-out capacity, and factor of safety to the RSM model's predicted values. The accuracy of the model can be evaluated by examining the points on the plot. A diagonal line that represents perfect agreement between the predicted and actual values can be drawn. If the points fall close to this line, the model is considered accurate. However, deviations from this line indicate that the model may be under or over-predicting the response variable. In such cases, adjustments may be needed to improve the model's accuracy. In Figures 6.9, 6.10, and 6.11, the plotted points are close to the diagonal line. This shows that the predicted values closely match the actual values.

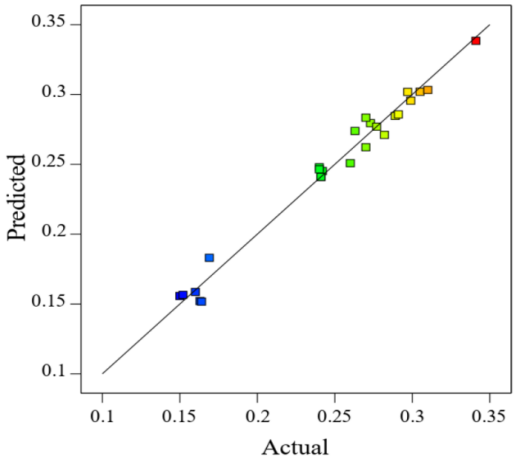

Figure 6.9. Predicted vs. Actual plots for installation torque

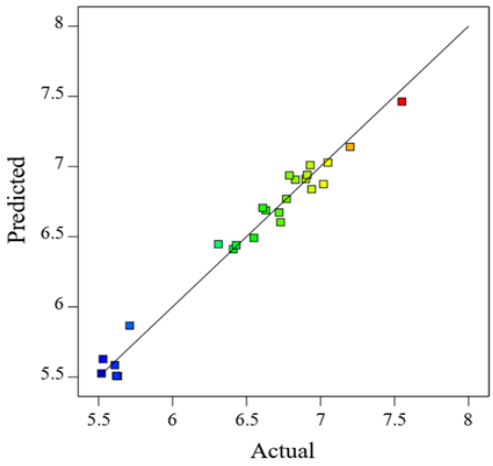

Figure 6.10. Predicted vs. Actual plots for pull-out capacity

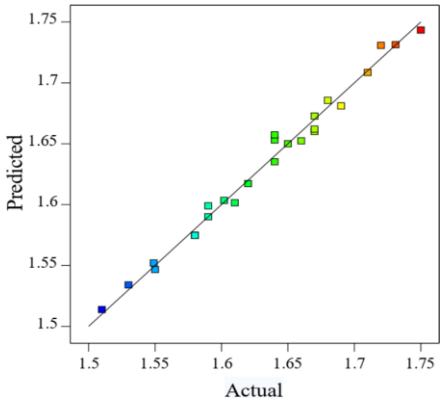

Figure 6.11. Predicted vs. Actual plots for factor of safety

6.6.4. Contour and 3D plots

Figure 6.12, 6.13, and 6.14 shows the RSM surface plot for the installation torque, pull-out capacity, and safety factor. In these plots, the interaction between shaft diameter and surcharge pressure is illustrated in Figures 6.12a, 6.13a, and 6.14a. The interaction between surcharge pressure and helical pitch is displayed in Figures 6.12b, 6.13b, and 6.14b. Lastly, figures 6.12c, 6.13c, and 6.14c demonstrate the interaction between surcharge pressure and inclination angle. The shaft diameter has a direct influence on the installation torque. An increase in surcharge pressure from 20kPa to 40kPa leads to an increase in installation torque. However, an increase in helical pitch does not improve pullout capacity and can even reduce it due to the auguring soil effect. This effect restricts forward helix movement and causes soil grain crushing, which can cause installation disturbances. The study found that shaft roughness and skin friction are important factors in enhancing pull-out capacity, with additional shaft roughness leading to maximum pull-out capacity. The increase in surcharge pressure also leads to higher maximum shear stresses in the nail shaft. This finding has been reported in previous research by Sharma et al. (2021c) and Sharma et al. (2022).

The inclination angle affects the installation torque, causing a slight increase before eventually decreasing. At an inclination angle of 15˚, the peak pull-out capacity and installation torque are typically observed in helical soil nailing. The pull-out capacity and installation torque are directly proportional to this type of nailing, and increasing the shaft diameter also results in an increasing trend for both parameters. The Mohr-Coulomb failure criterion governs the pull-out capacity under various surcharge pressures. As the inclination angle increases, the pull-out capacity decreases due to stress impact on the soil nail and soil parameters. When the inclination angle is raised, the compressive force within the soil nail also rises. The attainment of maximum pull-out capacity is linked to an escalation in surcharge temperatures. However, as the inclination angle, surcharge pressure, and shaft diameter increase, the effect on the factor of safety diminishes. Furthermore, increasing the helical pitch leads to a slight improvement in pull-out capacity until a certain threshold, beyond which it starts to decline.

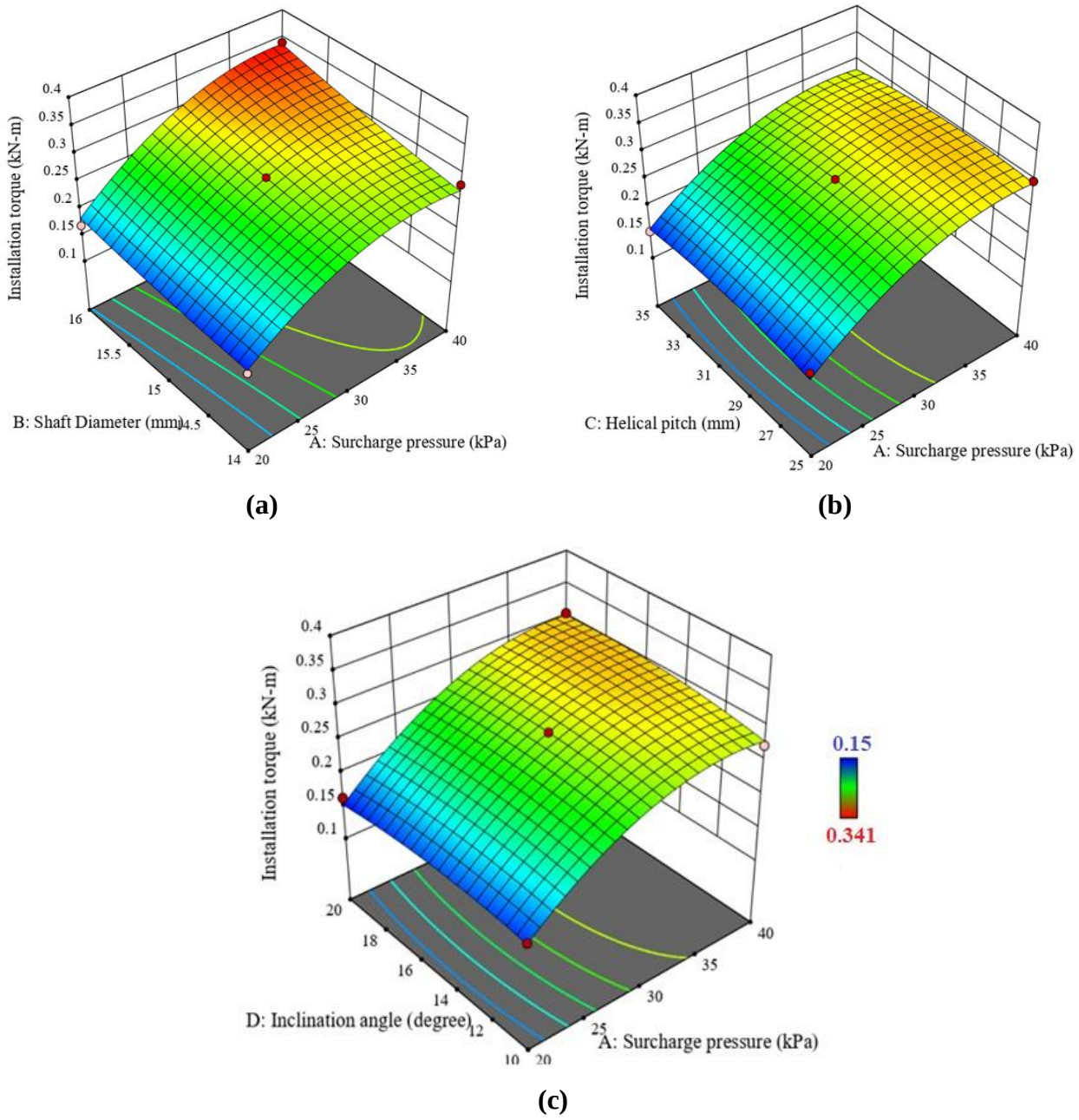

Figure 6.12. RSM Surface Plot for Installation Torque (a) Surcharge pressure vs shaft diameter, (b) Surcharge pressure vs helical pitch, (c) Surcharge pressure vs inclination angle

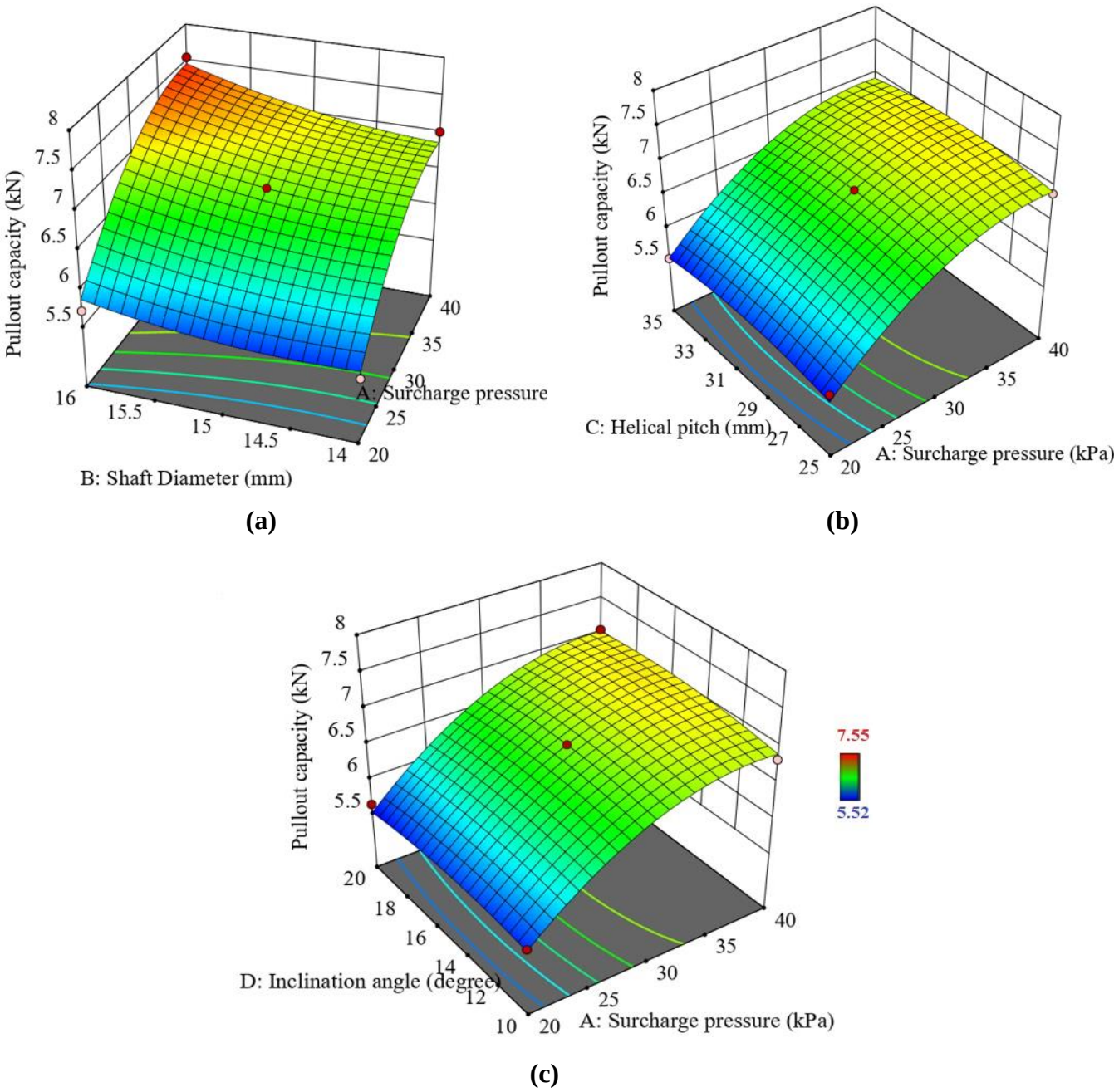

Figure 6.13. RSM Surface Plot for Pull-out capacity (a) Surcharge pressure vs shaft diameter, (b) Surcharge pressure vs helical pitch, (c) Surcharge pressure vs inclination angle

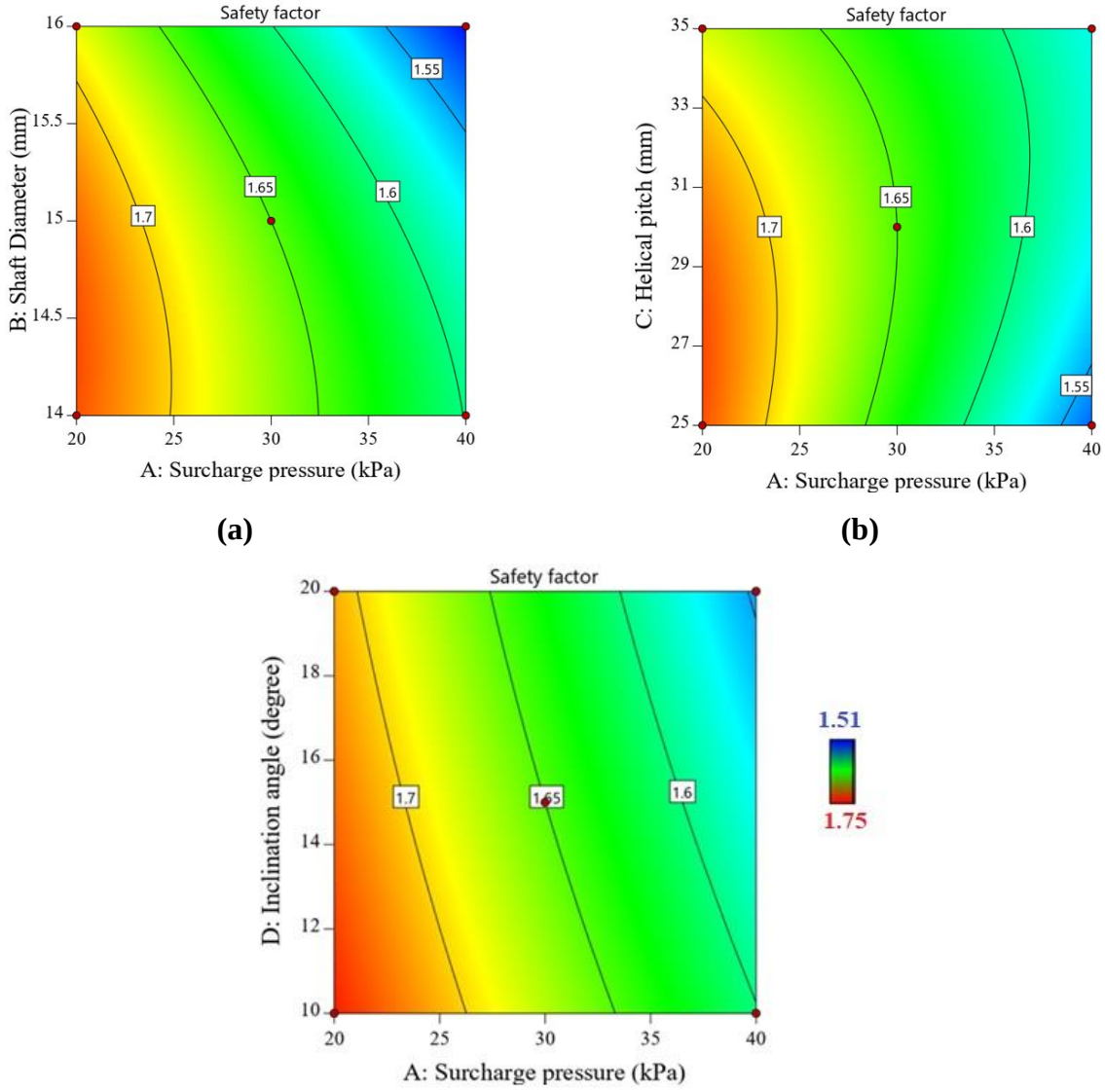

Figure 6.14. RSM Surface Plot for Factor of safety (a) Surcharge pressure vs shaft diameter, (b) Surcharge pressure vs helical pitch, (c) Surcharge pressure vs inclination angle

6.7. Performance of hybrid DBN-COOT model

The proposed hybrid DBN-COOT model is designed to predict soil nail parameters with high accuracy. The model represents the relationship between validated and target outcomes in Figure 6.15 using regression, which has a coefficient of 0.99. To improve the optimization of DBN, the

COOT algorithm is added to the neural network weight updating stage. To prevent overfitting, the hybrid DBN-CO approach only used six points for validation. This method of using a deep network with a small dataset and training is a viable option when large datasets are not available (Feng et al. 2019).

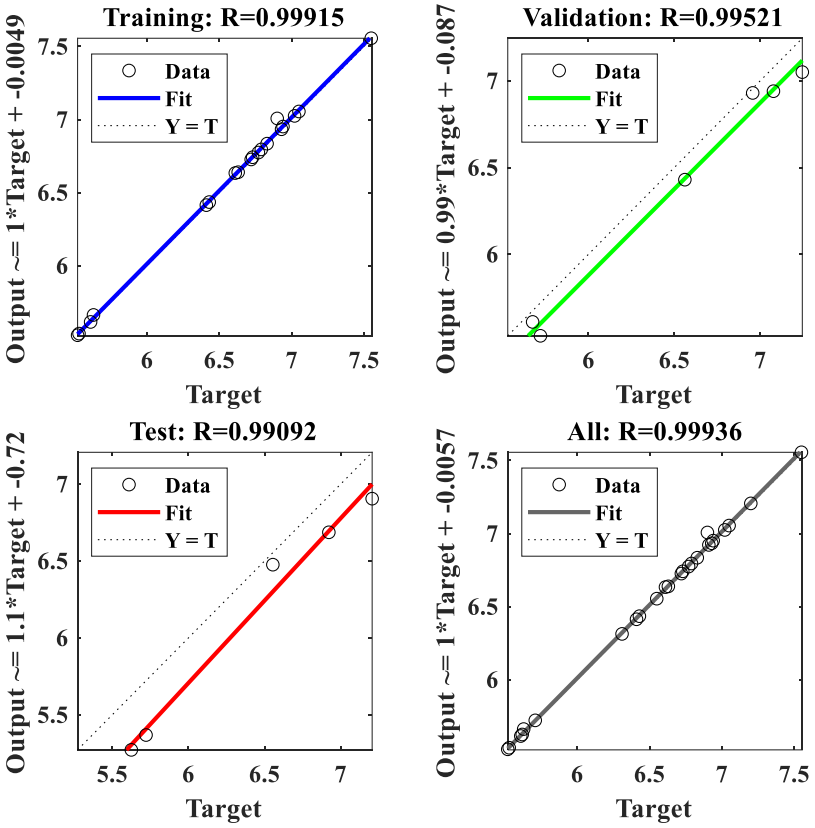

Figure 6.15. Performances of the DBN-CO at all stages

The graph plots the actual or target or experimental values on the X-axis and the values obtained from the hybrid DBN model on the Y-axis, showing that the predicted and actual values were close to each other with minimal error and good regression. The majority of the data points clustered around the 45˚ lines, indicating high accuracy of the model and better correlation between estimated and actual values. The regression plots demonstrate exceptional performance by the hybrid DBN-COOT model across various datasets, as indicated by the high correlation coefficients (R values). In the training set, the R value of 0.99915 reflects an almost perfect linear relationship

between the predicted and actual values. The data used in this context is related to soil nail parameters. The model is trained, tested, and validated on datasets containing information about these parameters. The limited dataset (only six points for validation) suggests that the model is designed to perform well even when large datasets are not available. The high correlation coefficients across different sets indicate that the model has learned meaningful patterns from the available data, and it can generalize well to new and unseen data.

Figure 6.16 demonstrates the comparison of the proposed DBN-COOT method with various validation models. The difference between the actual and DBN-CO predictions is lower compared to other methods such as RSM, DBN, and ANN. The non-hybrid approaches produce results that are almost identical to each other. In the experiments, the optimum pull-out capacity was found to be 7.55kN with a factor of safety of 1.51. The pullout capacity predictions from DBN-COOT, RSM, DBN, and ANN for this optimal condition were 7.56, 7.736, 7.01, and 7.46 respectively. The factor of safety predictions was 1.51, 1.53, 1.53, and 1.51 respectively.

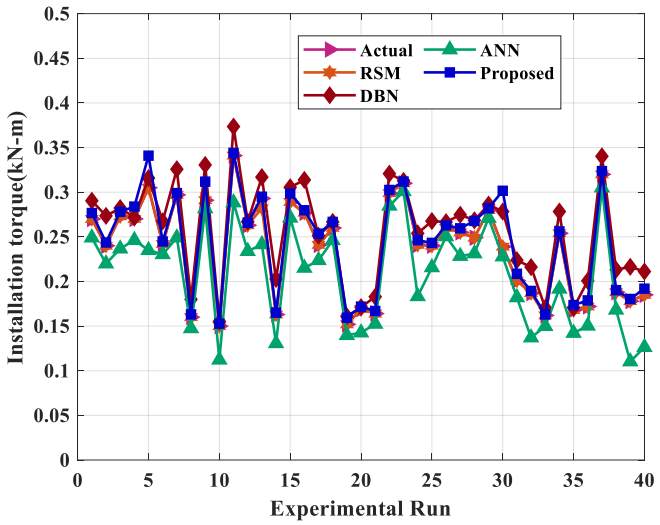

(a)

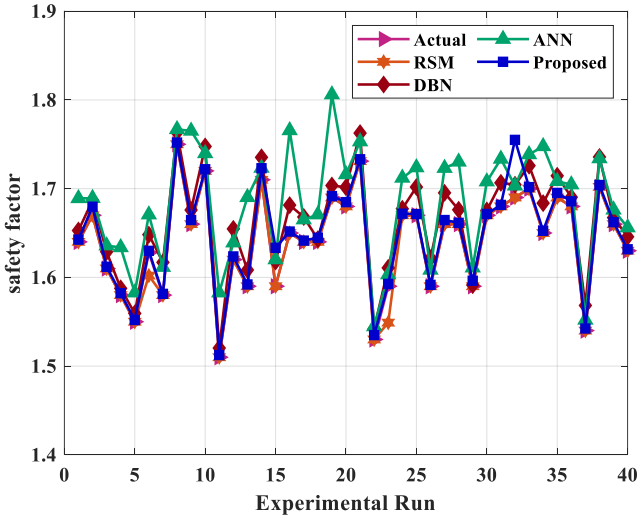

(b)

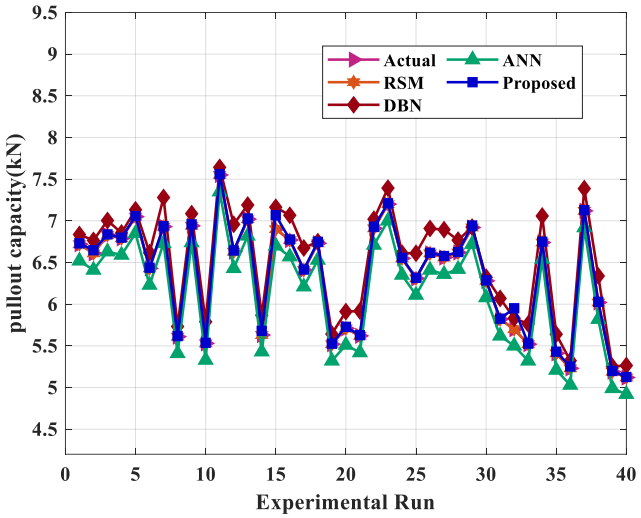

(c)

Figure 6.16. Contrast of Actual and predicted Results obtained from RSM, DBN-COOT, DBN, and ANN (a) Installation torque (b) Safety factor (c) Pull-out capacity

Table 6.6. Statistical Performance evaluation of different predictive Models

Parameter	RSM	DBN-COOT	DBN	ANN
R	0.98	0.99	0.985	0.982
R^2	0.979	0.98	0.97	0.96

MSE	0.0030	0.0018	0.0051	0.0117
RMSE	0.0230	0.0132	0.0226	0.0342

In Table 6.6, the statistical performance of various predictive models, including RSM, DBN-COOT, DBN, and ANN, is evaluated based on four parameters: R^2, R, RMSE, and MSE. All models exhibit high correlation coefficients with DBN-COOT and DBN having the highest values of 0.99 and 0.985 respectively. RSM and ANN models also show high correlation coefficients of 0.98 and 0.982, respectively. The observed result indicates a robust linear correlation between the predicted and actual values across all models. When evaluating the R^2, which gauges the predictability of the dependent variable in relation to the independent variable, the models demonstrate a high degree of accuracy. DBN-COOT performs the best with a value of 0.98, followed by RSM with 0.979. The DBN and ANN models show values of 0.97 and 0.96 respectively. This implies that DBN-COOT and RSM models can better explain the variability in the data compared to DBN and ANN models.

MSE is lowest for DBN-COOT with 0.0018 and for RSM with 0.0030. On the other hand, DBN and ANN models have higher MSE values of 0.0051 and 0.0117, correspondingly, which shows that DBN-COOT and RSM models exhibit better accuracy in predicting the values. Finally considering RMSE, DBN-COOT has the lowest value of 0.0132, followed by RSM with 0.0230. The DBN and ANN models have higher values of 0.0226 and 0.0342, respectively, indicating that DBN-COOT and RSM have better precision in predicting the values. Therefore, the high R-value and low error values of the proposed DBN-COOT model indicate a good correlation with the actual outcomes, suggesting that it has better predictive capability.

6.8. RSM and Hybrid DBN-COOT optimization analysis

The optimal soil nailing characteristics are determined in this study using RSM Optimization in Design-Expert Software. Using desirability analysis, 100 set solutions are generated, each assigned a desirability value of 0.99. The best solutions are then selected by considering the optimal solution as the benchmark. The fitness function used for the RSM can be found in Table 6.7. The chosen fitness functions were aimed at optimizing the performance of the soil nailing system during the

analysis. The input parameters considered were surcharge pressure, shaft diameter, helical pitch, and inclination angle, all of which were within their specified ranges. The installation torque was to be minimized, the pull-out capacity was to be maximized, and the factor of safety was to be minimized. These fitness functions were chosen because they are relevant to the soil nailing performance and assist in determining the input parameter's optimal combination to achieve the desired outcomes. The results obtained from RSM are plotted in Figure 6.17, showcasing the optimum values.

Table 6.7. Fitness functions of RSM

Input Parameter	Surcharge pressure	In range
	Shaft diameter	In range
	Helical pitch	In range
	Inclination angle	In range
Responses	Installation Torque	Minimize
	Pull-out capacity	Maximize
	Factor of safety	Minimize

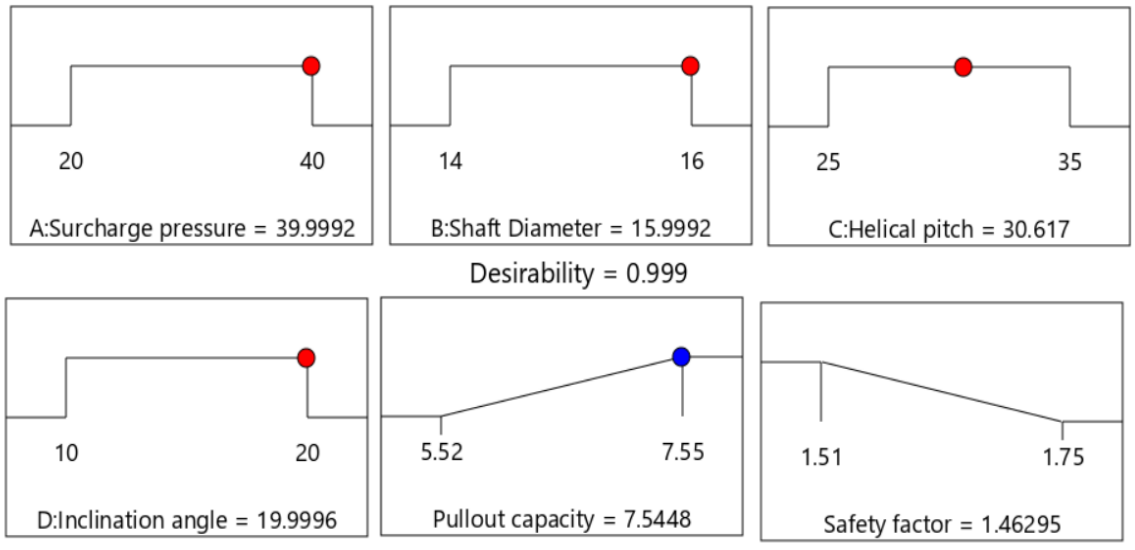

Figure 6.17. RSM-based Optimization Results

Within the scope of this research, it was observed that Response Surface Methodology (RSM) demonstrated comparatively lower effectiveness when contrasted with metaheuristic optimization techniques and machine learning algorithms. To enhance the optimization process, the COOT optimization algorithm is introduced and integrated with RSM, DBN, and ANN. This hybrid COOT optimization method is then applied to optimize the responses listed in Table 6.8. The fitness function of COOT is defined based on the outcomes derived from RSM, DBN, and ANN, as presented in equations (6.4) and (6.5). This integration of diverse techniques aims to augment the overall optimization performance and improve the accuracy of the results.

Fitness function=Min (Safety factor from RSM equation, DBN model, ANN model) (6.4)

Fitness function=Max (Pull-out capacity from RSM equation, DBN model, ANN model) (6.5)

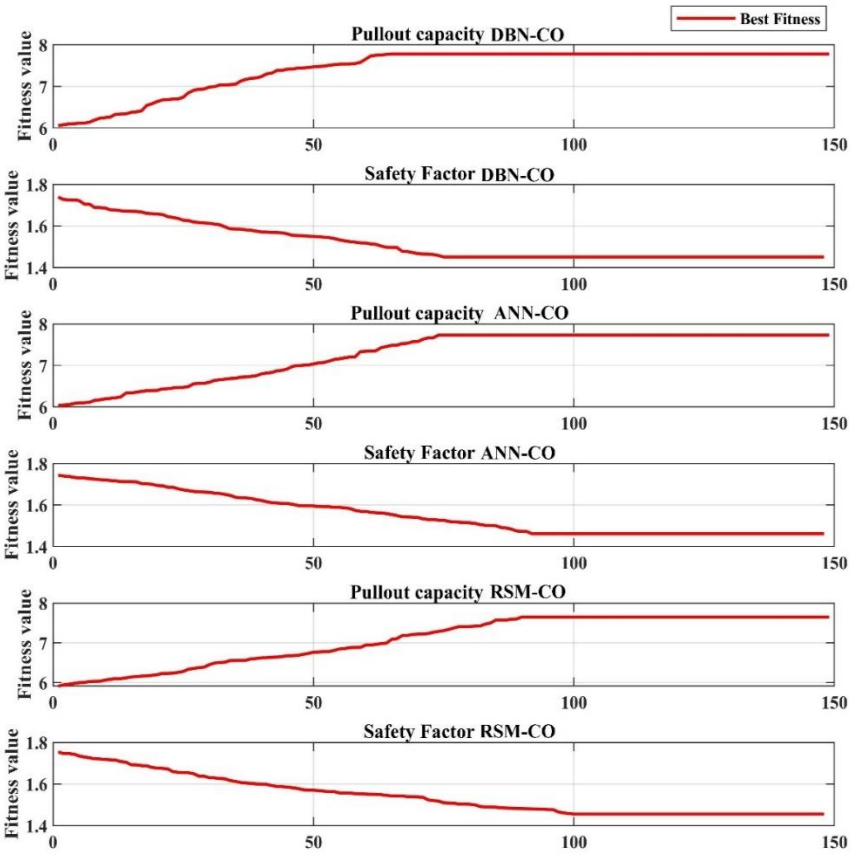

Figure 6.18. Best Fitness Value Analysis from different Optimization techniques

The best solutions obtained from the optimization process that is plotted in Figure 6.18. At the beginning of the plot, the fitness values fluctuate, either increasing or decreasing. However, eventually, the fitness values stabilize and remain constant from a particular point. This point is considered an intermediate point, where both the average and best fitness values are stable. The graph depicts 150 iterations, with DBN-COOT optimization achieving the fitness function in G75 for pull-out capacity and G85 for safety factor. Similarly, ANN-COOT satisfies the fitness conditions in G86 and G93.

The results obtained from the proposed optimization methods, namely RSM, DBN-COOT, ANN-COOT, and RSM-COOT, are demonstrated in Table 6.8.

Table 6.8. Comparison of optimization and the actual outcomes

Output	RSM	DBN-CO	ANN-CO	RSM-CO	Actual
Pullout capacity (kN)	7.5	7.77	7.75	7.64	7.68
Safety factor	1.46	1.44	1.46	1.463	1.453

Among these methods, the DBN-CO optimization approach yields the minimum safety factor and maximum pull-out capacity. Specifically, the DBN-COOT method produces an optimal pull-out capacity of 7.77 and a factor of safety of 1.44. In comparison, RSM optimization results in a pull-out capacity of 7.5 and a factor of safety of 1.46. As such, the proposed DBN-COOT model outperforms the RSM approach by 3%. The findings indicate that the DBN-COOT approach surpasses alternative optimization methods in pull-out capacity and factor of safety.

The ANN-COOT and RSM-COOT models also produce results that are comparable to the DBN-COOT method. To confirm the effectiveness of the DBN-CO model, a comprehensive confirmatory analysis is conducted through experimental testing with the optimized parameters. The outcomes derived from these experiments closely align with those predicted by the DBN-CO model. This convergence of results strongly supports the notion that the DBN-CO optimization

approach is both dependable and highly effective in optimizing parameters for achieving maximum pull-out capacity and ensuring the desired factor of safety.

6.9. Summary

This chapter discussed the experimental, numerical, and mathematical analysis of CN and HN. Derived from the analysis of pullout behavior, factor of safety, and deformation performance, the helical soil nail was selected as a better performance of the soil nail. Furthermore, helical soil nail characteristics were validated and optimized to improve the accuracy and effectiveness that are discussed in this chapter. The next chapter will cover the study's conclusions and future scope.

CHAPTER 7

CONCLUSIONS AND FUTURE SCOPE

In this study, a pullout test setup was employed to examine the pullout characteristics of CN and HN in cohesive soil using a consistent experimental procedure. After analyzing the pullout characteristics of CN and HN during the first phase of the research based on the analytical model, numerical model, and real-time experimentations. After analyzing the data, it became evident that helical soil nails (HN) exhibited superior performance in terms of factor of safety and deformation when subjected to comparable loading and soil conditions. Consequently, the latter part of the study focused on optimizing the working and soil nail installation processes of HN in cohesive soil, taking into consideration crucial factors such as installation torque, safety factor, and pull-out capacity. The machine learning algorithm (DBN-CO) and mathematical design of experiment (RSM-BBD) methods were utilized to optimize such installation phenomena of HN. The findings of this study, along with potential areas for future exploration, are summarized as follows.

7.1. Conclusions

- An experimental study shows that helical soil nails have a 42% greater pullout capability than conventional soil nails under varying surcharge pressures. This is because of the increased shear stress surrounding the helical nail, results in increased pullout capacity. So, the helical soil nail offers more resistance than conventional soil nails under varying surcharge pressure. The experimental and mathematical study shows that there is a direct relationship between surcharge stress and pullout shear stress, indicating that the pull-out force adheres to the Mohr-Coulomb trend for cohesive soil.
- Based on the mathematical model of the load-displacement behavior of a soil nail element the predicted results follow a similar trend with experimental results, however, the predicted result shows a slightly lesser value than the experimental value. The reason may that in mathematical modeling the result is based on soil nail stiffness value or interface friction value. The variations in the design parameters also may cause the difference in the experimental and calculated pullout forces. The experimental value is in good agreement

with the predicted values; hence the mathematical model can predict the approximate value of the pullout load results in the absence of laboratory testing.

- From experiments, progressive soil stresses were noticed on behalf of HN installation. Although for CN installation, the soil stress diminished significantly, such results indicate, that more disturbance might have occurred in CN than in HN. This shows that the HN's advancement leads to a significant increase in confining pressure, resulting in higher soil density around the nail's perimeter. In the end, the soil exerts a stronger pullout force on the soil nail.
- According to the results, the HN is 19% safer than CN for cohesive soil under similar soil and loading situations. From both the mathematical and numerical analysis it was observed that the results are in good agreement with each other and HN provides better FOS than CN under similar loading and soil conditions Also, HN shows 5% less deformation against equal soil mass compared to CN, thus HN is a safer and more convincing alternative for CN in cohesive soil. this may be due to the extra bearing resistance offered by the helices of HN. In the soil nailing, lesser deformation indicates to more strength. Based on theoretical and numerical analysis HN provide higher safety and less soil deformation than CN.
- Performance of RSM-BBD method and hybrid DBN-COOT method shows that the predicted and actual values were close to each other with minimal error and good regression. So, both the optimization methods validated the experimental results but the proposed DBN-CO predicted closer results toward experimented values with a greater regression coefficient over 0.99 for all output parameters and on the other hand, the ANOVA shows that, the shaft diameter and surcharge pressure as the most influencing parameters on HN installation torque, pullout capacity, and safety factor.
- The optimum results of DBN-CO are a safety factor of 1.44 and a pull-out capacity of 7.77kN. Similarly, the optimal outcomes achieved by RSM are a safety factor of 1.46 and a pull-out capacity of 7.5 kN. As a result, the DBN-CO optimized outcomes are 3% higher than the different existing RSM models. Thus, the DBN-CO approach is considered the

best validation and optimal technique to solve the optimization problems of different engineering disciplines.

7.2. Future scopes

- Even though, the proposed HNs are better than CNs. The performance of the proposed HN can be enhanced further in the future by understanding the influence of other parameters like soil nail length, number of nails involved in the nailing process, spacing between adjacent nails and orientation of nails, etc.
- Moreover, this study proved HN can produce greater safety factor and deformation against increased soil mass than CN. As a result, this research may motivate future researchers to investigate more and produce a variety of soil-nailing approaches to achieve more favorable results to implement advanced soil-nailing methods on construction sites.
- Besides, this research used PLAXIS 2D finite element analytical tool to numerically present and validate the proposed experiment. But, in the future, many advanced 3D simulation models and knowledge of respective simulation tools can be used to minimize the solving error percentage and achieve accurate results.

References

Ahmadi, M. M., and Borghei, A. (2018). Numerical investigation into the static behavior of stepped soil nail walls. Scientia Iranica, 25(1), pp.140-151.

Alhabshi, A. (2006). Finite element design procedures for hybrid MSE/Soil-nail retaining wall systems, Doctoral dissertation, Texas Tech University.

Alsubal, S., Harahap, I. S., and Babangida, N. M. (2017). A typical design of soil nailing system for stabilizing a soil slope: case study. Indian Journal of Science and Technology, 10(4), pp.1-7.

Anil, M., and Chen, C. H. (2004). Analytical solution for micropile design under tension and compression. Geotechnical and geological engineering, 22(2), pp.199-225.

Arvin, M. R., Ghavami, E., and Motamedi A., M. (2021). Optimization of Nail Inclination Angle in Soil Nail Walls Based on a Prevalent Limit Equilibrium Method. Indian Geotechnical Journal, pp.1-20.

Ayazi, M. F., and Tangri, A. (2022). Stabilization of soil nailed slope by flexible materials. Materials Today: Proceedings, 49, pp.1950-1955.

Ayazi, M. F., Tangri, A., and Jalota, S. (2020). Soil Nailing-A Review. International Research Journal of Engineering and Technology (IRJET), 7(12), pp.807-810.

Azzam, W., and Sobhey, M. (2019). Utilization of Soil Nailing Technique to Improve Sand Slopes under Seismic Loading. International Conference on Advances in Structural and Geotechnical Engineering ICASGE'19.

Azzam, W. R., and Basha, A. (2017). Utilization of soil nailing technique to increase shear strength of cohesive soil and reduce settlement. Journal of Rock Mechanics and Geotechnical Engineering, 9(6), pp.1104-1111.

Babu, G. S., and Singh, V. P. (2009). Appraisal of soil nailing design. Indian Geotechnical Journal, 39(1), pp.81-95.

Babu, G. L. S., Rao, R. S., and Dasaka, S. M. (2007). “Stabilization of vertical cut supporting a retaining wall using soil nailing: A Case Study.” Ground Improvement, 11(3), 157–162.

Basudhar, P. K., Anubhav, and Lakshminarayana, M. R. (2017). Three-dimensional limit-equilibrium stability analyses of slopes and effect of inclusion of soil nails. International Journal of Geomechanics, 17(9), p.04017067.

Benayoun, F., Boumezerane, D., and Bekkouche, S. R. (2021). Techniques for Optimizing Parameters of Soil Nailed Vertical Cut. Selected Scientific Papers-Journal of Civil Engineering, 16(1), pp.131-145.

Benayoun, F., Boumezerane, D., Bekkouche, S. R. and Bendada, L. (2020). Application of genetic algorithm method for soil nailing parameters optimization. In IOP Conference Series: Materials Science and Engineering. 800(1), p.012009. IOP Publishing.

Benayoun, F., Boumezerane, D., Bekkouche, S. R. and Ismail, F. (2021). Optimization of geometric parameters of soil nailing using response surface methodology. Arabian Journal of Geosciences, 14, pp.1-14.

Benmebarek, M. A., Benmebarek, S., Rad, M. M., and Ray, R. (2022). Pile optimization in slope stabilization by 2D and 3D numerical analyses. International Journal of Geotechnical Engineering, 16(2), pp.211-224.

Bhuiyan, M. Z. I., Wang, S., and Carter, J. (2022). New test facility for studying the behaviour of pressure-grouted soil nails. Transportation Geotechnics, 34, p.100752.

BIS (Bureau of Indian Standards), Methods of test for soils: Determination of water content–dry density relation using light compaction, IS 2720-7. New Delhi, India: BIS (1983)

BIS (Bureau of Indian Standards), Methods of test for soils: Direct shear test, IS 2720 13. New Delhi, India: BIS. (1986)

Bruce, D. A., and Jewell, R. A. (1986). Soil nailing: application and practice-part 1. Ground Engineering, 19(8), pp.10-15.

Burns, S. F. (2006). Landslides in Practice: Investigation, Analysis and Remedial/Preventative Options in Soils: (Derek H. Cornforth). Environmental & Engineering Geoscience. 12(1), 81-82.

Byrne, R. J., Cotton, D., Porterfield, J., Wolschlag, C., and Ueblacker, G. (1998). Soil Manual for design and construction monitoring of soil nail wall. Manual of the Federal Highway Administration Division, No. FHWA0-SA-96-069R.

Capilleri, P. P., Motta, E., and Raciti, E. (2016). Experimental study on native plant root tensile strength for slope stabilization. Procedia Engineering, 158, pp.116-121.

Chan, C.M., and Raman, M. H. A. (2017). Screw-in soil nail for slope reinforcement against slip failure: a lab-based model study. GEOMATE Journal, 12(29), pp.148-155.

Chavan, D., Mondal, G., and Prashant, A. (2017). Seismic analysis of nailed soil slope considering interface effects. Soil Dynamics and Earthquake Engineering, 100, pp.480-491.

Dai, Z. H., Guo, W. D., Zheng, G. X., Ou, Y., and Chen, Y. J. (2016). Moso bamboo soil-nailed wall and its 3D nonlinear numerical analysis. International Journal of Geomechanics, 16(5), p.04016012.

Deng, D. P., Li, L., and Zhao, L. H. (2017). Limit equilibrium analysis for stability of soil nailed slope and optimum design of soil nailing parameters. Journal of Central South University, 24(11), pp.2496-2503.

Dewedree, S., and Jusoh, S. N. (2019). Slope stability analysis under different soil nailing parameters using the SLOPE/W software. In Journal of Physics: Conference Series, 1174(1), p. 012008. IOP Publishing.

Dey, A. (2015). Issues and aspects of soil nailing. CAGERP 2015, Challenges and Recent Advances in Geotechnical Engineering Research and Practice, Guwahati, India, p.1-21.

Dhakal, D., and Acharya, I. P. (2019). Slope stability analysis of hill side steep cut slope and its stabilization by the method of soil nailing technique: A case study on narayanghat-mugling road section. In IOE Graduate Conference, 6, pp.189-196.

Ebrahimi, R., and Asakereh, A. (2016). Parametric evaluation of soil nailing method in slopes stabilization. International Journal of Basic Sciences & Applied Research, 5(2), pp.113-118.

Elahi, T. E., Islam, M. A., and Islam, M. S. (2022). Parametric Assessment of Soil Nailing on the Stability of Slopes using Numerical Approach. Geotechnics, 2(3), pp.615-634.

Elias, V., and Juran, I. (1991). Manual of practice for soil nailing. FHWA RD-89-198, Washington, D.C.

Farrokhzad, F., Tabari, S. M., Abdolghafoorkashani, H., and Tavakoli, H. (2021). Seismic Behaviour of Excavations Reinforced with Soil–Nailing Method. Geotechnical and Geological Engineering, 39(6), pp.4071-4091.

Feng, S., Zhou, H., and Dong, H. (2019). Using deep neural network with small dataset to predict material defects. Materials & Design, 162, pp.300-310.

Garg, A., Garg, A., Tai, K., and Sreedeep, S. (2014). An integrated SRM-multi-gene genetic programming approach for prediction of factor of safety of 3-D soil nailed slopes. Engineering Applications of Artificial Intelligence, 30, pp.30-40.

Gassler, G., and Gudehus, G. (1981). Soil nailing-some aspects of new technique. Proceedings of Tenth ICSMFE.

Gassler, G. (1995). Stabilization of a cutting slope along a high-speed railway line using extremely long nails. The practice of soil reinforcing in Europe organised by the Tenax Group under the auspices of the International Geosynthetics Society, and held at the Institution of Civil Engineers, pp. 214-226. Thomas Telford Publishing.

Ghareh, S. (2015). Parametric assessment of soil-nailing retaining structures in cohesive and cohesionless soils. Measurement, 73, pp.341-351.

Goyal, A., and Shrivastava, A. K. (2020). Soil Nailing for Highway Construction. AKGEC International Journal of Technology, 11(1), pp.32-36.

Goyal, A., and Shrivastava, A. K. (2021). Application of Different Types of Soil Nails for Slope Stabilization. International Conference on Advancements and Innovations in Civil Engineering. ICAICE-2021.

Goyal, A., and Shrivastava, A. K. (2022). Analysis of conventional and helical soil nails using finite element method and limit equilibrium method. Heliyon, 8(11), p.e11617.

Goyal, A., and Shrivastava, A. K., (2023). Optimization of helical soil nailing behaviors by response surface methodology and hybrid Coot optimization. International Journal for Numerical and Analytical Methods in Geomechanics. pp.1-23.

Halabian, A. M., Sheikhbahaei, A. M., and Hashemolhosseini, S. H. (2012). Three-dimensional finite difference analysis of soil-nailed walls under static conditions. Geomechanics and Geoengineering, 7(3), pp.183-196.

Han, W., Li, G., Sun, Z., Luan, H., Liu, C., and Wu, X. (2020). Numerical investigation of a foundation pit supported by a composite soil nailing structure. Symmetry, 12(2), p.252.

Hao, J., and Wang, B. (2014). Parameter sensitivity analysis on deformation of composite soil-nailed wall using artificial neural networks and orthogonal experiment. Mathematical Problems in Engineering.

Hong, C. Y., Liu, Z. X., Zhang, Y. F., Zhang, M. X., and Borana, L. (2017). Influence of critical parameters on the peak pullout resistance of soil nails under different testing conditions. International Journal of Geosynthetics and Ground Engineering, 3, pp.1-7.

Hong, C. Y., Yin, J. H., Zhou, W. H., and Pei, H. F. (2012). Analytical study on progressive pullout behavior of a soil nail. Journal of Geotechnical and Geoenvironmental Engineering, 138(4), pp.500-507.

Hong, C. Y., Zhang, Y. F., Guo, J. W., and Li, G. Y. (2016). Experimental study on the influence of drill hole roughness on the pullout resistance of model soil nails. International Journal of Geomechanics, 16(2), p.04015047.

Horn, R., Vossbrink, J., and Becker, S. (2004). Modern forestry vehicles and their impacts on soil physical properties. Soil and Tillage Research, 79(2), pp.207-219.

Imani, M., and BabaeiPouya, O. (2021). Seismic Stability Analysis of Soil Nail Walls Using the Upper Bound Method. Transportation Infrastructure Geotechnology, pp.1-24.

IS: 2720-4, Grain Size Analysis, Bureau of Indian Standard (BIS), New Delhi, 1985.

Issa, U., Saeed, F., Miky, Y., Alqurashi, M., and Osman, E. (2022). Hybrid AHP-fuzzy TOPSIS approach for selecting deep excavation support system. Buildings, 12(3), p.295.

Jewell, R. A. (1980). Some effects of reinforcement on the mechanical behaviour of soils. Ph.D. thesis, University of Cambridge.

Joshi, B. (2003). Behaviour of calculated nail head strength in soil-nailed structures. Journal of Geotechnical and Geoenvironmental Engineering, 129(9), 819-828.

Juran, I., and Elias, V. (1991). Ground anchors and soil nails in retaining structures. Foundation engineering handbook, pp.868-905.

Kim, Y., Lee, S., Jeong, S., and Kim, J. (2013). The effect of pressure-grouted soil nails on the stability of weathered soil slopes. Computers and Geotechnics, 49, pp.253-263.

Kotake, N., and Sato, E. (2021). Bearing capacity of a flexible plastic plate for soil nailing. International Journal of Physical Modelling in Geotechnics, 21(1), pp.26-39.

Kulczykowski, M., Przewłócki, J., and Konarzewska, B. (2017). Application of soil nailing technique for protection and preservation historical buildings. In IOP Conference Series: Materials Science and Engineering, 245(2), p.22055.

Lazarte, C. A., Robinson, H., Gomez, J. E., Baxter, A., Cadden, A., and Berg, R. R., (2015). Geotechnical engineering circular No. 7 soil nail walls-reference manual (No. FHWA-NHI-14-007). National Highway Institute (US).

Liu, D., Lin, P., Zhao, C., and Qiu, J. (2021). Mapping horizontal displacement of soil nail walls using machine learning approaches. ActaGeotechnica, 16(12), pp.4027-4044.

Liu, J., Shang, K., and Wu, X. (2016). Stability analysis and performance of soil-nailing retaining system of excavation during construction period. Journal of Performance of Constructed Facilities, 30(1), p.C4014002.

Löbmann, M. T., Geitner, C., Wellstein, C., and Zerbe, S. (2020). The influence of herbaceous vegetation on slope stability-a review. Earth-Science Reviews, 209, p.103328.

Lu, Y., Tan, Y., and Li, X. (2018). Stability analyses on slopes of clay-rock mixtures using discrete element method. Engineering Geology, 244, pp.116-124.

Majidian, S., and Panah, A. K. (2020). Hybrid experimental and numerical approach for assessment of non-linear dynamic behavior of soil-nailed retaining walls. International Journal of Non-Linear Mechanics, 123, p.103476.

Maleki, M., and Hosseini, S. M. M. (2022). Assessment of the Pseudo-static seismic behavior in the soil nail walls using numerical analysis. Innovative Infrastructure Solutions, 7(4), p.262.

Mickovski, S. B., Lindsay, F. M., and Smith, M. J. (2016). Construction and testing of self-drilled soil nails. Proceedings of the Institution of Civil Engineers-Geotechnical Engineering, 169(6), pp.541-553.

Milligan, G. W. E., and Tei, K. (1998). The pull-out resistance of model soil nails. Soils and Foundations, 38(2), pp.179-190.

Mirjalili, S., Gandomi, A. H., Mirjalili, S. Z., Saremi, S., Faris, H., and Mirjalili, S. M. (2017). Salp Swarm Algorithm: A bio-inspired optimizer for engineering design problems. Advances in engineering software, 114, pp.163-191.

Misra, A., and Chen, C. H., (2004). Analytical solution for micropile design under tension and compression. Geotechnical & Geological Engineering, 22, pp.199-225.

Mohamed, M. H., Ahmed, M., Mallick, J., and AlQadhi, S. (2023). Finite Element Modeling of the Soil-Nailing Process in Nailed-Soil Slopes. Applied Sciences, 13(4), p.2139.

Mohamed, M. S., Sagitaningrum, F. H., and Kamaruddin, S. A. (2019). Optimization of Soil-Nailed Wall Design using SLOPE/W Software. Open International Journal of Informatics, 7(Special Issue 1), pp.74-83.

Mohammad Zaki, M. F., Wan Ahmad, W. A. A., Ayob, A., and Ying, T. K. (2015). Analysis of soil nailing under earthquake loading in Malaysia using finite element method. In Applied Mechanics and Materials, 695, pp.526-529. Trans Tech Publications Ltd.

Mollaei, R., Yazdandoust, M., and Askari, F. (2022). Seismic evaluation of helical soil nailed walls using shaking table testing. Soil Dynamics and Earthquake Engineering, 163, p.107331.

Moniuddin, M. K., Manjularani, P., and Govindaraju, L. (2016). Seismic analysis of soil nail performance in deep excavation. International Journal of Geo-Engineering, 7, pp.1-10.

Mumtaz, M. W., Adnan, A., Mukhtar, H., Rashid, U., and Danish, M. (2017). Biodiesel production through chemical and biochemical transesterification: Trends, technicalities, and future perspectives. In Clean energy for sustainable development (pp. 465-485). Academic Press.

Naruei, I., and Keynia, F. (2021). A new optimization method based on COOT bird natural life model. Expert Systems with Applications, 183, 115352.

Niroumand, H., and Saaly, M. (2019). Design and construction of helical anchors in soils. In Sustainable engineering products and manufacturing technologies, pp.113-157, Academic Press.

Niu, G., Yi, X., Chen, C., Li, X., Han, D., Yan, B., Huang, M., and Ying, G. (2020). A novel effluent quality predicting model based on genetic-deep belief network algorithm for cleaner production in a full-scale paper-making wastewater treatment. Journal of Cleaner Production, 265, p.121787.

Nowroozi, V., Hashemolhosseini, H., Afrazi, M., and Kasehchi, E. (2021). Optimum design for soil nailing to stabilize retaining walls using FLAC3D. Journal of Advanced Engineering and Computation, 5(2), pp.108-124.

Oliaei, M., Norouzi, B., and Binesh, S. M. (2019). Evaluation of soil-nail pullout resistance using mesh-free method. Computers and Geotechnics, 116, p.103179.

Ortigao, J. A. R., and Palmeira, E. M. (1997). Optimised design for soil nailed walls. In Ground improvement geosystems Densification and reinforcement: Proceedings of the 3rd International Conference on Ground Improvement Geosystems London, pp.368-374.

Ortigao, J. A. R., Palmeira, E. M., and Zirlis, A. C. (1995). Experience with Soil Nailing in Brazil: 1970-1994. Proceedings of the Institution of Civil Engineers-Geotechnical Engineering, 113(2), pp.93-106.

Palmeria, E. M., and Milligan, G. W. E. (2015). Scale and other factors affecting the results of pull-out tests of grids buried in sand. Géotechnique, 39(3), 511-542.

Patra, C. R., and Basudhar, P. K. (2005). Generalized method of optimum design of nailed soil slopes. International Association for Computer Methods and Advances in Geomechanics, 4555-4562.

Pei, H., Yin, J., Zhu, H., and Hong, C. (2013). Performance monitoring of a glass fiber-reinforced polymer bar soil nail during laboratory pullout test using FBG sensing technology. International Journal of Geomechanics, 13(4), pp.467-472.

Perko, H. A. (2009). Helical piles: a practical guide to design and installation. John Wiley & Sons.

Pradhan, B., Tham, L. G., Yue, Z. Q., Junaideen, S. M., and Lee, C.F. (2006). Soil–nail pullout interaction in loose fill materials. International Journal of Geomechanics, 6(4), pp.238-247.

Rabie, M. (2016). Performance of hybrid MSE/Soil Nail walls using numerical analysis and limit equilibrium approaches. HBRC journal, 12(1), pp.63-70.

Raju, G. V. R. (1996). Behaviour of nailed soil retaining structures (Doctoral dissertation).

Ramkrishnan, R., Karthik, V., Sruthy, M.R., and Sharma, A. (2019). Soil reinforcement and slope stabilization using natural jute fibres. In New Solutions for Challenges in Applications of New Materials and Geotechnical Issues: Proceedings of the 5th GeoChina, pp.130-143.

Rawat, S. (2017). Testing and Modeling of soil–nailed slopes, Dissertation, Jaypee University of Information Technology, Waknaghat, Solan, Himachal Pradesh, India.

Rawat, S., and Gupta, A.K. (2016). An experimental and analytical study of slope stability by soil nailing. Electron J GeotechEng, 21(17), pp.5577-5597.

Rawat, S., and Gupta, A. K. (2016). Analysis of a nailed soil slope using limit equilibrium and finite element methods. Int. Journal of Geosynthetics and Ground Engineering, 2, pp.1-23.

Rawat, S., and Gupta, A. K. (2017). Numerical modelling of pullout of helical soil nail. Journal of Rock Mechanics and Geotechnical Engineering, 9(4), pp.648-658.

Rawat, S., and Gupta, A. K. (2018). Testing and modelling of screw nailed soil slopes. Indian Geotechnical Journal, 48, pp.52-71.

Rawat, S., Gupta, A. K., and Kumar, A. (2017). Pullout of soil nail with circular discs: a three-dimensional finite element analysis. Journal of Rock Mechanics and Geotechnical Engineering, 9(5), pp.967-980.

Rotte, V. M., and Viswanadham, B. V. (2013). Influence of nail inclination and facing material type on soil-nailed slopes. Proceedings of the Institution of Civil Engineers-Ground Improvement, 166(2), pp.86-107.

Seo, H., Lee, I. M., Ryu, Y. M., and Jung, J. H. (2019). Mechanical behavior of hybrid soil nail-anchor system. KSCE Journal of Civil Engineering, 23(10), pp.4201-4211.

Sharma, A., and Ramkrishnan, R. (2020). Parametric optimization and multi-regression analysis for soil nailing using numerical approaches. Geotechnical and Geological Engineering, 38(4), pp.3505-3523.

Sharma, A., Raju, P.T., Sreedhar, V., and Mahiyar, H. (2019). Slope stability analysis of steep-reinforced soil slopes using finite element method. In Geotechnical Applications: IGC 2016, 4, pp. 163-171, Springer Singapore.

Sharma, M., Choudhury, D., Samanta, M., Sarkar, S., and Annapareddy, V. R. (2020). Analysis of helical soil-nailed walls under static and seismic conditions. Canadian Geotechnical Journal, 57(6), pp.815-827.

Sharma, M., Samanta, M., and Punetha, P. (2019). Experimental investigation and modeling of pullout response of soil nails in cohesionless medium. International Journal of Geomechanics, 19(3), p.04019002.

Sharma, M., Samanta, M., and Sarkar, S. (2017). Laboratory study on pullout capacity of helical soil nail in cohesionless soil. Canadian Geotechnical Journal, 54(10), pp.1482-1495.

Sharma, M., Samanta, M., and Sarkar, S. (2019). Soil nailing: an effective slope stabilization technique. Landslides: Theory, practice and modelling, pp.173-199.

Sharma, P. (2021). Behavior of Helical Soil Nails: an experimental and theoretical study, Doctoral dissertation, Jaypee University of Information Technology, Solan, HP

Sharma, P., Rawat, S., and Gupta, A. K. (2020). Horizontal pullout behavior of novel open-ended pipe helical soil nail in frictional soil. International Journal of Civil Engineering, 18, pp.1179-1194.

Sharma, P., Rawat, S., and Gupta, A. K. (2021). Experimental investigation of helical soil nail group behavior under torque installation and monotonic pullout loading. Arabian Journal of Geosciences, 14(14), p.1376.

Sharma, P., Rawat, S., and Gupta, A. K. (2021). Force–displacement characteristics of helical soil nail under monotonic pullout loading: experimental and theoretical study. Indian Geotechnical Journal, 51(4), pp.757-772.

Sharma, P., Rawat, S., and Gupta, A. K. (2021). Laboratory investigation of pullout behavior of open-ended pipe helical soil nail in frictional soil. Geotechnical and Geological Engineering, 39, pp.2903-2914.

Sharma, P., Rawat, S., and Gupta, A. K. (2021). Laboratory investigation of pullout behavior of hollow and solid shaft helical nail in frictional soil. ActaGeotechnica, 16, pp.1205- 1230.

Sharma, P., Rawat, S., and Gupta, A. K. (2022). Experimental investigation of pullout behaviour of open-ended pipe helical soil nail in frictional soil. Geomechanics and Geoengineering, 17(3), pp.842-856.

Shirgir, S., Shamsaddinlou, A., Zare, R.N., Zehtabiyan, S., and Bonab, M.H. (2023). An efficient double-loop reliability-based optimization with metaheuristic algorithms to design soil nail walls under uncertain condition. Reliability Engineering & System Safety, 232, p.109077.

Spagnoli, G., Solarte, C. M. M., Tsuha, C. H. C., and Oreste, P. (2020). Parametric analysis for the estimation of the installation power for large helical piles in dry cohesionless soils. International Journal of Geotechnical Engineering, 14(5), pp.569-579.

Su, L. J., Chan, T. C., Shiu, Y. K., Cheung, T., and Yin, J. H. (2007). Influence of degree of saturation on soil nail pull-out resistance in compacted completely decomposed granite fill. Canadian Geotechnical Journal, 44(11), pp.1314-1328.

Su, L. J., Chan, T. C., Yin, J. H., Shiu, Y. K., and Chiu, S. L. (2008). Influence of overburden pressure on soil–nail pullout resistance in a compacted fill. Journal of geotechnical and geoenvironmental engineering, 134(9), pp.1339-1347

Su, L. J., Yin, J. H., and Zhou, W. H. (2010). Influences of overburden pressure and soil dilation on soil nail pull-out resistance. Computers and Geotechnics, 37(4), pp.555-564.

Tan, Y. C., and Chow, C. M. (2004). Slope stabilization using soil nails: design assumptions and construction realities. In Malaysia-Japan symposium on geohazards and geoenvironmental engineering, Bangi, Malaysia, pp.13-14.

Tao, C., Wang, X., Gao, F., and Wang, M. (2020). Fault diagnosis of photovoltaic array based on deep belief network optimized by genetic algorithm. Chinese journal of electrical engineering, 6(3), pp.106-114.

Tavakoli, S., and Aminfar, M.H. (2021). Numerical and Experimental Studies of the Effect of Mechanical Parameters on Nail Pull-Out Resistance in Sandy Soil. Iranian Journal of Science and Technology, Transactions of Civil Engineering, 45, pp.2477-2487.

Tokhi, H., Ren, G., and Li, J. (2016). Laboratory study of a new screw nail and its interaction in sand. Computers and Geotechnics, 78, pp.144-154.

Tokhi, H., Ren, G., and Li, J. (2018). Laboratory pullout resistance of a new screw soil nail in residual soil. Canadian Geotechnical Journal, 55(5), pp.609-619.

Villalobos, S. A., and Villalobos, F.A. (2021). Effect of nail spacing on the global stability of soil nailed walls using limit equilibrium and finite element methods. Transportation Geotechnics, 26, p.100454.

Wang, Q., Ye, X., Wang, S., Sloan, S. W., and Sheng, D. (2017). Experimental investigation of compaction-grouted soil nails. Canadian Geotechnical Journal, 54(12), pp.1728-1738.

Warner, M. F., and Barley, A. D. (1997). Cliff stabilisation by soil nailing, Bouley Bay, Jersey, CI. In Ground improvement geosystems Densification and reinforcement: Proceedings of the Third International Conference on Ground Improvement Geosystems London, pp.468-476.

Wei, W. B., and Cheng, Y. M. (2010). Soil nailed slope by strength reduction and limit equilibrium methods. Computers and Geotechnics, 37(5), pp.602-618.

Wolfram, S. (1992). Mathematica Reference Guide, Addison-Wesley, Redwood City, Calif, USA.

Wu, J. Y., and Zhang, Z. M. (2009). Evaluations of pullout resistance of grouted soil nails. In Slope Stability, Retaining Walls, and Foundations: Selected Papers from the 2009, GeoHunan International Conference, pp.108-114.

Xu, D. S., Liu, H. B., and Luo, W. L. (2018). Evaluation of interface shear behavior of GFRP soil nails with a strain-transfer model and distributed fiber-optic sensors. Computers and Geotechnics, 95, pp.180-190.

Ye, X., Wang, Q., Wang, S., Sloan, S. W., and Sheng, D. (2019). Performance of a compaction grouted soil nail in laboratory tests. ActaGeotechnica, 14, pp.1049-1063.

Ye, X., Wang, S., Wang, Q., Sloan, S. W., and Sheng, D. (2017). Numerical and experimental studies of the mechanical behaviour for compaction grouted soil nails in sandy soil. Computers and Geotechnics, 90, pp.202-214.

Ye, X., Wang, S., Wang, Q., Sloan, S. W., and Sheng, D. (2019). The influence of the degree of saturation on compaction-grouted soil nails in sand. ActaGeotechnica, 14, pp.1101-1111.

Yin, J. H., and Zhou, W. H. (2009). Influence of grouting pressure and overburden stress on the interface resistance of a soil nail. Journal of Geotechnical and Geoenvironmental Engineering, 135(9), pp.1198-1208.

Zhang, C. C., Zhu, H. H., Xu, Q., Shi, B., and Mei, G. X. (2015). Time-dependent pullout behavior of glass fiber reinforced polymer (GFRP) soil nail in sand. Canadian Geotechnical Journal, 52(6), pp.671-681.

Zhang, L. L., Zhang, L. M., and Tang, W. H. (2009). Uncertainties of field pullout resistance of soil nails. Journal of geotechnical and geoenvironmental engineering, 135(7), pp.966-972.

Zhang, C. C., Xu, Q., and Zhu, H. H. (2014). Evaluations of load-deformation behavior of soil nail using hyperbolic pullout model.

Zhou, W.H. (2015). Pullout resistance of grouted soil nails. Embankments with Special Reference to Consolidation and Other Physical Methods, pp.533-571.

Zhou, W. H., Yin, J. H., and Hong, C. Y. (2011). Finite element modelling of pullout testing on a soil nail in a pullout box under different overburden and grouting pressures. Canadian Geotechnical Journal, 48(4), pp.557-567.

Zhou, Y. D., Cheuk, C. Y., and Tham, L. G. (2009). Numerical modelling of soil nails in loose fill slope under surcharge loading. Computers and Geotechnics, 36(5), pp.837-850.

LIST OF PUBLICATIONS

1. Goyal, A., and Shrivastava, A. K. (2022). Analysis of conventional and helical soil nails using finite element method and limit equilibrium method. Heliyon, 8(11), p.e11617. https://doi.org/10.1016/j.heliyon.2022.e11617 (SCIE, IF-3.776)
2. Goyal, A., and Shrivastava, A. K. (2023). Optimization of helical soil nailing behaviors by response surface methodology and hybrid Coot optimization. International Journal for Numerical and Analytical Methods in Geomechanics, pp.1-23. https://doi.org/10.1002/nag.3533 (SCIE, IF-4.229)
3. Goyal, A., and Shrivastava, A. K. (2023). A novel Heuristic and Tunicate centered ANFIS and RCCRD optimization for soil nailing using a numerical approach. Soil Dynamics and Earthquake Engineering, 176, p.108289. https://doi.org/10.1016/j.soildyn.2023.108289 (SCIE, IF- 4)
4. Goyal, A., and Shrivastava, A. K. (2021) Application of Different Types of Soil Nails for Slope Stabilization. International Conference on Advancements and Innovations in Civil Engineering. ICAICE-2021. (International Conference Paper)
5. Goyal, A., and Shrivastava, A. K. (2022). Helical Soil Nail as an Alternative to Conventional Soil Nail for Slope Protection. International Conference on Smart Environment Management and Solutions. ICEMS-2022. (International Conference Paper)